



Rehabilitation of Deteriorated Steel Truss Members Using CFRP

By

Qaidar H. Tawfik

Supervised by:

Assoc. Prof. Karu Karunasena

Dr. Francisco Cardona

A dissertation submitted for the award of

Master of Engineering Research (MENR)

Centre of Excellence in Engineered Fibre Composites

Faculty of Engineering and Surveying

University of Southern Queensland

Toowoomba, Queensland, Australia

February 2012

Abstract

The main problem facing steel structures is corrosion which can lead to the failure in the design. Generally, retrofitting steel structures costs far less than replacement and it takes less time. With regards to this issue, there is a growing focus on the repair or rehabilitation of corroded steel structures. Repairing by welding, as a traditional method, is costly, time-consuming and has other problems related to quality control and safety instructions. As a consequence, many designers are seeking more economical solutions. This study aims to investigate the rehabilitation of corroded steel trusses using Carbon Fibre Reinforced Polymer (CFRP) as a new method. Angular steel samples were selected and tensile and compressive characteristics of the corroded rehabilitated steel were investigated.

The environmental temperature ($-20^{\circ}\text{C} - 60^{\circ}\text{C}$) and the effects of moisture (immersing the sample under tap water for 500 hrs – 2000 hrs) on corroded rehabilitated steel simulated by different sizes of notches (3 mm - 12mm) were considered in this investigation. To simulate the temperature difference during day and night or between seasons, the influences of the recycling temperature on the rehabilitation of the corroded steel were examined by subjecting the sample to fluctuated temperature.

The results revealed that CFRP is able to rehabilitate the corroded steel at different conditions, i.e. there is high gain in the tensile strength of the corroded steel which nearly reaches the original value of the raw steel in some conditions. However, the influence of the environmental temperature is very pronounced, i.e. recycling of low and high values of temperature compromise the rehabilitation

process; where the improvement on the tensile and compressive properties are not remarkable compared to the room temperature condition.

Moisture effect caused gradual reduction in ultimate tensile capacity when the immersion time increased. The reduction recorded a maximum value of about 6.9% less than the original sample at 2000 hours. For the compression test, moisture had a faster effect on ultimate compression capacity, especially in the first 1000 hours which recorded a reduction of about 9.4% compared with the original sample.

For field applications, it is recommended that the percentage of CFRP area to steel area at the corroded section, should be about 35% to 45%, to achieve the most economic use of the CFRP and maintain the corroded steel member within the allowable elastic strain. The finite element model, developed using the Strand 7 program, showed good agreement with the experimental work regarding the strain value of CFRP strips.

CERTIFICATION OF DISSERTATION

I certify that the ideas, experimental work, results, analyses, software and conclusions in this dissertation are entirely my own effort, except where otherwise acknowledged. I also certify that the work is original and has not been previously submitted for any award, except where otherwise acknowledged.

.....

Signature of Candidate

Date / /

ENDORSEMENT

.....

Signature of Principal Supervisor

Date / /

.....

Signature of Associate Supervisor

Date / /

Acknowledgements

I am truly grateful to my supervisor Associate Professor Dr. Karu Karunasena for the efforts and time that he spent supporting me through research tasks and finding solutions for problems related to my research. I appreciate his kind attention and continued encouragement throughout the semesters of my Master Programme. I would like to extend my great thanks to my associate supervisor Dr. Francisco Cardona for his advice and guidance that helped me in preparing and dealing with adhesive chemical materials.

I would like to thank the Iraqi government, especially the Ministry of Higher Education and Scientific Research for nominating me to study aboard and supporting me and my family with a fully-funded scholarship.

I am also thankful to the technical team of the Faculty of Engineering and Surveying (FOES) and the Centre of Excellence in Engineered Fibre Composites (CEEFC), who helped me complete the experimental work and to all the staff and postgraduate students at CEEFC for sharing ideas, discussion and friendship.

For all the staff of University of Southern Queensland (USQ), I so greatly appreciate the opportunity you granted me to do a Master Programme at this university. Special thanks also go to Associate Professor Dr. Talal Yusaf for his support prior to and during my study. I especially acknowledge Ms. Sandra Cochrane for her proof-reading of my thesis.

I would like to express my deepest gratitude to my wife for her sacrifice and support throughout my learning journey at USQ.

To everybody who helped me but I forgot to mention, please forgive me and thank you very much.

Table of Contents

Chapter One	1
1.1 Introduction.....	1
1.2 Objectives of this work	4
1.3 Scope of the work	5
1.4 Contributions.....	6
1.5 Organization of the thesis.....	7
Chapter Two.....	9
Literature Review.....	9
2.1 Introduction.....	9
2.2 Carbon fibre reinforced polymers	9
2.3 CFRP for rehabilitating deteriorated steel trusses.....	14
2.3.1 CFRP with steel under tensile forces.....	15
2.3.2 CFRP with steel under compression forces	28
2.4 Numerical simulation of CFRP/steel technique.....	34
2.5 Conclusion and gap of current research.....	36
Chapter Three.....	37
Methodology	37
3.1 Introduction.....	37
3.2 Material selection.....	37
3.2.1 Steel plates	37
3.2.2 CFRP laminates	38
3.2.3 Steel angles	40
3.2.4 Primer and adhesive materials	40
3.3 Experimental apparatus and procedure	41

3.3.1	Universal tensile machines	41
3.3.2	Other equipment	45
3.3.3	Deterioration technique	45
3.3.3.1	Heating	45
3.3.3.2	Cooling	46
3.4	Preliminary tests and results for notched steel plates	47
3.5	Evaluation technique for corroded steel angle	53
3.6	Environmental effect on CFRP bonded to steel	60
3.6.1	Effect of environmental temperature	60
3.6.2	Effect of moisture	62
3.7	Summary	63
Chapter Four		66
Results and discussions		66
4.1	Introduction	66
4.2	Tensile characteristics of the rehabilitated steel	66
4.2.1	Influence of corrosion	66
4.2.1.1	Effect of notch sizes on steel alone without CFRP	66
4.2.1.2	Effect of notch sizes on steel attached with CFRP	68
4.2.2	Effect of environmental temperature	79
4.2.3	Effect of moisture	82
4.2.4	Finite Element Model for notched reinforced tensile member	83
4.3	Compressive characteristics of the rehabilitated steel	87
4.3.1	Influence of notch sizes	87
4.3.3	Effect of moisture	90
4.4	Failure modes	91

4.5	Summary	94
	Chapter Five	95
	Conclusions and recommendations	95
5.1	Introduction	95
5.2	Conclusions on tensile behaviour	95
5.3	Conclusions on compression behaviour	97
5.4	Recommendations and proposals for future works	98
	References	101
	Bibliography	107
	Appendix A	108
	Tables of maximum loads	108
A.1	Maximum loads in tensile test	108
A.2	Maximum loads in compression test	111

List of Figures

Figure 1.1: Corrosion effects on low level Bridge Northbound (Lima et al., 2008) ...	1
Figure 1.2: Layout of the thesis	8
Figure 2.1: Development of fibre matrix composite from the 1970s into the 21st century (Hollaway, 2010)	10
Figure 2.2: Amount of carbon fibre sheet alone used in Japan (Ueda, 2005).....	12
Figure 2.3: Number of applications for carbon fibre sheet by type of structures from 1987 to 2003 (Ueda, 2005)	12
Figure 2.4: Possible failure modes in a CFRP bonded to steel system (Zhao and Zhang, 2007)	14
Figure 2.5: Different retrofit schemes (Mertz and Gillespie, 1996)	16
Figure 2.6: Methods of CFRP strengthening and their load-deflection curves (Zhao et al., 2006)	17
Figure 2.7: Schematic drawing of CFRP/steel double strap joints (Nguyen et al., 2011)	26
Figure 2.8: Shear strength versus lasting time in man-made seawater (Yang et al., 2005)	27
Figure 2.9: Shear strength versus lasting time in hot/wet cycle (Yang et al., 2005) .	28
Figure 2.10: Experimental and numerical failure modes of the (a) short columns (b) long columns (Silvestre et al., 2008)	29
Figure 2.11: Tee sections and retrofit scheme (unit: mm) (a) aspect ratio of web; (b) CFRP-retrofit scheme; and (c) slenderness ratio of member with $h_w/t_w = 29$ (Kim and Harries, 2011b).....	31
Figure 2.12: Energy comparison between wrapped and unwrapped C12 x 20.7 specimens (C12 x 20.7 = unwrapped C12 x 20.7W = wrapped) (El-Tawil et al., 2011)	33
Figure 2.13: Definition of four material states and three transitions (Bai et al., 2008)	34
Figure 3.1: Picture of CFRP specimen after failure.....	39
Figure 3.2: Plates testing machine in the CEEFC.....	42
Figure 3.3: The tensile and compression testing machine used for angles.....	43

Figure 3.4: The original and converted jaws.....	44
Figure 3.5: Grooved steel disc used in compression test	44
Figure 3.6: The specimens inside the oven	46
Figure 3.7: The specimens inside the fridge	47
Figure 3.8: Geometrical dimensions of steel plates (not to scale)	48
Figure 3.9: Steel specimens after failure.....	50
Figure 3.10: Reinforcing steel specimens after failure	51
Figure 3.11: Load-extension diagrams for circular notched plate	52
Figure 3.12: Load-extension diagrams for edge notched plate	53
Figure 3.13: Method of reinforcement.....	55
Figure 3.14: Notched steel angle.....	55
Figure 3.15: Effective bond length for normal modulus CFRP joint (Fawzia et al., 2006)	57
Figure 3.16: Angle specimens after 1000 hours under water.....	63
Figure 4.1: Load-extension diagrams for control and notched specimens without CFRP.....	67
Figure 4.2: Effect of CFRP on load-extension diagram for 3mm notch specimen....	69
Figure 4.3: Effect of CFRP on load-extension diagram for 6 mm notch specimen... 70	
Figure 4.4: Effect of CFRP on load-extension diagram for 9 mm notch specimen... 70	
Figure 4.5: Load behavior of 12 mm notch specimen with and without CFRP and of the original steel specimen.....	71
Figure 4.6: Stress-strain diagram for the original sample	72
Figure 4.7: Stress-strain diagram for 12 mm notch with CFRP specimen.....	72
Figure 4.8: Attaching of strain gauge to CFRP strip.....	73
Figure 4.9: Increase in ultimate loads for rehabilitated notched samples	75
Figure 4.10: Increase in yield loads for rehabilitated notched samples	75

Figure 4.11: Relationship between percentage of CFRP to steel area for notched reinforced specimens and yield stress (from 3 to 12 mm notch, blue colour).....	77
Figure 4.12: Stress increments by increasing the ratio of carbon to corroded steel ..	78
Figure 4.13: Load-extension graph for the specimen at -20° C	80
Figure 4.14: Load-extension graph for the specimen at 60° C.....	80
Figure 4.15: Average ultimate stresses with different temperatures.....	81
Figure 4.16: Moisture effect on ultimate tensile stress	83
Figure 4.17: The mesh used for the FEA	84
Figure 4.18: Strain distribution (FE model).....	85
Figure 4.19: Enlarged view of the strain dialogue box	86
Figure 4.20: Compression load-extension diagrams for 9 mm notched samples with and without CFRP	87
Figure 4.21: Ultimate compression stresses for 9 mm notched samples with and without CFRP	88
Figure 4.22: Ultimate compression stresses under different temperature.....	90
Figure 4.23: Moisture effect on ultimate compression stress	91
Figure 4.24: Delaminating failure in tensile test.....	92
Figure 4.25: Delaminating failure in compression test.....	93
Figure 4.26: Debonding failure in tensile test.....	93
Figure 4.27: Debonding failure in compression test.....	94

List of Tables

Table 2.1: Properties of different types of CFRP.....	11
Table 2.2: Details of the test beams (Kim and Harries, 2011a).....	20
Table 2.3: Geometric and physical properties of materials (Kerboua et al., 2011) ...	21
Table 2.4: All of the tested configurations (Täljsten et al., 2009)	22
Table 3.1: Tensile test results of two steel specimens	38
Table 3.2: Tensile test results of 0.5 mm thick CFRP specimens.....	39
Table 3.3: Tensile test results of 0.8 mm thick CFRP specimens.....	39
Table 3.4: Characteristics of SWANCOR 984 (Primer).....	40
Table 3.5: Characteristics of Hysol EA 9330 (adhesive material).....	41
Table 3.6: Results of different bond length (Fawzia et al., 2006).....	56
Table 3.7: Dimension properties for angle sections from British Standard (BS-4848- part4, 1972)	60
Table 3.8 Numbers of specimens required for tensile test.....	64
Table 3.9 Numbers of specimens required for compression test.....	65
Table 4.1: Differences between ultimate and yield loads affected by edge notch.....	68
Table 4.2: Yield load, delaminating occurrence and ultimate loads for reinforced samples.....	74
Table 4.3: Load increments for rehabilitated notched specimens.....	74
Table 4.4: Equivalent area and yield stress for rehabilitated samples	77
Table 4.5: Effect of moisture on ultimate tensile stress	82
Table 4.6: Readings provided by strain gauge at 40 kN	86
Table 4.7: Ultimate stresses in compression test	89
Table 4.8: Effect of moisture on ultimate compression stress	90
Table A.1.1: Maximum tensile load of original samples (steel alone)	108
Table A.1.2: Maximum tensile load of 3 mm samples with and without CFRP	108

Table A.1.3: Maximum tensile load of 6 mm samples with and without CFRP	109
Table A.1.4: Maximum tensile load of 9 mm samples with and without CFRP	109
Table A.1.5: Maximum tensile load of 12 mm samples with and without CFRP ...	109
Table A.1.6: Maximum tensile load of samples affected by temperature	110
Table A.1.7: Maximum tensile load of samples affected by moisture	110
Table A.2.1: Maximum compression load of 9 mm samples with and without CFRP	111
Table A.2.2: Maximum compression load of samples affected by temperature	111
Table A.2.3: Maximum compression load of samples affected by moisture.....	111

Chapter One

Introduction

1.1 Introduction

The main problem facing steel structures is corrosion which can lead to structural failure. Corrosion reduces the total sectional area of the steel members in a structure which, in turn, increases stress in the corroded area due to the inverse proportional relationship between area and stress. Figure 1.1 shows the effect of corrosion on steel members. In reinforced concrete structures, corrosion of steel bars can, not only lead to reduction in the steel sectional area but, also to a fall of the concrete cover and bonding loss (AL-Ibweini and Ziara, 2011).



Figure 1.1: Corrosion effects on low level Bridge Northbound (Lima et al., 2008)

Generally, the cost of replacing deteriorated steel trusses is very high, especially when the failed structure affects the other structures, as what can happen

in transmission towers (a type of truss structure). If one suspension tower collapses, suspension towers on either side collapse, adding to the other costs which usually result from power disruption. In such cases, the rehabilitation of deteriorated trusses and resulting increase in service life, is unquestionably a useful procedure.

Corroded steel structures are traditionally repaired by cutting out the damaged sections and replacing them with new steel plates attached to the existing structure by welding, bolting or adhesive bonding. Such methods are costly, time-consuming, and require heavy lifting equipment to carry the heavy and bulky plates. In addition, new plates add more dead load to the structure, are prone to corrosion, and create, stress concentration resulting from welding or drilling (Tavakkolizadeh and Saadatmanesh, 2003; Colombi and Poggi, 2006). Also, welding introduces additional problems such as quality control, difficulty in tight locations, unknown residual stresses, cracking in the zones affected by welding heat and a dramatic reduction in fatigue life cycles (El-Tawil et al., 2011).

Moreover, repairing by welding in a highly explosive environment like steel fuel tanks can only be undertaken under strict safety conditions, and can cause interruption to production. For storage and offloading vessels used widely in offshore oil and gas mining, this is particularly significant. All of these procedures lead to production interruption and dramatic increases in repair cost (Tsouvalis et al., 2009; McGeorge et al., 2009). So, the need for economical and fast solution is the aim of many designers.

Fibre reinforced polymers (FRP) have been used in the rehabilitation of concrete structures. Currently, carbon fibre reinforced polymer (CFRP) is being considered for use in the rehabilitation of steel structures. The characteristics of each type of the three components forming CFRP/steel systems (CFRP composite, steel

member and adhesive material) play a vital role in determining the performance of this technique.

CFRPs have superior characteristics such as a high strength to weight ratio, very good durability in ambient conditions; are anti-corrosive; and are highly resistance to severe environments. These characteristics make CFRP a good candidate in several applications particularly the retrofitting of old steel structures (rather than using the traditional method of welding and/or cutting out and replacing steel parts as solutions for corroded parts in steel structures). As well, the weight of CFRP laminates is less than one fifth of the weight of similar size steel plates, making them easy to handle and able to be installed in less time than an equivalent number of steel plates (Shaat et al., 2003). Also, this technique helps avoid the welding problems mentioned previously.

Reducing the time of retrofitting of steel structures means reducing the cost of equipment, labour and materials. Increasing the construction speed through retrofitting also leads to reduce environmental impact (Lee and Jain, 2009). In Delaware, for instance, severely damaged bridge girders of a total length of 180 m were repaired. A comparison study between the cost of replacement and the cost of rehabilitation using CFRP pultruded laminates showed that total replacement cost was 3.65 times higher than the cost of rehabilitation at an assumed 25 percent section loss (Gillespie et al., 1996). Along with the reduction in cost and time of rehabilitation of corroded steel components, the Young modulus of CFRP composites is close to, or higher than, that of steel (Nguyen et al., 2011) which adds another reason for choosing it for steel structures rehabilitation.

One disadvantage of this technique is the phenomenon of galvanic corrosion. This phenomenon is a result of the high electric conductivity of CFRP composite

when it contacts steel directly. Galvanic corrosion can only happen when these three factors are available (Francis, 2000): an electrolyte like salt water linking the two materials (carbon fibre and steel), an electrical connection between the materials, and a sustained cathode reaction on the carbon. Removing any one of those factors prevents this problem. Fortunately, structural adhesives are mostly insulators that provide a continuous film of adhesive when used to bond CFRP with steel which means disruption of the galvanic cell and having no possibility for galvanic corrosion (Shaaf et al., 2003). Both the adhesive and the primer materials used in this experimental work are structural adhesives which formalised an insulator layer between the CFRP and the steel. An experimental study (Tavakkolizadeh and Saadatmanesh, 2001a) mentioned that galvanic corrosion can be eliminated by following certain applications such as using an isolating epoxy film, a nonconductive layer of fabric between the two bonded materials (steel and carbon), or applying a moisture barrier to the bonded area.

Almost all steel member rehabilitation work using CFRP has been limited to flexural type (i.e. bending type) members. There is a clear gap in research on the rehabilitation of truss type members subjected to axial load only. In this research project, the focus will be on the rehabilitation of truss type members using CFRP as the strengthening material.

1.2 Objectives of this work

The main objectives of this work are:

1. To overcome corrosion issues in steel structures by using CFRP composites. The study will provide information about the ability of CFRP composites to meet the loss of cross sectional areas of steel members and restore strength lost through corrosion

2. To study the efficiency of using CFRP in steel structures by investigating the tensile and compressive properties of a steel truss member (angle)
3. To evaluate the effect of using CFRP as rehabilitation for corroded angle steel parts under different conditions of temperature and moisture. The evaluation will be based on tensile and compressive testing.

1.3 Scope of the work

The study focused on using the positive aspects of CFRP composites to provide a durable and economical technique for the rehabilitation of deteriorated steel structures and contribute to solving the problem of corrosion and, as a result, save significant amounts of money. The project deals with three important parameters: the corrosion, and the temperature and the moisture which affect steel structures across the world. These parameters were chosen to simulate real environmental conditions, and small margins were added to each end to the temperature range to accommodate laboratory conditions and provide additional useful information.

Thus, corrosion is simulated as a deficiency in the cross-sectional area of steel truss members starting from 12.5 percent (3mm notch both legs of 25 * 25 * 3 mm angle) to approximately 50 percent (12 mm notch both legs of 25 * 25 * 3 mm angle) of the total sectional area. The effect of temperature is limited to between -20° C and +60° C. This simulates the normal distribution of annual temperatures worldwide with a little expansion in scope to present the effect of temperature clearly. The moisture effect is limited from 500 hours to 2000 hours by immersing specimens in tap water under the room temperature in the laboratory. Where possible, some of the

experimental results will be compared with the results of a numerical simulation using the STRAND7 programme.

1.4 Contributions

It is expected that this work makes a significant contribution to civil and mechanical engineering as it paves the way for other applications of the technique on corroded steel trusses. The main contributions will be:

1. Improved performance of corroded steel trusses and increased service age for these structures, allowing the delay of replacement by many years
2. An economic and accessible method of steel truss rehabilitation. The new technique of rehabilitation introduced through research can be applied directly to the corroded member without removing it from the original structure. Thus, associated problems can be avoided, especially when the corroded member is a critical part of the structure. The chosen type of CFRP in this project is a normal modulus one which makes the technique cheaper than those which use high modulus CFRP
3. Providing guidelines on applying this technique in different environmental conditions (i.e. temperature and moisture)
4. Choosing a new type of steel truss member (angle) to be rehabilitated by CFRP. The research will provide experimental results on retrofitting corroded steel angles which are used mainly in truss construction. Research results will be valuable in the field of reinforcing telecommunication and transmission towers which consist of angles, and attract significant attention because of the vital role they play in modern life

5. The study will contribute to the civil and mechanical engineering fields through publication. One conference paper has been published (Tawfik and Karunasena, 2010). A further conference paper has been accepted for publication and an international journal article will be submitted in the near future.

1.5 Organization of the thesis

The thesis contains five chapters (as shown in the layout in Figure 1.1.). Chapter One presents a brief introduction to the importance of CFRP in the rehabilitation of steel structures and the positive aspects that make it to a preferred solution in the steel retrofitting field. The chapter also considers the costly traditional method of steel structure rehabilitation and the problems associated with this. Finally, it summarizes the objectives and presents a brief overview of the research efforts and findings.

Chapter Two contains a comprehensive literature review on the development and application of the technique of bonding CFRP to steel and its benefits to steel members. It discusses recent research dealing with attaching CFRP material to steel members (which could be intact, naturally corroded, or artificially notched) and the results obtained after subjecting CFRP/steel members to different types of loads and environments.

Chapter Three explains the tests which conducted on the selected material of steel and carbon. It describes the tests on notched steel plates rehabilitated by selected carbon strips in order to discover the effect of carbon strips before moving to reinforce steel angles by these strips. The chapter addresses the manufacturing of new testing machine jaws that catch the angle during tensile tests. It also includes the

experimental steps that have been conducted to find the effect of corrosion; temperature and moisture.

Chapter Four presents the results of this study. The chapter discusses the effect of notch (corrosion), temperature and moisture on the efficiency of CFRP to rehabilitate steel members. Chapter Five concludes the outcome of this thesis, and gives recommendations for future work.

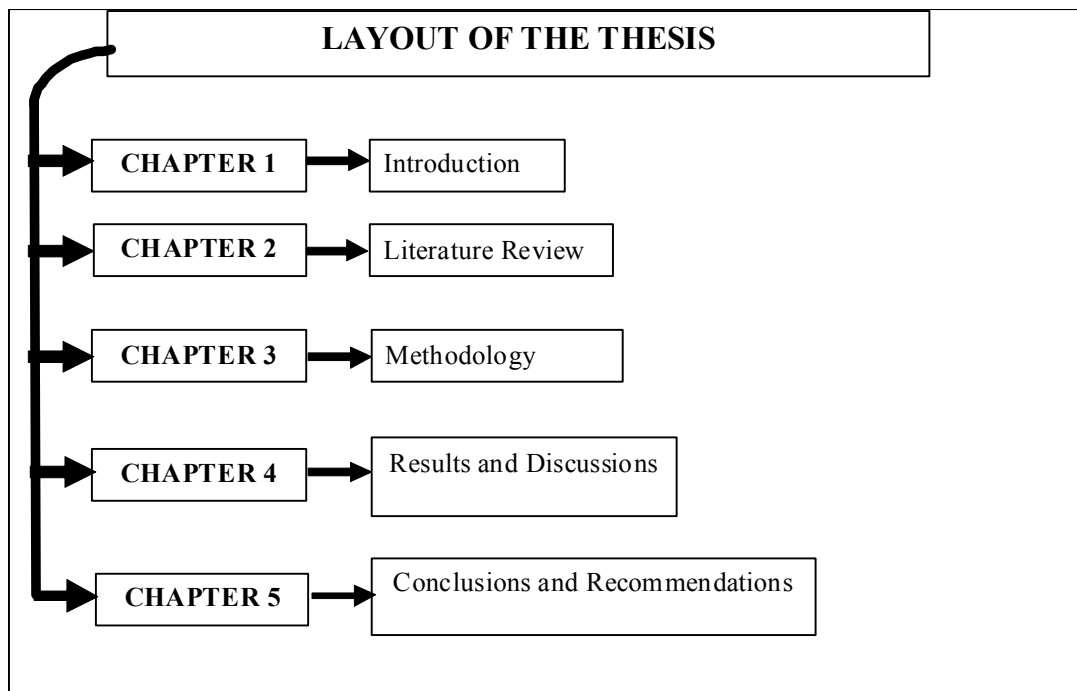


Figure 1.2: Layout of the thesis

Chapter Two

Literature Review

2.1 Introduction

This chapter presents an overview of the importance of Carbon Fibre Reinforced Polymer (CFRP), its applications and developing uses. The chapter demonstrates a comprehensive background of previous works that deal with attaching CFRP to intact, artificially notched and naturally deteriorated steel flexural members subjected to tension and compression forces. In addition, the chapter reviews some studies regarding the application of numerical simulation to CFRP/Steel technique.

2.2 Carbon fibre reinforced polymers

Carbon fibre reinforced polymer (CFRP) can be defined as a composite material consisting of carbon fibres, which provide strength, stiffness, and load carrying capacity, and a polymer matrix (Smith et al., 2005). During the past few decades (1960s onwards), the aerospace, marine and automobile industries have witnessed expanded use of advanced composite materials. More recently, the construction industry has started to use composites as strengthening materials (Pendhari et al., 2008). While the strengthening and rehabilitation of concrete structures by FRP composites have attracted considerable interest (Hollaway, 2003), the first application of bonding FRP material to metallic structure was in mechanical engineering (Shaat et al., 2003).

The types of fibre used in FRP composites are glass, aramid, carbon, other organic fibre like Polyacetal fibre (PAF), or polyester fibre like Polyethylene

Terephthalate (PET) (Ueda, 2005). A number of papers provide a historical review of FRP composite materials in civil infrastructure. Figure 2.1 summarizes the development of these materials from 1970s into the 21st century (Hollaway, 2010).

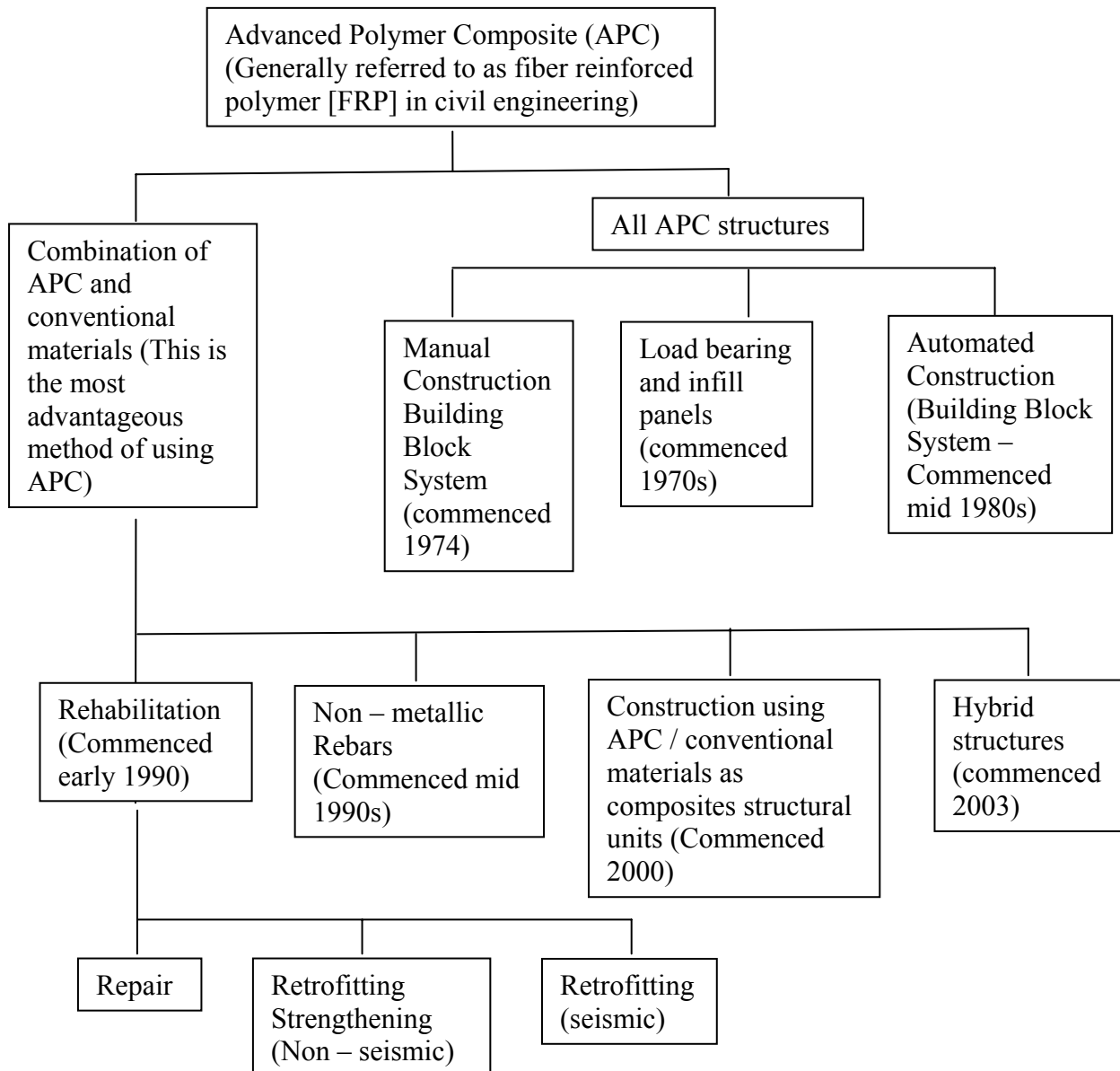


Figure 2.1: Development of fibre matrix composite from the 1970s into the 21st century (Hollaway, 2010)

The mechanical properties of CFRP composites depend on the type and orientation (transverse or longitudinal direction) of carbon fibre, percentage of resin material and curing conditions. Some researchers focused on the effect of the adhesive materials because of the fact that the success of this technique depends

mainly on the ability of the adhesive material to keep transferring the load between steel and the CFRP composite. This transferring is affected by many factors such as surface preparation, bonded length, type of adhesive material, thickness of adhesive and thickness of CFRP laminate. Table 2.1 shows the main mechanical properties of different types of carbon fibre composites used in the indicated research.

Table 2.1: Properties of different types of CFRP

CFRP composite type	Young`s Modulus (GPa)	Tensile strength (MPa)	Elongation at failure, %
Unidirectional pultruded Sika Carbodur strips (Bocciarelli et al., 2009)	>200	>280	>1.35
High modulus unidirectional sheets (Al-Shawaf et al., 2008)	640	2650	0.4
M Brace CF 130 sheets (Liu et al., 2009)	240	3800	1.55
M Brace CF 530 sheets (Liu et al., 2009)	640	2650	0.4
Sika Carbodur M 914 pultruded plates (Fam et al., 2009)	125	1914	
Sika Carbodur H 514 pultruded plates (Fam et al., 2009)	313	1475	
H S strips (Harries et al., 2009)	155	2790	1.8

FRP materials have been given a lot of attention in many countries, especially the industrial countries like USA, Japan and those in Europe. An example of carbon fibre sheet use in Japan (Figure 2.2) shows the amount of carbon fibre sheet alone use up to 2003, while Figure 2.3 shows number of applications for carbon fibre sheet by types of structures from 1987 to 2003 as reported by Ueda (2005). CFRP laminates have been used to retrofit damaged aluminium and steel aircraft structures (Armstrong, 2003), and thick steel for constructing ship structures (Hashim, 1999). It

is also worth mentioning that CFRP can be used with timber structures (Lees and Winistörfer, 2011) or with masonry arch bridges (Tao et al., 2011) especially as these structures include examples of historical or architectural value.

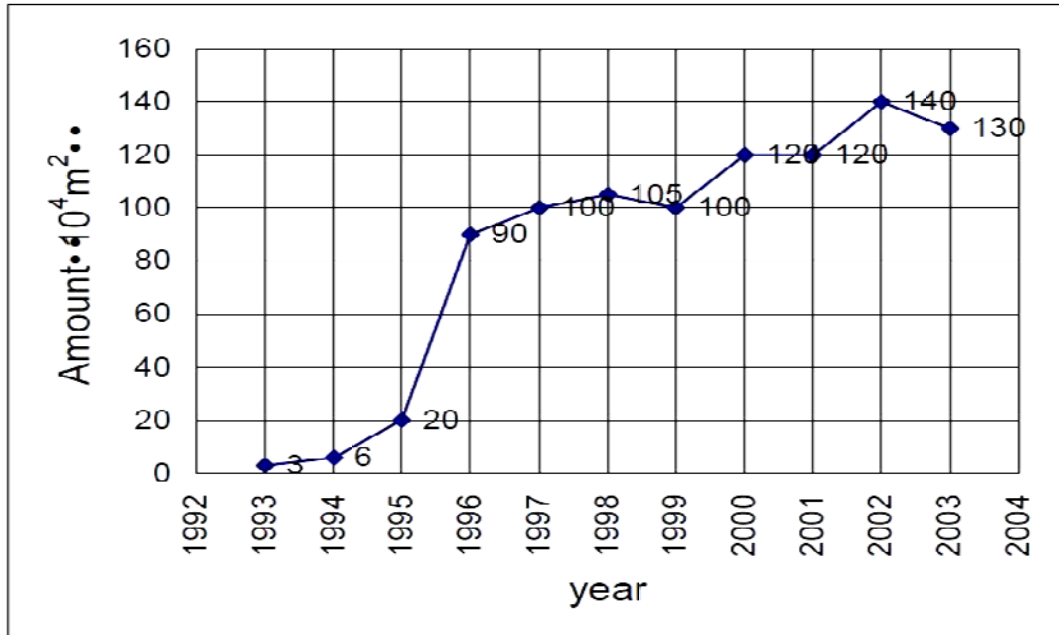


Figure 2.2: Amount of carbon fibre sheet alone used in Japan (Ueda, 2005)

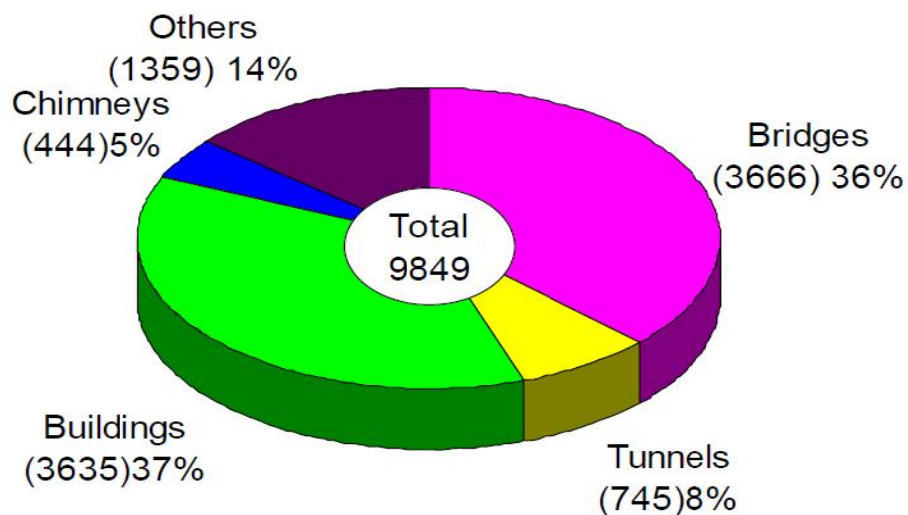


Figure 2.3: Number of applications for carbon fibre sheet by type of structures from 1987 to 2003 (Ueda, 2005)

Bonding techniques are critical to the success of attaching CFRP to steel members. To provide a strong bond between the CFRP composite and a steel member, the steel surface needs to be prepared by using an abrasive disk or sand blasting to remove rust and paint, and then cleaned by acetone or “degreased with a xylene based solvent to obtain a rough and clean, chemically active surface” (Bocciarelli et al., 2009). At the same time, the surface of CFRP strips can be treated by very fine sandpaper (grit P240) to provide sufficient roughness and more bond strength (Bocciarelli et al., 2009).

It is recommended that bare steel be pretreated by an adhesion promoter or a primer/conditioner which leaves a thin layer attached to the oxide surface of steel. Because water displacement is unlikely to happen through this coating, this bond remarkably improves the long-term durability of bonding (Mays and Hutchinson, 1992).

Failure in this technique can take different forms. Zhao and Zhang (2007) explained the possible failure modes associated with bonding of CFRP composite to a steel system subjected to a tensile force. These failure modes are shown in Figure 2.4 and they can include:

- (a) Interfacial debonding between the steel and adhesive layer,
- (b) Failure of the adhesive layer,
- (c) Interfacial debonding between CFRP and the adhesive layer,
- (d) Delaminating of CFRP composites,
- (e) Rupture failure of CFRP composites,
- (f) Yielding of steel members.

Failure mode type (b) is a common failure which is usually associated with a thin or low quality adhesive layer. Failure mode type (d) can happen when there is a separation of carbon fibres from the resin matrix of CFRP which means low elastic modulus CFRP composite, while failure mode type (f) happens rarely because there is usually a sufficient thickness of the steel member. So, elastic modulus of CFRP, elastic modulus of steel, and the quality and quantity (layer thickness) of adhesive material can all affect the failure mode of this technique.

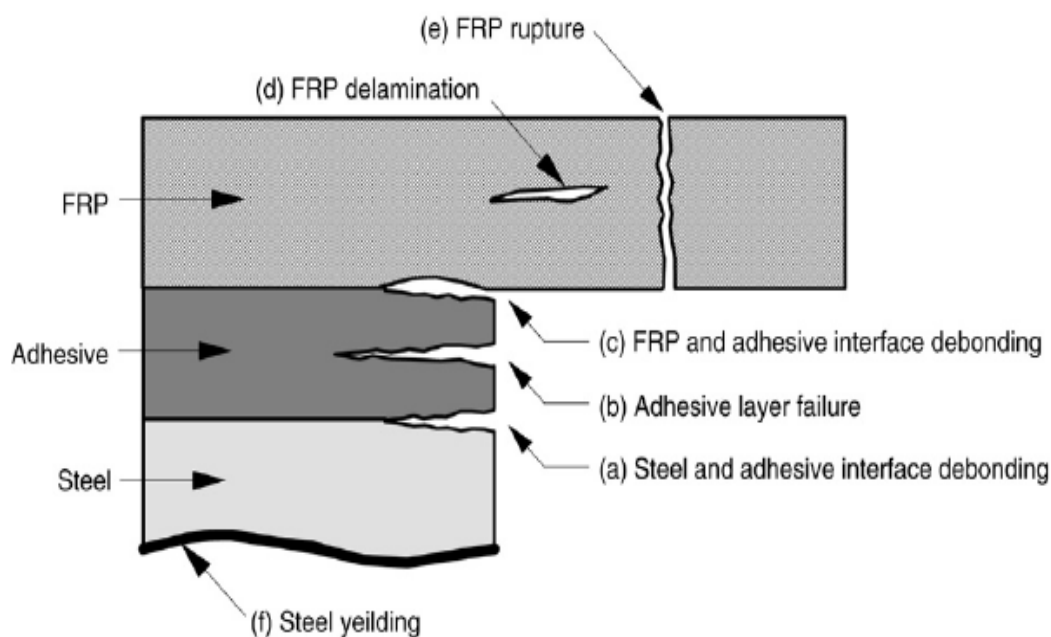


Figure 2.4: Possible failure modes in a CFRP bonded to steel system(Zhao and Zhang, 2007)

2.3 CFRP for rehabilitating deteriorated steel trusses

Occupying a large area in civil construction, steel structures regularly require attention for repair and rehabilitation. Generally, retrofitting of steel structures cost far less than replacement, and takes less time for construction. Thus, the service interruption time will be reduced. Retrofitting schemes are a very important due to the huge numbers of deteriorated steel structures. In Europe, about 50% of existing

bridges need to be retrofitted but the situation differs from one European country to the next (Radomski, 2002). Similarly, more than 40% of bridges in Canada were built before the 1970s and most of them need repair or rehabilitation (Intelligent sensing for innovative structures (ISIS), 2000/01). Few researchers have used Glass Fibre Reinforced plastic (GFRP) sheets for the rehabilitation composite steel bridges (El Damatty et al., 2005), even though the characteristics of CFRP (mentioned in Table 2.1) suggest it to be a promising solution for the strengthening of steel structures.

2.3.1 CFRP with steel under tensile forces

Many experimental works and theoretical studies address the bonding of CFRP composite on steel members; each dealing with a different parameter to discover more advantages of the material and its suitability for steel structures. Patnaik and Bauer (2004) used four I-sectioned undamaged beams. Two beams were reinforced by CFRP strips along the tension flange and exposed to a flexure failure test. The other two beams were reinforced by CFRP strips along their webs and exposed to a shear failure test. The first two beams recorded about a 14% increase in the capacity of flexure strength. For two shear-strengthened beams, one failed while the other recorded a 26% increase in strength. Mertz and Gillespie (1996) dealt with different reinforced schemes for W8x10 (American steel sections standard) members each 1.52 m long. All tested specimens showed a noticeable increase in strength and stiffness. Figure 2.5 shows the different retrofit schemes use for the specimens.

Vatovec et al (2002), 50 mm x 1.2 mm CFRP strips were used to reinforce the tension and compression flanges of rectangular steel tubes which were filled with concrete and submitted to a simple beam test. The results showed an increase in the ultimate moment capacity from 6% for specimens with one strip bonded to the

compression flange, to 26% for specimens with two strips bonded to the tension flange and one strip to the compression flange.

A theoretical study by Toutanji and Dempsey (2001) proved that using CFRP sheets around damaged steel pipe lines (circular hollow section) improve the internal pressure capacity of pipes better than other types of FRP sheets (glass or aramid). Zhao et al.(2006) used different styles of CFRP strengthening techniques to improve the web crippling capacity of cold-formed rectangular hollow sections. It was found that CFRP composite remarkably increase the web crippling capacity, especially when the ratio of web depth-to-thickness was large.

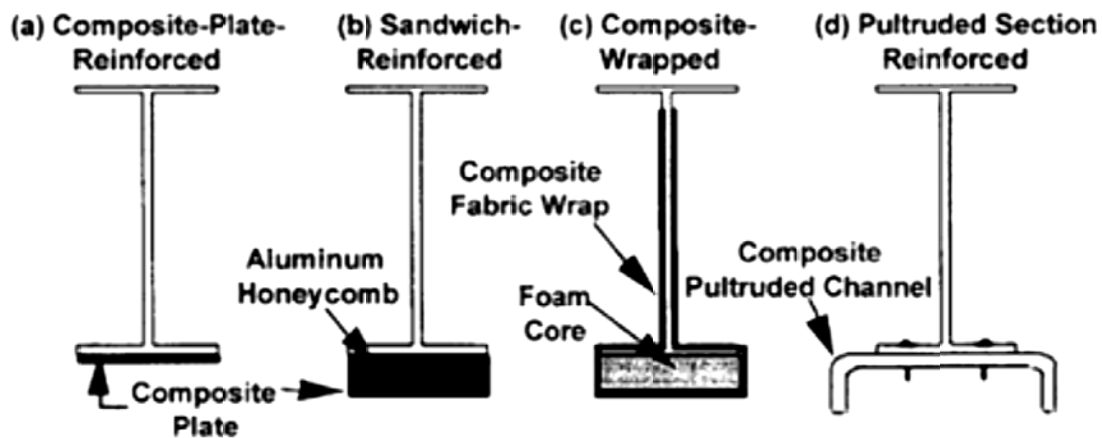
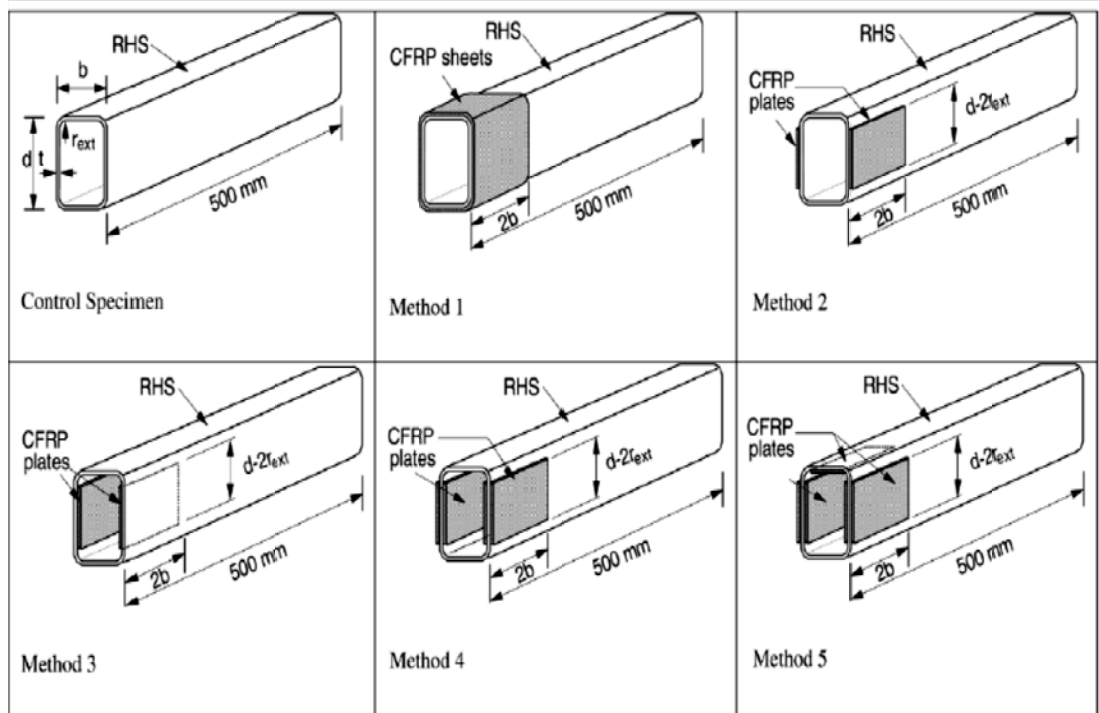
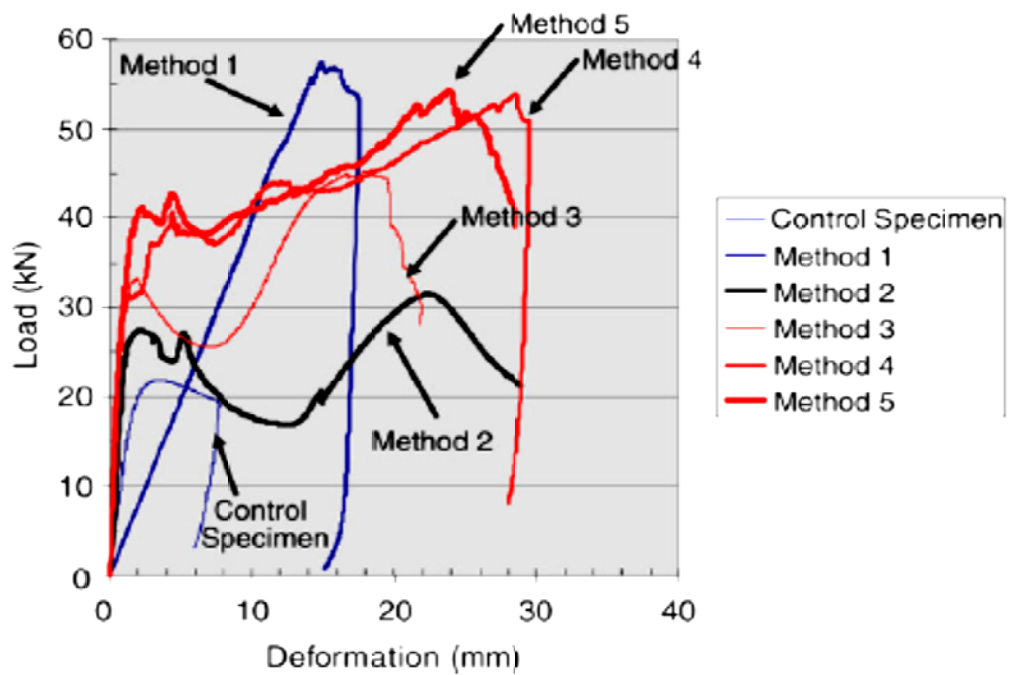


Figure 2.5: Different retrofit schemes (Mertz and Gillespie, 1996)

Figure 2.6 shows the adopted methods of CFRP strengthening and the typical behaviour of each method compared with the bare specimen. Zhao et al.'s investigation was focused on Method 2 because it was very simple in construction and Method 4 because it increased strength and ductile behaviour.



(a) Methods of strengthening



(b) Load-deflection curves

Figure 2.6: Methods of CFRP strengthening and their load-deflection curves (Zhao et al., 2006)

To simulate the effect of corrosion, some researchers used notched steel members while others used naturally deteriorated members. A cyclic loading test was done for naturally corroded bridge girders which were moved aside from deteriorated bridges (Gillespie et al., 1996). The test included using a single layer of CFRP to reinforce the entire length of the bottom flanges of two girders which were affected by corrosion more than webs or top flanges (this is typical for many bridges). Results showed that CFRP reinforcement increased the elastic stiffness of the girders in the range of 10% to 37%. Also, the ultimate capacities of the two girders increased to 17% and 25%, and the inelastic strains in the bottom of the flange were reduced by 75% compared with unreinforced girders at the same load level.

A three-point bending test on artificially notched beams was done at the University of Missouri-olla (Liu et al., 2001). Four W12x14 (American steel sections designation) with a length of 2438mm were used in this test. The first two specimens were tested without a CFRP retrofit but one of them contained 106 mm notch in the tension flange to simulate the effect of corrosion. Two CFRP laminates of 100 mm width were used to cover the same notch in the second two specimens but one covered the entire length of tension flange and the other covered one quarter of the beam length. Use of CFRP caused an increase of 60% in the plastic load capacity for the full length specimen and 45% for the one quarter length specimen.

Tavakkolizadeh and Saadatmanesh (2001b) used four-point bending on two groups of S5 x 10 (American steel sections designation) steel beams, 1300 mm length which were cut in the middle of tension flange to depths of 3.2mm for the first group and 6.4 mm for the second group. Both groups were reinforced by different

lengths of CFRP sheets with 0.13 mm thickness. The results demonstrated that, regardless of the length of the CFRP patch, the ultimate load carrying capacity and the stiffness of retrofitted specimens were close to their original values in the control specimen. The results of the deep cut group showed a distinct loss of ductility in comparison with the shallow cut group. Bassetti et al. (1999) proved that using CFRP plates of 1.2 mm thickness to reinforce central-notched specimens can sharply decrease crack growth and increase fatigue life by a factor up to twenty.

An experimental program by Kim and Harries (2011a) included use of 50 mm wide by 1.4 mm thick CFRP strips to repair W150 x 18 (American steel sections designation) steel beams in order to present flexural behaviour. Except for the control specimen, all beams were damaged by notching the tension flange. The purpose of the notch was to initiate a vertical crack in the steel web and initiate debonding of CFRP propagating towards the required support. A three-point flexural loading test was done for all beams over a 1830 mm simply-supported span. Three beams were loaded monotonically to failure while the others were subjected to cycling load. The details of each beam are shown in Table 2.2 below.

Table 2.2: Details of the test beams (Kim and Harries, 2011a)

Beams	Notch	CFRP-repair	Moment of inertia (10^6 mm^4)	Monotonic to failure ^a		Fatigue characteristics			
				P_y (kN)	P_u (kN)	Stress range ^d and loading frequency	Load (kN)	Stress range (MPa) ^e	Fatigue life (cycle)
A	None	None	9.20	b	102.3	–	–	–	–
FEA values for beam A				104.0	116.4	–	–	–	–
B	Yes	None	3.34	31.1 c	81.8	–	–	–	–
FEA values for beam B				78.0	97.6	–	–	–	–
C	Yes	Yes	4.54	42.6 c	84.5	–	–	–	–
FEA values for beam C				105.0	123.0	–	–	–	–
D	Yes	Yes	4.54	–	–	0.73 P_y @ 1 Hz	4.4–35.6	274	20,000
FEA values for beam D				–	–	N/A	4.4–35.6	274	15,000
E	Yes	Yes	4.54	–	–	0.42 P_y @ 2 Hz	4.4–22.2	158	152,380
FEA values for beam E				–	–	N/A	4.4–22.2	158	150,000
F	Yes	Yes	4.54	–	–	0.21 P_y @ 2.5 Hz	4.4–13.3	81	1,703,020
FEA values for beam F				–	–	N/A	4.4–13.3	81	2,100,000

^a P_y = yield load; P_u = ultimate load

^b lateral torsional buckling failure

^c yield load at root of notch

^d stress range based on yield of Beam C (i.e.: $P_y = 42.6 \text{ kN}$)

^e stress range at notched location

^{FEA} Finite Element Analysis

The results showed that CFRP strengthening can improve the monotonic capacity of damaged beams compared to that of undamaged ones, even though the local plasticity near the damage was not significantly improved. Moreover, the level of damage was not affected by the stress range up to nearly 60% of the fatigue life, while the effect of the stress range on damage levels clearly appeared with further

increases in fatigue cycles. The vertical crack propagation in the web grew slightly up to 40%-50% of the fatigue life, but after that increased substantially. The increase of fatigue cycle led to a gradual increase in CFRP debonding strains especially near the damage. The increment in plastic strains was affected by the stress range however, their magnitude was not significantly influenced by the stress range when it was below 40% of the steel yielding strength.

Regarding attaching FRP material to steel beams, a study carried out by Kerboua et al. (2011) investigated practical difficulties that could be associated with applying the FRP/steel technique to existing structures. The analytical solution of the study included some basic assumptions. The authors considered their study as an original one that can provide the benefits of FRP prestressed laminate to improve the structural strength by avoiding the premature failure of the reinforcing scheme and ensure sufficient adhesive capacity at plates' ends. The chosen steel beams were I cross-section simply supported bridge girders of 7.9 m free span, and subjected to 500 kN/m uniformly distributed loads. The geometric and physical properties of beams, types of FRP materials and adhesive layer used in this study are shown in Table 2.3.

Table 2.3: Geometric and physical properties of materials (Kerboua et al., 2011)

Material	b (mm)	t (mm)	E (GPa)
Steel beam	300	874	210
GFRP plate	70	2	50
FRP plate	70	2	140
Adhesive layer	70	2	2

It was found that the increasing values of prestressing force can lead to high concentrations of interfacial stresses, and when there is no prestressing force the

distribution of stresses will be normal like any other reinforced beam subjected only to mechanical load. It was found that shear modulus of the adhesive layer has a large effect on the magnitude of interfacial stresses at the laminate end, and using more flexible adhesives can reduce the value of maximum critical interfacial stresses at the laminate end by giving more uniform distribution of interfacial stresses. An inverse proportionality has been recorded between the variation of FRP plate thickness and the numerical values of the stresses concentration.

Täljsten et al. (2009) presented the results of old steel plates with a central notch and reinforced by prestressed and non-prestressed CFRP laminates loaded in fatigue. The test plates were fabricated from a deteriorated steel girder, originally taken from a demolished truss bridge in Sweden, built in 1896. The purpose of this procedure was to have a test specimen with the surface and mechanical properties the same as the original old structure would have. Two types of adhesives and CFRP laminates were used in this study. The test specimens included five different configurations. A is the control unstrengthened specimen; B and C are strengthened with different non-prestressed laminates and adhesives; D and E are strengthened with prestressed laminates and D has a slightly more prestressing force. Table 2.4 shows these configurations in details.

Table 2.4: All of the tested configurations (Täljsten et al., 2009)

Configuration	Lam.*	Ad.*	t_a [mm]	P_{pre} [kN]	$\Delta\sigma$ [MPa]
A (1)	–	–	–	0	97.5
B(1,2,3,4)	E*	S*	1	0	97.5
C (1)	M*	B*	2	0	97.5
D(1,2,3)	E*	S*	1	15	97.5
E (1)	M*	B*	2	12	97.5

*Lam. -, laminate; Ad.-adhesive., B (BPE 567); S (Pox SK 41); S (E 50 C); M (M 50 C); t_a (adhesive thickness); P_{pre} (prestressing load); $\Delta\sigma = \sigma_{max.} - \sigma_{min.}$; 1,2,3,4 (number of tested specimens)

It has been seen that the fatigue life of the test specimens in configurations B and C (non-prestressed laminates reinforcement) was prolonged to 2.45-3.74 times, while the prestressed laminates reinforcement as in configurations D and E presented the ability to stop crack propagation and extend the fatigue life of the structures. The study concluded that the crack propagation rate and fatigue life depend mainly on the prestressing force of the laminate and laminate stiffness for non-prestressed laminates. The thickness of the adhesive layer used has not proved significant influence, but other adhesive types could create different effects. Moreover, the study focused on plate surface treatment as an important issue for members reinforced for fatigue life.

A similar study to Täljsten et al. (2009) was done by Huawen et al. (2010). Double-edge-notched steel plates strengthened with prestressed CFRP laminates were tested to investigate the fatigue behaviour of tension steel members. The fourteen test specimens were divided to five configurations A, B, C, D, and E according to different prestress levels, and a simple model of fracture mechanics was proposed to predict the fatigue life. It has been noticed that prestressed reinforcements significantly prolong the remaining fatigue life of the structure in comparison with non-prestressed reinforcements. The measurements of crack growth proved that pre-treatments of the initial crack have a positive effect on the remaining fatigue life of a deteriorated structure. Also, the study mentioned two critical parameters in determining the fatigue behaviour of steel plates which were the prestressing level and the applied stress range. The study of debonding behaviour showed that the debonding area decreased by nearly 50% at a higher prestress level and there was a correlation between theoretically predicted results and experimental ones.

Some researchers have dealt with the effect of environment on the CFRP/steel bonding system. Temperature and moisture are the common factors for all geographic locations while other environmental factors such as alkaline solutions, fire, radiation, Ultra-violet, etc exist only in specific geographic locations. It is for this reason, that this research project focuses on temperature and moisture factors. The environmental effect could be on FRP components (fibre + resin) or on the total system of CFRP/steel rehabilitation. For FRP components whose glass transition temperatures (T_g) are well above normal ambient temperature, a beneficial post curing can result in a slight increase in the ambient temperature, while the performance of the FRP composite can significantly decrease when the surrounding temperature is above the glass transition temperature (Veselovsky and Kestelman, 2002; ACI-Committee-440, 2007). Karbhari et al.(2003) added to the already mentioned effects that freeze-thaw cycles could lead to an accelerated degradation, and that under 0°C , hardening and micro cracking of the matrix and then bond degradation can occur.

Naruse et al. (2001) studied the effect of thermal degradation behaviour on fatigue strength for unidirectional CFRP rings. The strength of CFRP rings was evaluated using a ring tensile test. The fatigue-tested control CFRP rings were compared with several thermally degraded ones. The results showed that the reduction ratio of fatigue strength reduced proportionally with degradation time. A prediction based on their developed method to accelerate the thermal degradation mentioned that the reduction ratio of fatigue strength will be 0.7 when unidirectional CFRP rings are heated at 120°C for 1500-7000 hours.

For the whole CFRP/steel system, Al-Shawaf et al. (2008) carried out a series of tensile tests on CFRP/steel plates specimens subjected to a range of ambient

temperatures between 20° C and 60° C. Three types of epoxy resins with different glass transition temperatures (T_g) were used for specimens fabrication. The results showed that the generic failure mode is debonding failure of CFRP/steel specimens subjected to temperature condition above their adhesive/matrix's (T_g). In addition to this, they found that the general relationship between joint capacity and operating temperature is inversely proportional with significant deterioration in joint capacity when the temperature is above the adhesive's (T_g). Moreover; joint capacity for identical wet-lay upped CFRP/steel joints depends mainly on adhesive type and its properties. In another work, Nguyen et al. (2011) studied the mechanical performance of adhesively bonded CFRP/steel double strap joints with different lengths of bond subjected to temperature around the glass transition temperatures (T_g) of adhesive material which was (T_g , 42 °C). Figure 2.7 shows a schematic view of these double strap joints. It was found through experiments that the effective bond length of CFRP adhesively attached to steel double strap joints increased with temperature. The effective bond length was twice larger when the temperature is close to the (T_g) of the adhesive material than it was at room temperature. The research also mentioned that the stiffness of CFRP/steel double strap joints sharply decreased when temperature was elevated. The reduction in joint stiffness was 20% at the (T_g), 50% at 10° C above the (T_g) and 80% at 20° C above the (T_g). The failure mode of CFRP/steel double strap joints was CFRP delamination at a lower temperature and then the joints failed through cohesive failure at temperatures equal to, or more than, the (T_g). It was noticed that joint strength behaviour is similar to joint stiffness degradation. The drop in joint strength was about 15%, 50% and 80% when temperature elevated to (T_g), 10° C above the (T_g) and 20° C above the (T_g) respectively.

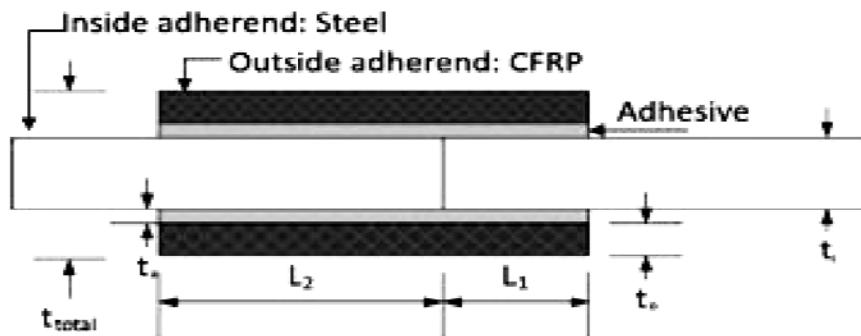


Figure 2.7: Schematic drawing of CFRP/steel double strap joints (Nguyen et al., 2011)

The effect of moisture can appear through the amount of water absorbed by resin matrix. Absorption depends on the type of resin and the temperature of water. Water absorption can result in a stiffening of the resin and a reduction of (T_g) (Smith et al., 2005). But, it has been shown that the general effect of moisture can lead to even more of a reduction in strength. Karbhari et al. (2003) mentioned that the effect of moisture exposure for long periods of time, and under certain conditions, may cause irreversible degradation especially for an under-cured system which then results in a significant decrease in the load carrying capacity.

Studying the combined effect of moisture and temperature has shown different outcomes. Karbhari and Shulley (1995) studied the effect of hot/wet cycling on CFRP/steel joints. The specimens were exposed to 65° C hot water for 14 days duration. The wedge-test showed significant bond degradation of CFRP/steel specimens. In contrast with this observation, Yang et al. (2005) investigated the effect of two environments (man-made seawater and the hot/wet cycle) on CFRP/steel joints for an exposure duration from 500 hours to 3000 hours. In the man-made seawater environment, a significant decrease in the shear strength for the first 1000 hours and a slow decrease after that with the lasting time, were shown. The reduction

in strength is due to water penetration to the adhesive, but this effect exists only to a certain point, after which a new balance system is formed and the rate of reduction stabilises or ceases. So, the reduction rate in strength becomes slow with the lasting time. Figure 2.8 shows the relationship between shear strength and lasting time for man-made seawater.

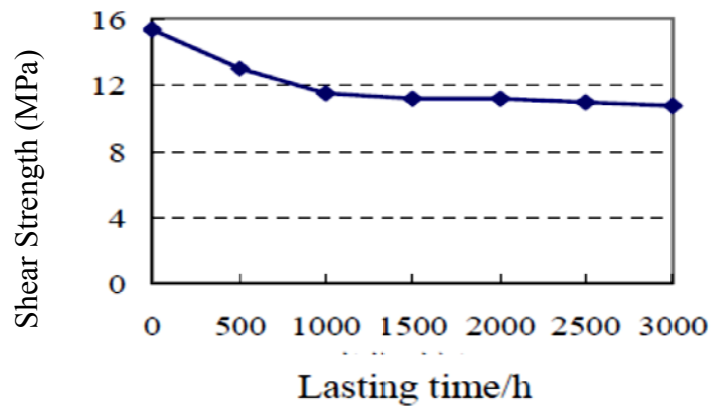


Figure 2.8: Shear strength versus lasting time in man-made seawater (Yang et al., 2005)

For the hot/wet cycle effect, they found an increase in the shear strengths of the single-lap joint specimens. The increase in bond strength of the joints which results from diffusing, filtering and entwisting of the adhesive molecules was attributed to temperature increase which enhances resin curing and improves the bond strength between the adhesive and the steel. The bond strength decrease, for the same hot/wet cycle, was attributed to differences in the thermal expansion coefficients between CFRP adhesive and steel which led to the production of cyclic thermal stress that can weaken the strength of the bond between the CFRP and steel. Figure 2.9 shows the relationship between shear strength and lasting time for hot/wet cycle.

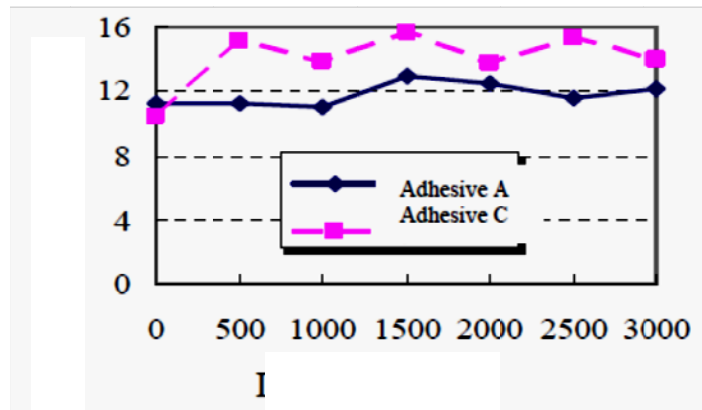


Figure 2.9: Shear strength versus lasting time in hot/wet cycle (Yang et al., 2005)

2.3.2 CFRP with steel under compression forces

As for using CFRP to retrofit columns or other steel members subjected to compression forces, a few researchers have worked in the field of loading conditions. Some researchers have studied the behaviour of CFRP with steel members under axial compression. For example, Shaat and Fam (2009) tested longitudinally square hollow sections reinforced by CFRP sheets and subjected them to monotonic axial loads. It was noticed that load carrying capacity of these reinforced sections increased up to 71% compared to the original section but the axial stiffness did not show improvement.

Ekiz and El-Tawil (2006) tried to find the effect of CFRP sheets on sandwiched steel plates with core material (mortar or PVC). The plates were subjected to compressive axial load under fixed-fixed ends boundary condition. Different failure modes were noticed such as plates buckling failure and the fracture of CFRP-wraps, but there was also enhancing of the post-buckling response of strengthened plates. Also, the CFRP- wrapping with core materials led to an increased failure load of steel plates up to 215%.

Silvistre et al.(2008) studied the behaviour of CFRP-strengthened steel long and short channel columns. This study included experimental and numerical

investigations of the non linear behaviour of CFRP, and found, local or global buckling failure type associated with most of the columns, whereas some columns showed debonding failure of the CFRP sheets. On the other hand, the presence of a single carbon fibre sheet increased the load-carrying capacity up to 15% for the short columns and up to 20% for the long columns. The numerical investigation demonstrated that the best option is employing when the carbon fibre sheets were longitudinally oriented. The study demonstrated that carbon fibre sheet failure could happen near to web-flange corners (for long and short columns) and next to lip free ends (for long columns only). Figure 2.10 shows experimental and numerical failure modes for columns used in this study.

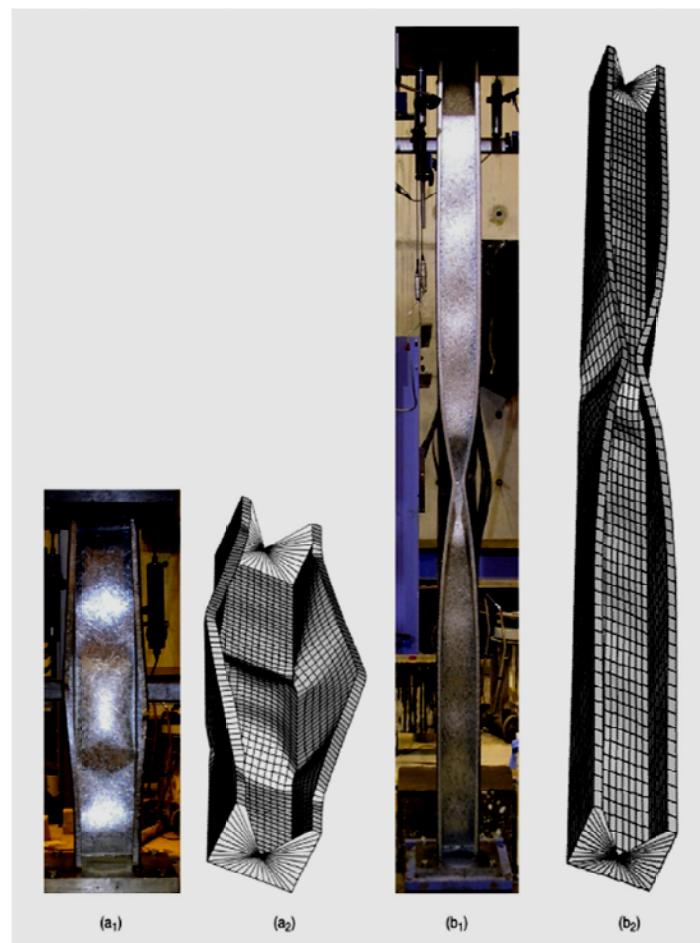


Figure 2.10: Experimental and numerical failure modes of the (a) short columns (b) long columns (Silvestre et al., 2008)

Recently, Kim and Harries (2011b) presented the response of steel tee-section bracing members when they were reinforced by CFRP strips and subjected to axial compression force. The study dealt with the effects of different factors such as CFRP-retrofit schemes, slenderness ratio of retrofitted sections and material properties of the CFRP strips. It has been found that increasing the number of CFRP bonded layers or the modulus of elasticity had little impact on the performance of the reinforced tee-sections. They also found that, the slenderness ratio affected the load-carrying capacity of CFRP retrofitted tee-sections sharply, the load-carrying capacity for these sections decreased about 50% when the slenderness ratio increased from 27 to 109. The aspect ratio of the web affected the stiffness of the load versus displacement responses for reinforced sections. The experimental work proved that attaching CFRP strips to tee-section bracing members reduced the stress up to 25% especially at the web-flange junction where critical hysteretic stress concentrations were expected to occur. The study mentioned that a CFRP-retrofit scheme could not be recommended for tee-sections having a slenderness ratio or web aspect ratio more than 60. Figure 2.11 shows details of tee sections and the retrofit scheme.

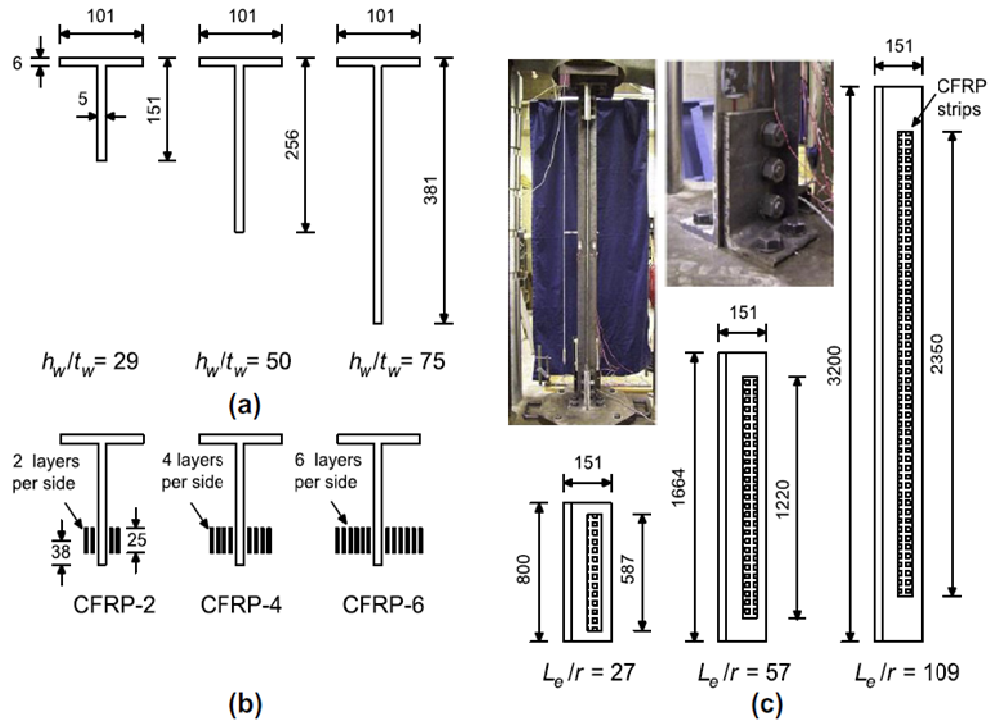


Figure 2.11: Tee sections and retrofit scheme (unit: mm) (a) aspect ratio of web; (b) CFRP-retrofit scheme; and (c) slenderness ratio of member with $h_w/t_w = 29$ (Kim and Harries, 2011b)

Bambach et al. (2009a) conducted a study on a short square hollow sections (SHS) compressed axially and bonded with CFRP externally. The width-to-thickness ratios of these sections were between 42 and 120 which lead to plate slenderness ratios between 1.1 and 3.2. It was mentioned that the application of CFRP could contribute to increasing the axial capacity of up to two times compared with the capacity of the steel section alone and could provide increases in strength-to-weight ratio of up to one and half times. In addition, the use of CFRP delayed local buckling by restraining the development of elastic buckling deflections. This restraining provided increases in the buckling stress of up to four times for reinforced sections compared to the control. Since the increase of capacity depend on restraining buckling, the capacity can be increased by increasing the plate slenderness ratio in

order to reach the optimum benefit of the steel plate slenderness ratio which was approximately 2.5 according to this study.

Another study by Bambach et al. (2009b) included a series of tests on square hollow section tubes (SHS) composite of steel-CFRP loaded dynamically under axial impact. It was noticed that enhancing steel SHS with CFRP can provide positive effects on the crushing load, energy absorption capacity and load uniformity. The dynamic mean crushing load of the member was increased up to 82% when CFRP was applied to existing steel SHS. Furthermore, the value of specific energy absorption for the steel-CFRP SHS was 52% greater than the value of that for steel SHS, and 94% greater than that for CFRP SHS.

Since flexural loading is a combination of tensile and compressive loads, a brief literature on flexural performance of steel members reinforced with CFRP is presented in the following paragraphs. Recently El-Tawil et al. (2011), presented a failure test for many large-scale steel flexural members under reversed cyclic loading. Some of the beams were wrapped in the plastic hinge region by various combinations of CFRP sheets. Others were unwrapped and considered as control specimens. The purpose of the study was to find out the effect of CFRP on the behaviour of steel plastic hinges. The results showed that wrapping the plastic hinge region of flexural members with CFRP can provide beneficial effects such as increasing the size of the yielded plastic hinge region and delaying the occurrence of local buckling and lateral tensional buckling. These benefits could contribute to a reduction in strain demands in the plastic hinge region, improving low cyclic fatigue behaviour and totally increasing energy dissipation of the plastic hinge region. Figure 2.13 shows energy comparison between wrapped and unwrapped C12 x 20.7 specimens.

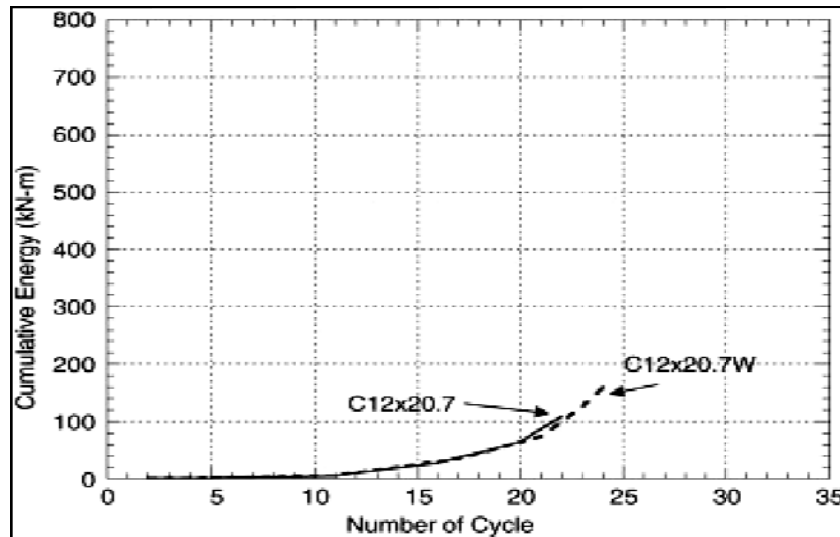


Figure 2.12: Energy comparison between wrapped and unwrapped C12 x 20.7 specimens (C12 x 20.7 = unwrapped C12 x 20.7W = wrapped) (El-Tawil et al., 2011)

As most of the available research on attaching CFRP composite to steel members has focused on flexural strengthening of corroded bridge girders and bonding FRP materials on the tension flange of beams (Harries et al., 2009), there is a scarcity of research dealing with the effect of temperature or moisture on CFRP materials attached to steel compression members. Only a few studies can be mentioned.

Akaro (2006) focused on determining the longevity of open steel grate decking filled with epoxy resin. The compression test through this study proved that the performance of open filled deck systems can be affected by high cyclic temperature, and the compressive strength was lower for all samples tested under high cyclic temperatures. Another study by Bai et al. (2008) proposed new models to calculate the heating effect on mechanical properties of FRP composite materials. The study concluded that FRP composites suffer dramatic changes under high and elevated temperatures. These changes can be divided into four temperature-dependent material states and three different transitions. The four states can be defined as

(glassy, leathery, rubbery and decomposed), while the three transitions can be defined as (glass, leathery-to-rubbery and rubbery-to-decomposed). Figure 2.14 shows definition of these material states and transitions.

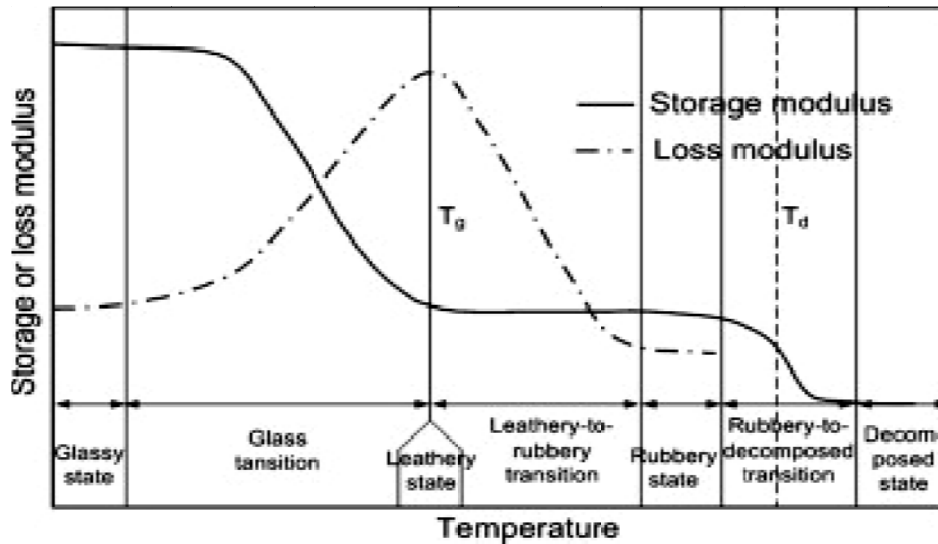


Figure 2.13: Definition of four material states and three transitions (Bai et al., 2008)

2.4 Numerical simulation of CFRP/steel technique

In this study, STRAND 7 programmes will be used to simulate the effect of CFRP on an artificially-notched steel member. So, it is necessary to provide a brief history of the Finite Element (FE) method and mention some research comparing numerical and experimental results of bonding CFRP to steel members. In the early of 1940s, Courant published a paper investigating torsion problems by using piecewise polynomial interpolation over triangular subregions, and for this reason, he has been selected as the first person who developed the finite element method. According to Moaveni (1999), the next significant step to utilize FE method was by Boeing in the 1950s when he used stress elements for modelling airplane wings. During the 1960s and after Clough made the term “finite element” popular, researchers started to apply the finite element method to different areas of engineering (Moaveni, 1999). A general purpose and comprehensive finite element

computer programme (ANSYS) was released for the first time in 1971 (Moaveni, 1999). The development of finite element theory still continues.

Tsouvalis et al. (2009) studied the fatigue behaviour by using low cost carbon/epoxy patches on one side of large cracked steel plates and then modelled them with finite element method based on some simplified assumptions. It was noticed that the relationship between patch thickness and bending resulting from the non-symmetric cross-section of the one-sided patched plate was verified experimentally and numerically. Also, an accurate prediction for the crack propagation rate and strains on the carbon/epoxy patch was obtained by the FE method.

A study done by Haghani (2010) provided analytical results about adhesive joints by bonding two CFRP laminates to steel plate both sides experimentally and utilizing FE method numerically. It was shown that the experimental work at mid-thickness of the adhesive layer was consistent with the results of the linear-elastic FE analysis. It was also found that the linear-elastic FE model for adhesive material can provide sufficiently precise approximations in terms of maximum strain in the adhesive joints used in the study. For joints made from a non-linear adhesive, the linear-elastic FE model failed to produce accurate predictions relating to the maximum stress/strain because the non-linear deformation of the adhesive can contribute to the redistribution of the strain and joint capacity.

Al-Shawaf (2011) studied the reasons for failure and failure loads of double strap joints under environmental conditions of extreme subzero and elevated temperature. The joints included three different resins, two grades of CFRP layers and mild steel plate; all investigated exposures were adopted by non-linear finite element models. The FE method and micro structural modelling approach opted for

the wet lay-up CFRP layer and presented good behavioural simulations to the experimental specimens of extreme temperature exposures. There was very good agreement between FE predictions and experimental results for CFRP superficial strain distributions. The current FE models confirmed that the most common triggering failure pattern for 89% of the specimens was “interfacial adhesive debonding”. The FE failure load predictions were generally conservative for all CFRP-material joint configurations and conditioning temperatures. For joint strength, and when the conditioning temperatures were increased towards the joint’s adhesive (T_g) temperature, the FE predictions seemed to be more accurate relative to their experimental values.

2.5 Conclusion and gap in current research

Through the mentioned studies, it can be said that almost all of previous research studies on tension and compression were conducted in the context of flexural member applications. There were no studies in the direct applications to angle members in truss type structures. Hence, the present study is focussed on a new method of applying direct axial tensile and compression loads to notched angle members reinforced by CFRP strips. This new method will provide new results on the effect of CFRP on the tensile and compression characteristics of truss members affected by corrosion and other environmental conditions such as temperature and moisture.

Chapter Three

Methodology

3.1 Introduction

Chapter Three shows the dimensions and characteristics of the materials used in this study including steel angles, CFRP, primer and adhesive materials. It presents the specifications of testing machines and the standards that are followed in tension and compression tests, as well as all other instruments used to prepare the specimens or to conduct the deterioration procedures. The details of samples' preparation have been explained in this chapter.

3.2 Material selection

3.2.1 *Steel plates*

At the preliminary stage of this project, steel plates were used to study the effect of CFRP laminate on corroded steel. This is a common technique used by many and reported in the literature. Steel plates were sourced from Blue Scope Steel (SMORGON STEEL) company, Australia. The plates were machined by electrical saw into samples of 3 mm thickness x 25 mm width x 350 mm length. The mechanical properties of the supplied materials were not provided by Blue Scope. However, the mechanical properties of the material were experimentally tested with reference to AS-1391(2007). The tensile testing was performed using the universal tensile machine (MTS Insight, Electromechanical-100KN Standard Length). Table 3.1 lists the general mechanical properties of the selected steel.

Table 3.1: Tensile test results of two steel specimens

Specimen #	Avg Thick mm	Avg Width mm	Area mm ²	Peak Load N	Peak Stress MPa	Modulus of Elasticity MPa
1	3.00	25.00	75.00	33404	445.39	282328
2	3.00	25.00	75.00	31874	424.99	262538
Mean	3.00	25.00	75.00	32639	435.19	272433

3.2.2 CFRP laminates

The CFRP laminates were supplied by H. E. Supplies Pty Ltd, Australia. There are four dimensions of the available CFRP strips (0.5 mm x 10 mm, 0.8 mm x 25.4 mm, 1mm x 3 mm and 2 mm x 12 mm). All these strips are provided with 1000 mm length and were cut according to the required lengths.

As the supplier of CFRP does not provide information about the laminates, it was necessary to test them to ascertain their mechanical properties. In the experimental testing, four CFRP specimens were chosen, two with dimensions of 0.5 mm thickness x 10 mm width x 300 mm length and two with dimensions of 0.8 mm thickness x 25.4 mm width x 300 mm length. All of them were subjected to tensile testing with reference to EN-ISO-527-5 (1997) to obtain its elastic modulus value. The speed of the testing machine was 2 mm per min. Table 3.2 gives the results of the elastic modulus of 0.5 mm CFRP strips thickness while table 3.3 shows the results of 0.8 mm CFRP strips thickness. Both sets of results were obtained from the universal tensile machine. The average value for all four specimens was nearly 125 GPa. It must be noted that only the CFRP strips with dimensions of 0.8 mm thickness x 25.4 mm width, were used in this project. These strips were chosen as they are the dimensions most suited to the width of the steel plates and angles. Figure 3.1 shows a picture of one of the CFRP specimens after failure.

Table 3.2: Tensile test results of 0.5 mm thick CFRP specimens

Specimen #	Peak Stress MPa	Modulus of Elasticity MPa
1	2048.60	124911
2	1976.66	124117
Mean	2012.63	124514

Table 3.3: Tensile test results of 0.8 mm thick CFRP specimens

Specimen #	Peak Stress MPa	Modulus of Elasticity MPa
1	1165.43	124186
2	1341.44	125889
Mean	1253.43	125038



Figure 3.1: Picture of CFRP specimen after failure

3.2.3 *Steel angles*

The steel angles were also provided by Blue Scope Steel. The dimensions of the angle specimen was 25mm equal legs angle x 3mm thickness x 350mm length, and the tensile test was done with reference to AS-1391(2007) standard and were proved to possess the same mechanical properties as the ones given on the steel plates in Section 3.1.1.

3.2.4 *Primer and adhesive materials*

Bare steel should be pretreated by an adhesion promoter or a primer/conditioner which leaves a thin layer attached to the oxide surface of steel. Because water displacement is unlikely to happen with this coating layer, the coating layer remarkably improves the long-term durability of the bond (Mays and Hutchinson, 1992). The chosen primer was SWANCOR 984 as recommended by the supplier (Swancor Ind. Co.) and the Technical Manager of the CEEFC Centre. Table 3.4 shows the characteristics of the primer according to manufacturer (Swancor Ind. Co.).

Table 3.4: Characteristics of SWANCOR 984 (Primer)

Product	Appearance	Viscosity (25°), cps	Heat Distortion Temperature °C	Shelf Life Months	Description
SWANCOR 984	Opaque two-phase liquid	400	82	4	Vinyl ester primer for concrete, carbon steel, stainless steel and old FRP. Excellent resilience and adhesion to metal.

The adhesive used in this study is Hysol EA 9330, as recommended by the supplier to be the optimal type of adhesive for a CFRP/steel material system. This adhesive is a two-part epoxy resin. The percentage of mixing between part A- to part B-components (Epoxy and Hardener) is 1:3. Table 3.5 shows the characteristics of this adhesive according to the material provider (Logistics Ltd.).

Table 3.5: Characteristics of Hysol EA 9330 (adhesive material)

Product	Form	Consistency	Service Temperature °F/°C	Tensile Lap Shear 25 °C MPa	Description
Hysol EA 9330	Two-parts epoxy	Moderate Viscosity	180/82	34.5	* High peel strength * High shear strength * Easy to mix * Good general purpose adhesive * Ideal for thermoplastic bonding

3.3 Experimental apparatus and procedure

3.3.1 *Universal tensile machines*

Two universal tensile machines (MTS) have been used in this work. The first MTS machine is 100 kN capacity and has been used for conducting tensile testing of steel plates and CFRP laminates. The machine is located at the Centre of Excellence for Engineered Fibre Composite (CEEFC) at the University of Southern Queensland (USQ). Figure 3.2 shows the testing machine in the CEEFC.

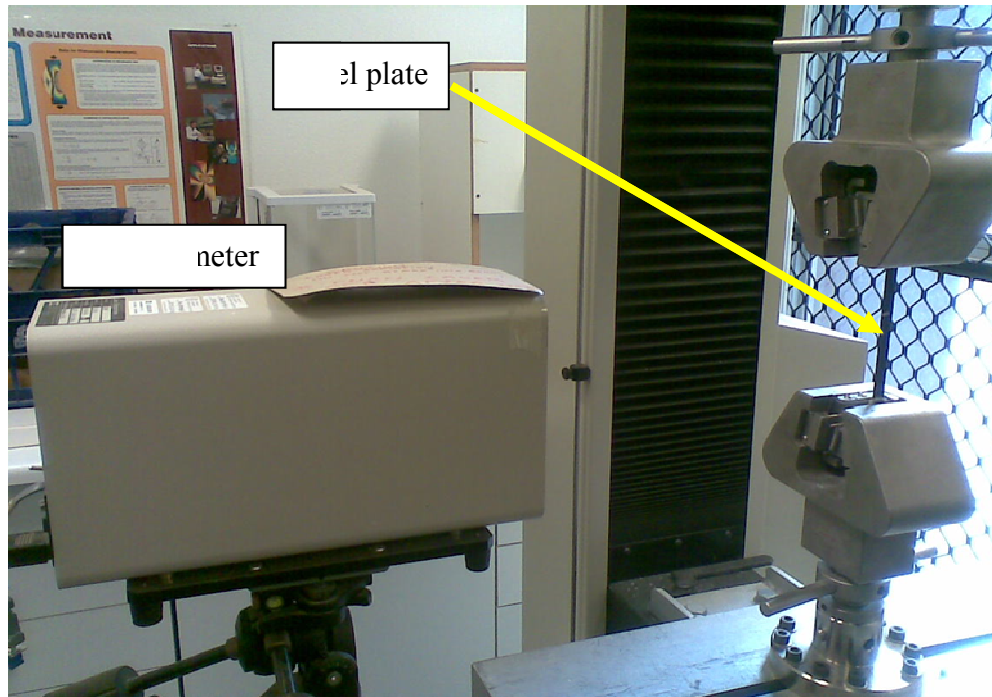


Figure 3.2: Plates testing machine in the CEEFC

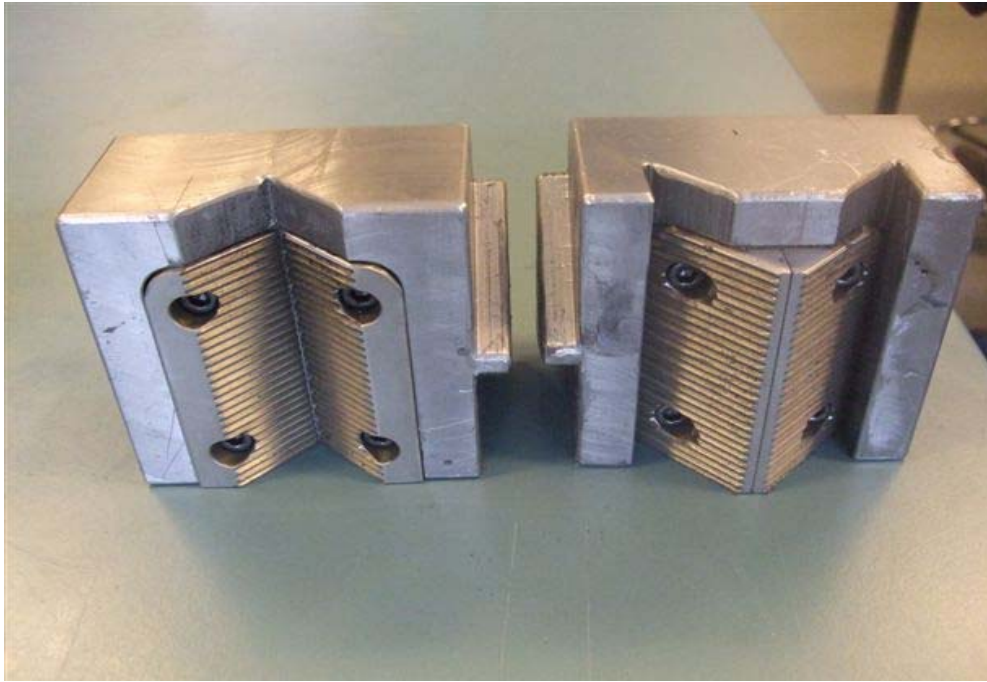
The second MTS machine has a 500 kN capacity and has been used for conducting tensile and compressive tests of steel angles. The machine is located in the laboratory of the Faculty of Engineering and Surveying (FOES) at USQ. Conducting tensile test demands the conversion of the jaws of the tensile testing machine to catch angles because the original jaws are designed to test flat plates or round bars. Figure 3.3 shows the tensile testing machine used for angles test while Figure 3.4 shows the original and converted jaws. For compressive testing, a grooved steel disk was manufactured in order to prevent the angle from slipping out of the machine during the compressive test. The disk was 150 mm diameter with 20 mm total depth and the cross groove was 10 mm depth and 5 mm width. Figure 3.5 shows the manufactured steel disk.



Figure 3.3: The tensile and compression testing machine used for angles



(a) The original jaws of the tensile machine



(b) The converted jaws for angles tensile testing

Figure 3.4: The original and converted jaws



Figure 3.5: Grooved steel disc used in compression test

3.3.2 Other equipment

Two electrical saws were used in this project, one was used to cut steel plates and angles (Makita, cut off saw) and the other was used to cut CFRP laminates (Hitachi C10RC, table saw).

One electrical smoothing machine (Linisher, 200 mm Industrial Bench Grinder) was used for smoothing the edges of steel plates and angles and for preparing their surfaces. The other electrical smoothing machine (Disk Sander) was used for smoothing the edges of CFRP specimens after cutting.

The electrical drill machine (HAF CO Pedestal drill, Metal Master) was used to make hole notches in the steel plates. Another machine (HAAS, VF 3, CNC Machining centre) was used to make edge notches in the steel angles.

3.3.3 Deterioration technique

The experimental work of this project includes submitting reinforced steel angles to deterioration techniques such as heating and cooling to find out the deterioration effect on CFRP/steel reinforcing system.

3.3.3.1 Heating

An electrical oven was used in order to expose reinforced steel angles to 60° C for the required period. Figure 3.6 shows a picture of the specimens inside the oven.



Figure 3.6: The specimens inside the oven

3.3.3.2 Cooling

An electrical fridge was used in order to expose reinforced steel angles to -20° C for the required period. Figure 3.7 shows a picture of the specimens inside the fridge. This fridge provides freezing degrees up to -20° C, and it is for this reason, that -20° C was chosen to study the effect of freezing temperatures on notched rehabilitated specimens.



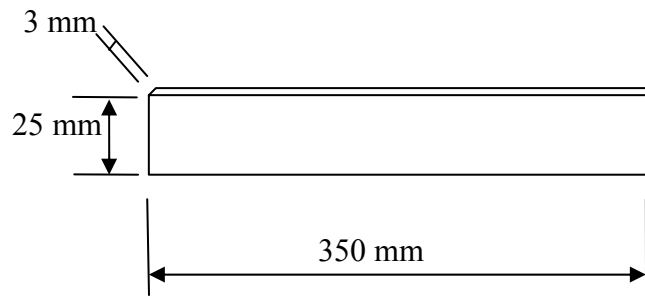
Figure 3.7: The specimens inside the fridge

3.4 Preliminary tests and results for notched steel plates

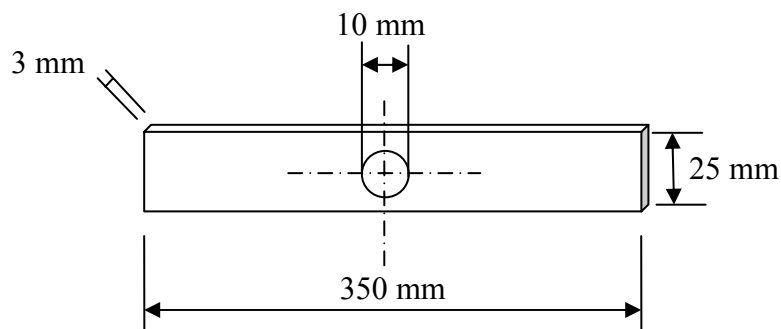
As an initial step, it was decided to undertake preliminary tests on steel plates before moving to angle specimens. It was determined that different sizes and shapes of notches (hole and edge notches) should be used in these tests. After receiving the adhesive material and CFRP laminate, it was necessary to perform some laboratory tests in order to find the capacity of the adhesive material to transfer the load between steel and CFRP.

Four steel specimens with the dimensions of 3 mm thickness x 25 mm width x 350 mm length were subjected to tensile tests with reference to AS-1391(2007). Two of specimens were control specimens while other two specimens contained different shapes of notch. One of them was punched to make a 10 mm diameter hole as a circular notch in the middle and the other one was notched to make 6 mm edge cut

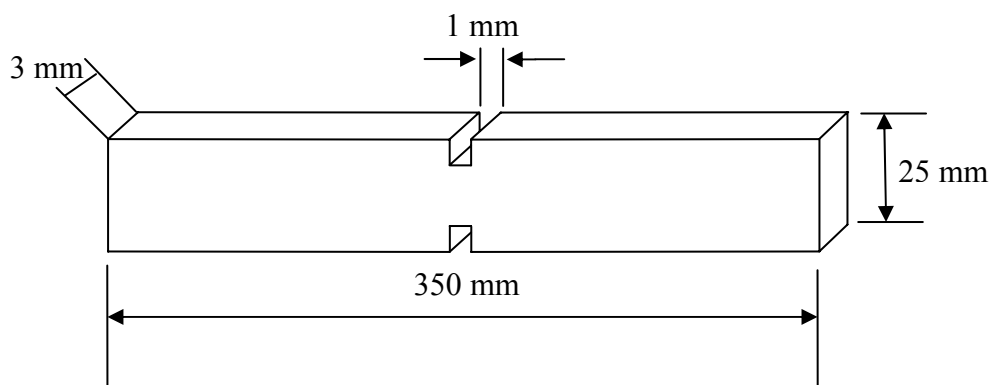
on the both sides of the steel plate. The results of notched specimens were compared with other notched plates which were reinforced by CFRP. Figure 3.8 shows geometrical dimensions of the control and notched specimens. Figure 3.9 shows a picture for control (a), circular notch (b) and edge notch (c) plates after failure.



(a) Steel plate without notch



(b) Steel plate with hole

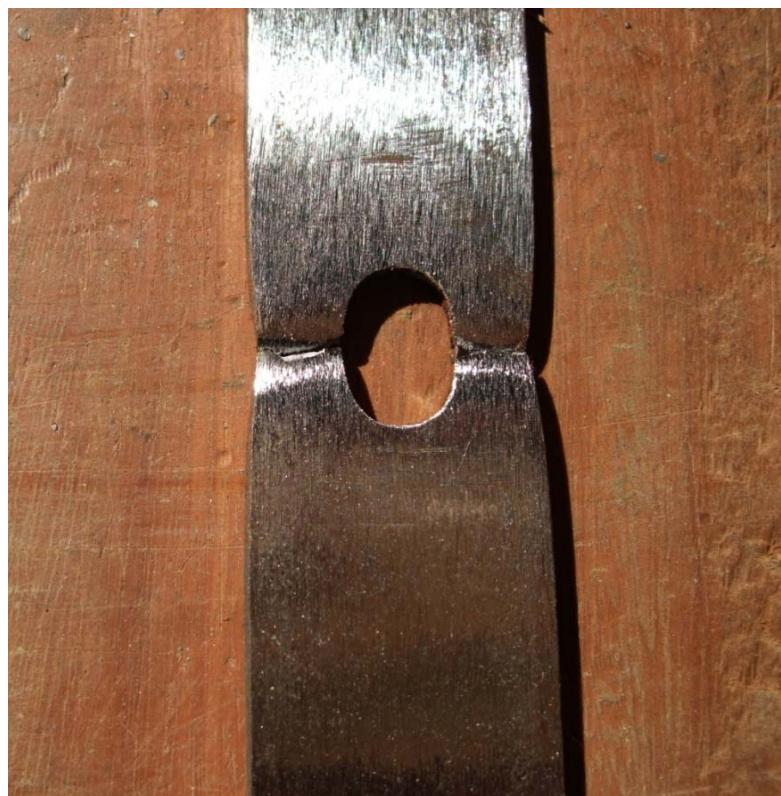


(c) Steel plate with edge notch

Figure 3.8: Geometrical dimensions of steel plates (not to scale)



(a) Specimen with no hole after failure



(b) Specimen with hole after failure



(c) Specimen with edge notch after failure

Figure 3.9: Steel specimens after failure

To find the effect of CFRP attached to steel, the notched steel plate reinforced by CFRP was tested. The steel specimen was notched with a 10 mm diameter hole in the middle (at 25 mm width) as in Figure 3.9 (b). The notch helped to create the failure in the reinforcing area and to cause about 40% reduction of the total cross sectional area of steel plate, which is assumed in this study to represent the corrosion effect. A CFRP laminate with dimensions of 0.8 mm thickness x 25.4 mm width x 150 mm length was bonded to the middle of one side of the notched steel plate. Then, the reinforced specimen was submitted to a tensile test. Figure 3.10 shows a picture of this specimen after failure. The load-extension diagrams for steel with no hole (steel alone), steel with a 10 mm hole and steel with a 10 mm hole reinforced by CFRP are shown in Figure 3.11.



Figure 3.10: Reinforcing steel specimens after failure

Another similar test was done on plates but with different sized and shaped notch. A steel plate of dimensions 3 mm thickness x 25 mm width x 350 mm length was notched 6 mm both sides from the edges in the middle length (as shown in Figure 3.8 (c)). This notch caused about a 50% reduction of the total cross sectional area of steel plate. The notched area of the plate was reinforced by a 0.8 mm thickness x 25.4 mm width x 150 mm length CFRP laminate. After that, a tensile test was completed on three plates: a plate with a notch reinforced by CFRP, a plate of the same notch but without CFRP, and the control plate. Figure 3.12 shows the load-extension diagrams for the three plates.

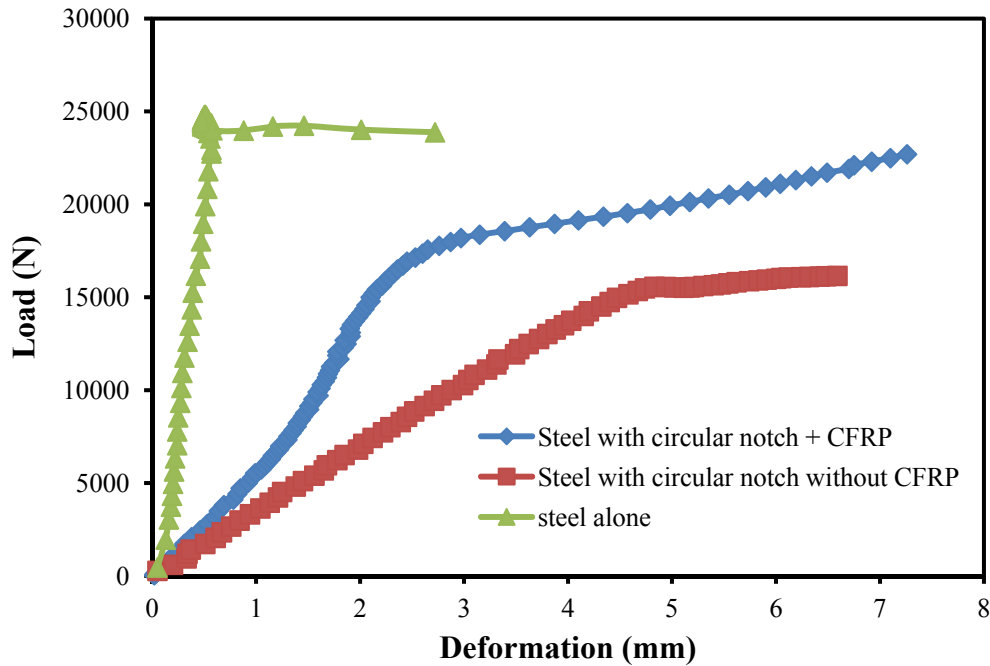


Figure 3.11: Load-extension diagrams for circular notched plate

The preliminary tests showed successful results in solving the adhesion problem of the FRP laminate to the steel plate. The initial tensile tests demonstrate that the CFRP laminate adhered to the surface of the damaged steel plate and definitely increased the load capacity of the damaged plate (in comparison with the damaged plate without CFRP laminate). The effect of CFRP provided better results with edge notch than the results with the circular notch and that can be attributed to the effect of notch shape. Figure 3.12 shows that CFRP significantly improved the strength, and the load carrying capacity of notched sample with CFRP was similar to the intact sample (steel plate alone). For this reason, it was decided to chose an edge notch instead of a hole notch to conduct this study. This result confirms that CFRP laminates are able to rehabilitate and fix a steel structure damaged by corrosion or by a physical/mechanical effects, and allows the project to continue on dealing with steel angles as truss members.

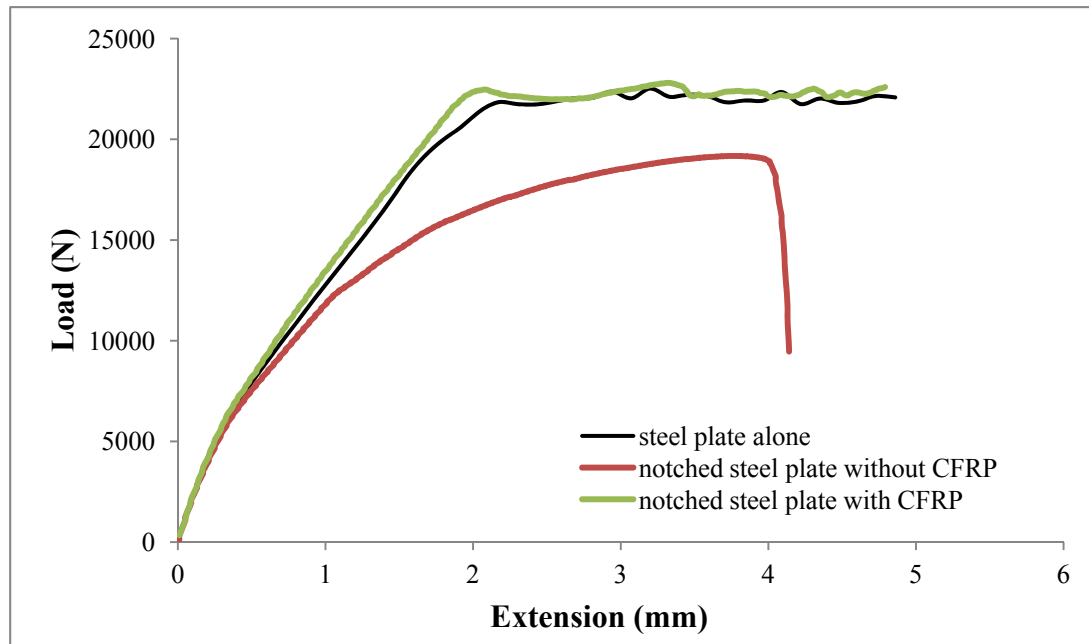


Figure 3.12: Load-extension diagrams for edge notched plate

3.5 Evaluation technique for corroded steel angle

There is a scarcity of information about using CFRP to rehabilitate steel trusses. Steel trusses are affected by weather conditions like other steel structures. Transmission towers, as a type of steel truss, can be affected by many changes in weather patterns like extreme winds and heavy ice (Albermani et al., 2004). As well as the negative effects of standard weather conditions, the high cost of replacement must also be considered. For example, Behncke (2002) reported that, in 2002, it cost over \$30 million to replace 40 km of double circuit line.

This is the motivation for studying the effect of corroded steel truss members strengthened with CFRP. The steel angle shaped truss member was chosen for this study as it is a commonly used. Although angles are common members in truss structures, especially in transmission towers, another factor for choosing angles in this study is to provide new information and new data on tensile and compression tests of steel angles rehabilitated with CFRP.

It is well known that truss members are subjected to tension and compression axial loadings. For tensile testing in this study, each angle specimen, with the dimensions of 25 mm equal legs angle x 3 mm thickness x 350 mm length, was subjected to a tensile test. This angle size was selected because it can be caught by the converted jaws of the machine and the width of the angle was equal to the width of CFRP strip. The first three specimens served as control specimens. The test was done with reference to AS-1391(2007). The CFRP laminate had already been subjected to a tensile test with reference to EN-ISO-527-5(1997) and the elastic modulus was obtained. After that, the steel angle specimens were notched to simulate the corrosion effect. The reduction in the cross-sectional area for notched steel specimens began with a 3 mm edge notch in both angle legs from the edges in the middle length (Figure 3.8 (c)), and then 6 mm and 9 mm up to 12 mm for each leg of the angle. This caused a reduction in the cross-sectional area of the angle from 12.5% for the 3 mm notch and up to 51% for the 12 mm notch which assisted the study of the effect of CFRP on different percentages of steel corrosion and helped to investigate the maximum level of corrosion that can be rehabilitated by this CFRP. These notches were made using the machine mentioned in Section 3.2.2.

The experimental work required a large number of notched angles with different notch sizes. Utilisation of the artificial notch method is suggested in order to deal with this large number of corroded specimens, and also to control the percentage of area reduction. Each notched steel angle was reinforced by two separate CFRP laminates, each one attached separately to the outside edge of the angle legs. Figure 3.13 represents a cross section of reinforced steel angle that shows the method of reinforcement and remaining steel area after the notch while Figure 3.14 shows a picture of a notched steel angle.

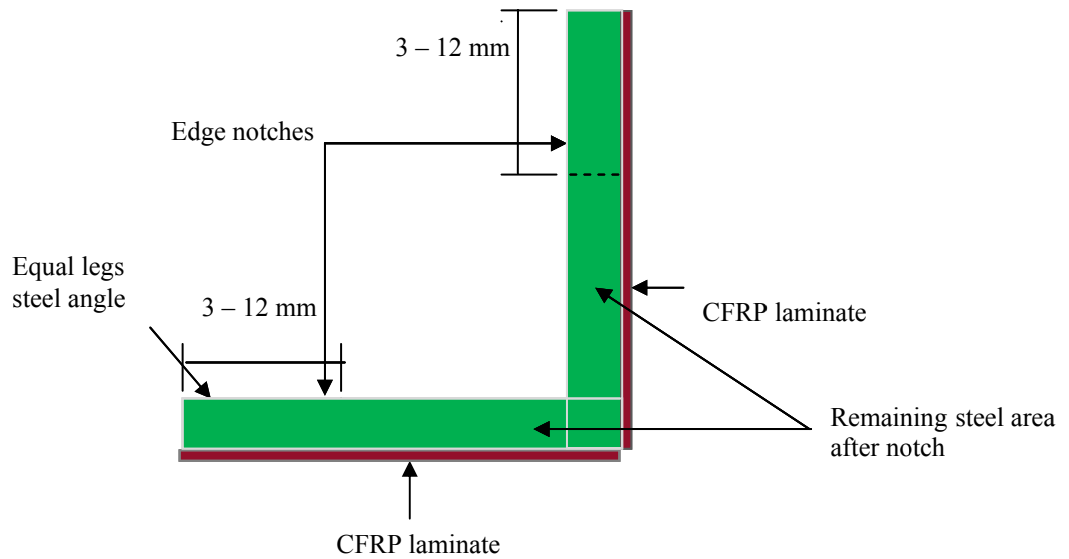


Figure 3.13: Method of reinforcement



Figure 3.14: Notched steel angle

For each size of notch, three CFRP reinforced steel specimens and three with the same notch but without reinforcing, were tested and the average for each three was compared with the average of the three intact specimens (the control). The results show the effect of CFRP on steel samples with different sizes of notches, which represent different percentages of reduction in steel area caused by corrosion.

The width of CFRP laminate was similar to the width of the angle leg. The length of CFRP laminate was calculated based on research carried out by Fawzia et

al. (2006). The research dealt with different bond lengths of normal modulus CFRP to find an effective bond length by testing CFRP/steel double strap joints. The effective bond length of CFRP is a certain value that “beyond which no significant increase in load carrying capacity will occur” (Fawzia et al., 2006). Table 3.6 shows the test results for different bond lengths and Figure 3.15 shows the plotting of ultimate load capacity verses the bond length. According to Figure 3.15, the effective bond length is 75 mm on the each side of the joint which means 75 mm on notch right side and 75 mm on notch left side. Thus, the calculation of CFRP length will be:

Minimum required length for CFRP = 2 x effective bond length + notch width.

CFRP length = 2 x 75 + notch width = 150 mm + notch width.

As the notch width was equal to the thickness of saw blade (approximately 1mm), it was disregarded and the minimum required length for CFRP will be 150 mm.

Table 3.6: Results of different bond length (Fawzia et al., 2006)

Specimen label	Bond length L_1 (mm)	Ultimate load P_{ult} (KN)	Failure mode
SN40	40	49.9	Bond failure
SN50	50	69.8	Bond failure
SN70	70	80.8	Bond failure
SN80	80	81.3	Bond failure

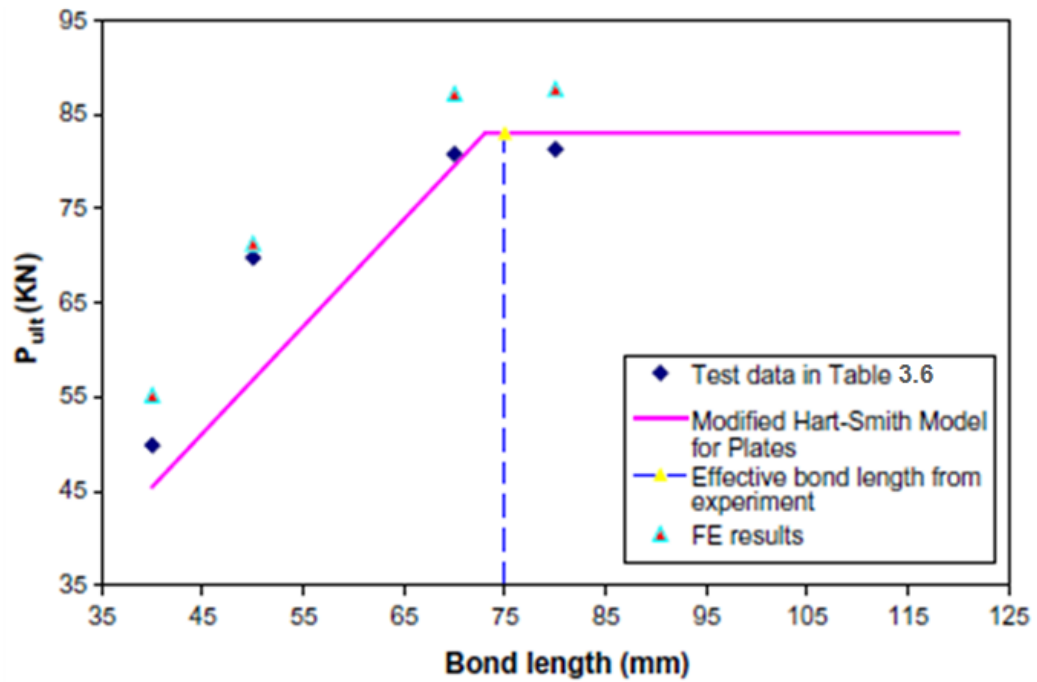


Figure 3.15: Effective bond length for normal modulus CFRP joint (Fawzia et al., 2006)

After cutting CFRP strips to the required length (150 mm), the surfaces of steel angle specimens were prepared by using the electrical machine (mentioned in Section 3.2.2) to remove rust and paint, and to obtain a rough steel surface which was cleaned by Acetone to remove dust. Then, the primer type SWANCOR 984 was used after mixing it with 2% by weight of Methyl Ethyl Ketone Peroxide (MEKP) as a catalyst to start the chemical reaction. Cobalt Naphthenate (CoNap) was also added as a promoter with a ratio from 1/3 to 1/10 of catalyst weight. After that, the primer was left for at least 24 hours at room temperature to complete curing. Sand paper was used to provide enough roughness for the CFRP surface and then the surface was cleaned by Acetone. The CFRP specimen was attached to a steel angle on both outside edges. Finally, the reinforced angular specimens were subjected to a tensile test with reference to AS-1391(2007).

To understand the compression behaviour of corroded steel angles rehabilitated with CFRP, this study focuses on studying compression tests of reinforced specimens, but their lengths are different from those mentioned previously in the tensile tests. The length of the specimens in the compression test must be calculated in such a way that the effect of buckling can be avoided as the failure will occur according to the effect of axial compression load only. In order to achieve this, the Licence Review Manual (Fattaleh, 1984) for steel design mentions that, if the slenderness ratio (KL/r) is less than the value of (C_c), the member will be considered a short compression member and its failure would occur because of compression yielding. Herein, K is Effective Length Factor, L is Length of the specimen, r is Radius of Gyration and C_c is dimensionless constant which is used to compare with the slenderness ratio in order to distinguish between the long and short steel columns. The value of C_c according to this manual is calculated as:

$$C_c = \sqrt{\frac{2\pi^2 E}{F_y}} \quad (3.1)$$

where: F_y =Yield Stress

E = Modulus of Elasticity

The value of K depends on the end conditions of the member. In the test procedure used in this study, the lower end of the angle specimen was placed in the machine on the grooved steel disk shown in Figure 3.5. Then, the load was applied directly to the upper end of the angle. Thus, these ends of the specimen can be considered as pinned ends connection and the value of K for this condition is 1 according to the Licence Review Manual (Fattaleh, 1984). The value of r can be found from tables of steel sections and must be the least radius of gyration of the section (Young and Budynas, 2002). Table 3.7 for steel angle dimension properties

BS-4848-part4 (1972) shows that the value of r for 25x 25x3 mm angles is 0.48 cm for the weak axis. On the basis of r value and in order to find the length of the specimen, the formula of $KL/r < C_c$ will be:

$$1 \times L / 0.48 < C_c$$

$$C_c = \sqrt{\frac{2\pi^2 E}{F_y}}$$

where: F_y = yield load/cross sectional area.

$$F_y = 52125 \text{ kN (from the test)} / 1.42 \text{ (Table 3.7)} = 367 \text{ MPa}$$

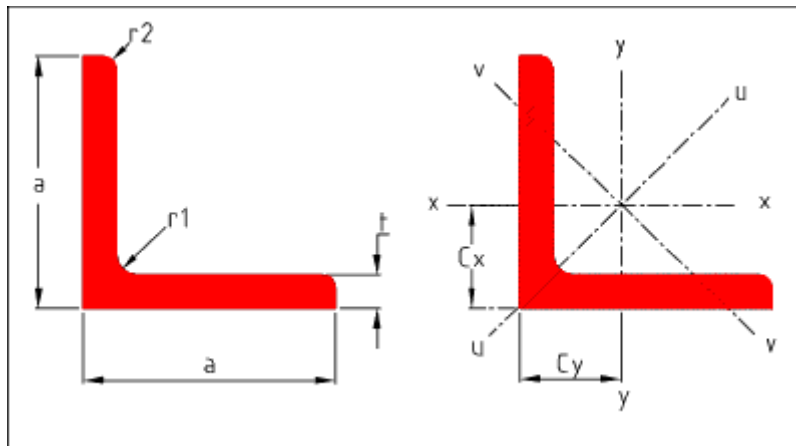
$$E = \text{Modulus of Elasticity} = 272433 \text{ MPa (from the test)}$$

$$\text{So } C_c = 121 \quad \text{and } 1 \times L / 0.48 < 121$$

$$\text{So } L < 58.1 \text{ cm} = 581 \text{ mm}$$

Thus, to avoid the effect of buckling, the length of the angle specimen must be less than 581 mm. It was suggested that the length of angle in the compression test will be 220 mm. The total length of the specimen in compression of 220 mm is considered the gauge length of the specimen because the load in the compression test was applied directly to the specimen without catching by the jaws and at the same time it was equal to the gauge length of the specimen in the tension test (350 mm – 130 mm (each 65 mm to be caught by the upper and lower jaws) = 220 mm). The speed of the testing machine for steel specimens reinforced by CFRP was 3 mm per min. which is between the speed for testing CFRP alone (2 mm per min.) according to EN-ISO-527-5 (1997) and the speed for testing steel alone (6-60 MPas⁻¹ (stress rate)) according to AS-1391(2007).

Table 3.7: Dimension properties for angle sections from British Standard (BS-4848-part4, 1972)



a x a	T	M	r1	r2	A	C of G		Moment Of Inertia			Radius Of Gyration			Z
						Cx, Cy	X-X, Y-Y	U-U	V-V	X-X, Y-Y	U-U	V-V		
mm	mm	kg	mm	mm	cm ²	cm	cm ⁴	cm ⁴	cm ⁴	cm	cm	cm	cm ³	
25 x 25	3	1.11	3,5	2,4	1.42	0.72	0.80	1.26	0.33	0.75	0.94	0.48	0.45	
	4	1.45	3,5	2,4	1.85	0.76	1.01	1.60	0.43	0.74	0.93	0.48	0.58	
	5	1.77	3,5	2,4	2.26	0.80	1.20	1.87	0.52	0.73	0.91	0.48	0.71	
30 x 30	3	1.36	5,0	2,4	1.74	0.84	1.40	2.23	0.58	0.90	1.13	0.58	0.65	
	4	1.78	5,0	2,4	2.27	0.88	1.80	2.85	0.75	0.89	1.12	0.58	0.85	
	5	2.18	5,0	2,4	2.78	0.92	2.16	3.41	0.92	0.88	1.11	0.57	1.04	
40 x 40	4	2.42	6,0	2,4	3.08	1.12	4.47	7.09	1.85	1.21	1.52	0.78	1.55	
	5	2.97	6,0	2,4	3.79	1.16	5.43	8.60	2.26	1.20	1.51	0.77	1.91	
	6	3.52	6,0	2,4	4.48	1.20	6.31	9.98	2.65	1.19	1.49	0.77	2.26	
A x B	T	M	r1	r2	A	C of G		Moment Of Inertia			Radius Of Gyration			Z
mm	mm	kg	mm	mm	cm ²	Cx, Cy	X-X, Y-Y	U-U	V-V	X-X, Y-Y	U-U	V-V	cm ³	

M = Mass per m , A= Depth of Section, B= Width of Section,
 T = Flange Thickness, A = Area of Section, Z = Section Modulus (Elastic Modulus)
 = I/y_{max} x-x & y-y

3.6 Environmental effect on CFRP bonded to steel

3.6.1 Effect of environmental temperature

As the study deals with the rehabilitation of steel trusses, the effect of temperature must be taken into consideration. Two techniques were considered in evaluating the effect of environmental temperature which can be stated as continuous and fluctuating techniques.

In the continuous technique, the service temperature for civil constructions vary within the range of -30° C and + 60° C, depending on the seasons of the year,

geographical site and daily fluctuation (Barkatt, 2001; Jiang and Zhao, 2007). So, it was decided to study the effect of different temperatures from -20°C to $+60^{\circ}\text{C}$ with 40°C increments. Six of notched steel specimens reinforced by CFRP were tested at each temperature, i.e. three for a tensile test and three for a compression test. In other words, the set of three specimens was exposed to each of these temperatures -20°C , 20°C , and 60°C and subjected to a tensile test. Another set of three specimens was tested at same temperatures for compression. . The under zero degrees temperature reflected the effect of freezing while the highest temperature degree $+60^{\circ}\text{C}$ reflected the effect of continuous heating for steel structures in hot climates during the day. The freezer and the oven (see Section 3.2.3) were used for this purpose, and each sample of the six specimens remained under the target temperature for a duration of 24 hours and then the specimens were taken directly from the freezer or the oven to the testing machine.

Regarding the fluctuating technique, a cycle of temperature fluctuations between -20°C and 60°C was considered. Six of the notched steel specimens reinforced by CFRP were put at -20°C for 11 hours, then 1 hour in the laboratory temperature, then 11 hours at 60°C , then 1 hour in the laboratory temperature, and this cycle was repeated for 30 times (over 30 days). This one hour in the laboratory or room temperature allows the gradual transition in temperature between heating and freezing, and the number of cycles depended on the available time for experimental work in the Masters program. After that, the three specimens were subjected to a tensile test and three to a compression test, and the results were compared with those tested at -20°C , 20°C , and 60°C to assess the effect of temperature recycling on them.

3.6.2 *Effect of moisture*

It is necessary to identify the effect of moisture on this rehabilitation technique because it is a significant parameter which can influence the characteristics of the developed system. The worst possible attack of moisture occur when the specimens are immersed in water (Selzer and Friedrich, 1997). This procedure is considered in the current study because it is a technique commonly used to determine the effect of moisture. Yang et al.(2005) studied the moisture effect of each 500 hour period of exposure time starting from 500 hours and ending at 3000 hours. The current study follows the similar procedure to the one suggested by Yang et al. (2005), but up to 2000 hours because it is suitable for the period of experimental work in the Masters program.

Thus, twenty four notched steel specimens reinforced by CFRP were immersed in tap water for different durations up to 2000 hrs with increments of 500 hrs. Figure 3.16 shows the deteriorated samples after 1000 hrs under water. After the immersing procedure, the samples were collected and mechanical testing (tensile and compression) were performed.



Figure 3.16: Angle specimens after 1000 hours under water

3.7 Summary

After providing the required details about the selected materials and their preparation and testing, Tables 3.8 and 3.9 summarise the program plan and the numbers of specimens which were tested in each of the tensile and compression tests.

Table 3.8 Numbers of specimens required for tensile test

Tensile test			
	Steel control specimens S	Steel + notch + CFRP S+N+C	Steel + notch only S+N
Steel angle samples to study corrosion effect	3 specimens of steel angles alone	3 specimens of 3 mm notch + CFRP	3 specimens of 3 mm notch
		3 specimens of 6 mm notch + CFRP	3 specimens of 6 mm notch
		3 specimens of 9 mm notch + CFRP	3 specimens of 9 mm notch
		3 specimens of 12 mm notch + CFRP	3 specimens of 12 mm notch
Steel angle samples to study temperature effect	9 mm notch was chosen to study temperature effect		
	At -20° C temperature	3 specimens of 9 mm notch + CFRP	
	At 20° C temperature	3 specimens of 9 mm notch + CFRP	
	At 60° C temperature	3 specimens of 9 mm notch + CFRP	
	Recycle the specimens between -20 °C and 60 °C	3 specimens of 9 mm notch + CFRP	
Steel angle samples to study moisture effect	9mm notch is chosen to study moisture effect		
	3 specimens at 500 hours	3 specimens of 9 mm notch + CFRP	
	3 specimens at 1000 hours	3 specimens of 9 mm notch + CFRP	
	3 specimens at 1500 hours	3 specimens of 9 mm notch + CFRP	
	3 specimens at 2000 hours	3 specimens of 9 mm notch + CFRP	

Table 3.9 Numbers of specimens required for compression test

Compression test			
Steel angle samples to study corrosion effect	9 mm notch is chosen to study corrosion effect		
	Steel control specimens Steel + notch only S+N	Steel + notch + CFRP S+N+C	
	3 specimens of 9 mm notch	3 specimens of 9 mm notch + CFRP	
Steel angle samples to study temperature effect	9 mm notch is chosen to study temperature effect		
	At -20° C temperature	3 specimens of 9 mm notch + CFRP	
	At 20° C temperature	3 specimens of 9 mm notch + CFRP	
	At 60° C temperature	3 specimens of 9 mm notch + CFRP	
	Recycle the specimens between -20 °C and 60 °C	3 specimens of 9 mm notch + CFRP	
Steel angle samples to study moisture effect	9 mm notch is chosen to study moisture effect		
	At 500 hours	3 specimens of 9 mm notch + CFRP	
	At 1000 hours	3 specimens of 9 mm notch + CFRP	
	At 1500 hours	3 specimens of 9 mm notch + CFRP	
	At 2000 hours	3 specimens of 9 mm notch + CFRP	

Chapter Four

Results and discussions

4.1 Introduction

In this chapter, the experimental results are presented and evaluated. A comparison of the results obtained of the steel angle specimens with and without the CFRP reinforcement is included. Both tensile and compressive properties of the tested specimens are also included.

4.2 Tensile characteristics of the rehabilitated steel

This section includes the results of all specimens subjected to tensile testing in order to find the effect of corrosion, temperature and moisture on rehabilitated steel members.

4.2.1 *Influence of corrosion*

4.2.1.1 *Effect of notch sizes on steel alone without CFRP*

Before discussing the reinforcement character of the CFRP laminates on the notched steel members, it is necessary to mention the effect of different notch sizes cut into the steel plates without any CFRP reinforcement. Figure 4.1 shows the results obtained in load-extension of four steel specimens which are notched longitudinally in the middle span of the angle legs from 3 mm up to 12 mm and for comparison also the load-extension diagram of a control specimen (without notch). It is important to mention that the preliminary tests on steel plates (Figures 3.11 and 3.12) which proved that the particular effects of the notch on the mechanical

properties of the steel panels depend not only of the length of the notch but also on the particular shape of the notch. For the notch with a circular or edge shape, the effects will change due to different distribution of forces and stresses within the steel specimens.

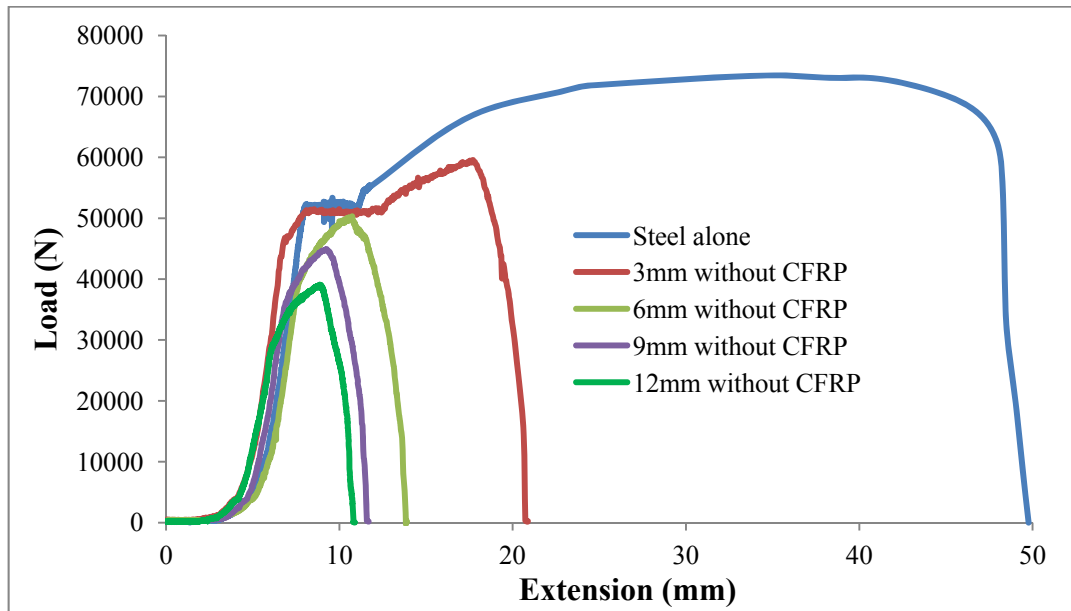


Figure 4.1: Load-extension diagrams for control and notched specimens without CFRP

Figure 4.1 clearly shows the relationship between notch size and the ultimate load. As expected, the ultimate tensile load decreases with the increasing size of the notch. The obvious effect of the edge notch appears to reduce the hardening zone which translates to a decrease in ductility of the steel sample. Also, the edge notch affected the difference between ultimate and yield loads, while the difference ratio between them was about 41% in the control specimen. For the 3 mm notch this ratio was reduced to about 32% and to 31% for 6 mm notched specimens.

This difference in ratio began to increase sharply for specimens notched at 9 mm, and 12 mm to about 51% for the last one. These aspects of load behaviour

between the control and notched specimens can be attributed to the distribution of load through the notched area which mainly depends on the size of the notch. Table 4.1 shows the differences between the ultimate and yield loads affected by edge notch.

Table 4.1: Differences between ultimate and yield loads affected by edge notch

Sample	Yield Load (N)	Ultimate Load (N)	Difference between ultimate and yield loads (N)	Difference ratio
Average of Steel alone	52125	73521	21395	41%
Average of steel 3 mm notch	45803	60608	14805	32%
Average of steel 6 mm notch	39133	51222	12089	31%
Average of steel 9 mm notch	32311	45321	13009	40%
Average of steel 12 mm notch	25836	39128	13292	51%

4.2.1.2 Effect of notch sizes on steel attached with CFRP

Figure 4.2 shows the effect of CFRP on the load-extension diagram for the 3mm notch sample compared with sample without CFRP and both are compared with the control sample. Figure 4.2 demonstrates that the CFRP layers increased the average ultimate load (4.6%) and the average yield load (14%) in comparison with the steel specimen without CFRP. In addition to this, there was an increase in ductility. There is a similarity between these results and the experimental work of Zhao et al. (2006) who also found increasing in strength and ductile behaviour (see Figure 2.6 (b)).

For all three tested specimens of a 3mm notch with CFRP, the delamination of CFRP layers occurred after the yielding point which delayed the occurrence of yielding to a point or to a load higher than the yield load in the specimens without CFRP and consequently resulted in a higher ultimate stress load than the specimens without CFRP reinforcement. A similar mechanical behaviour was observed for the 6 mm and 9 mm notched reinforced specimens. Figures 4.3 and 4.4 show the effect of CFRP on the load-extension diagram for the 6 mm and 9 mm notched samples compared with those without CFRP and with the control sample. To summarise, the delaminating behaviour of steel samples reinforced with CFRP and with 3, 6 and 9 mm notches were similar because delamination occurred after the yield point of steel and before the ultimate load of the specimens.

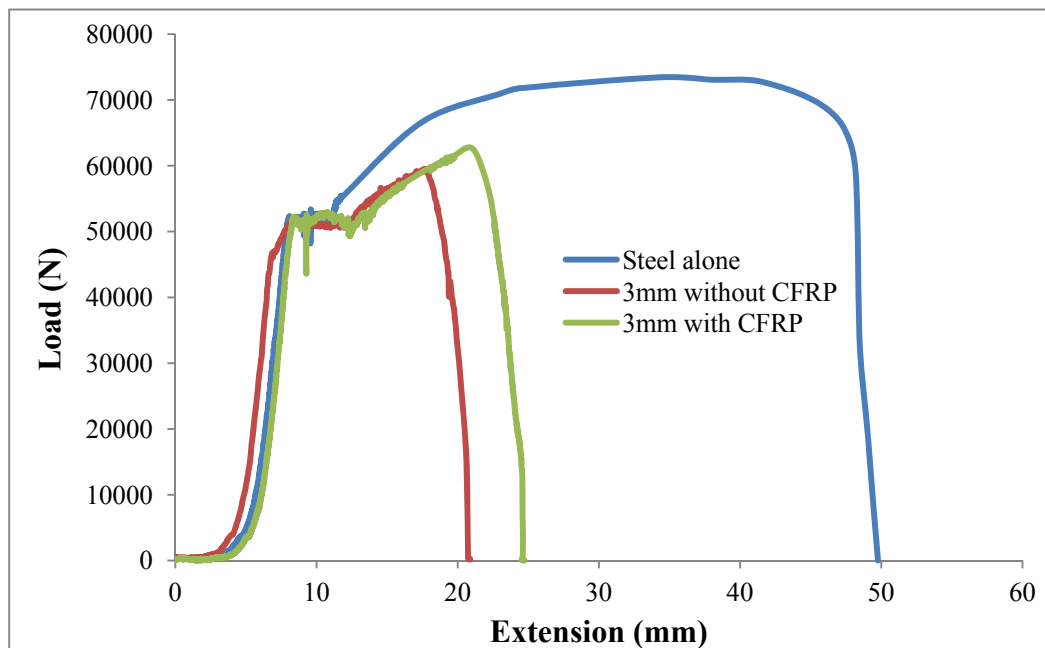


Figure 4.2: Effect of CFRP on load-extension diagram for 3mm notch specimen

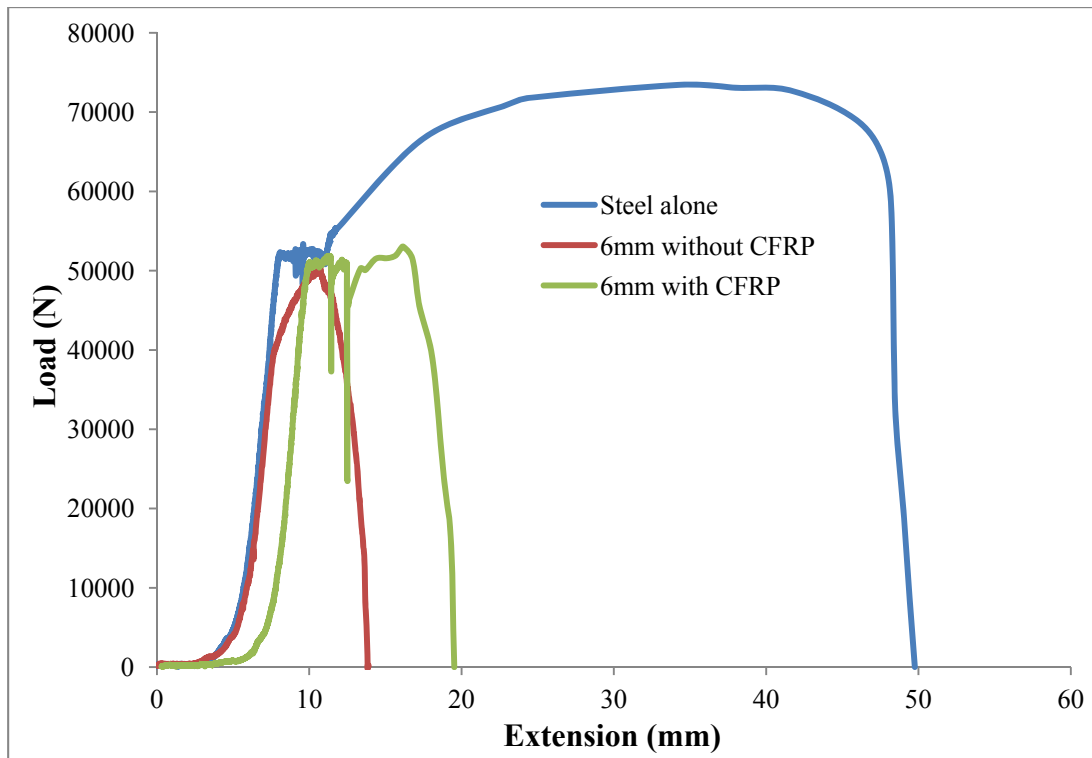


Figure 4.3: Effect of CFRP on load-extension diagram for 6 mm notch specimen

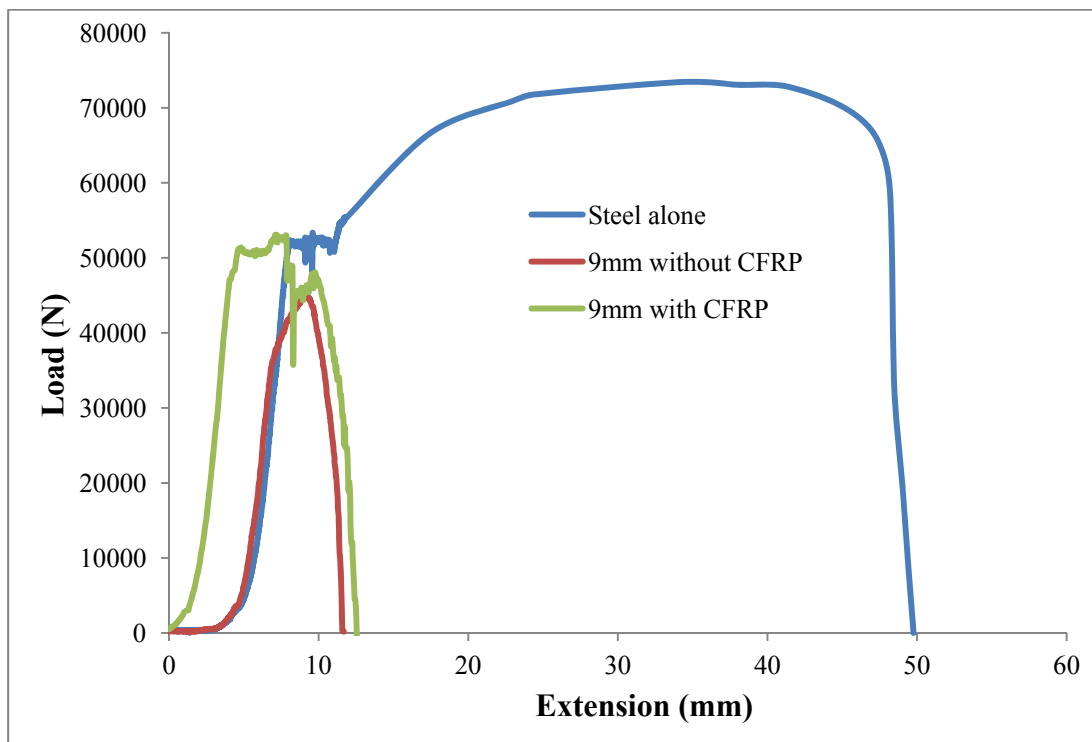


Figure 4.4: Effect of CFRP on load-extension diagram for 9 mm notch specimen

In contrast, a different load behaviour was found during the test of the specimens with 12 mm notches and reinforced with CFRP (see Figure 4.5).

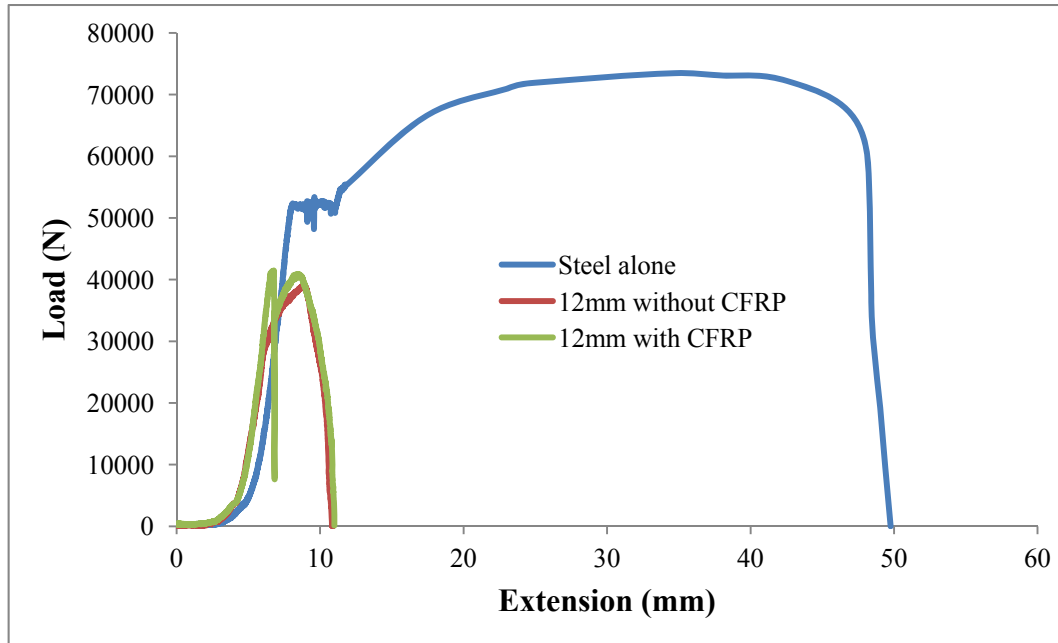


Figure 4.5: Load behavior of 12 mm notch specimen with and without CFRP and of the original steel specimen

Through the test of 12 mm notched reinforced specimen (Figure 4.5), it was observed that the initial load was taken by steel and the CFRP together and as the load continue increasing the delamination of the CFRP and the ultimate load took place simultaneously at the point where previous samples (with 3 to 9 mm notch) reached just the yield load point. This indicates that the samples with the 12 mm notch and the CFRP reinforcement behaved like brittle material when there is no real yielding point, or in another words, the yield point of steel cannot be easily determined as the CFRP helped in increasing the load linearly up to the ultimate load. In such cases and in order to know where the yield of steel occurred, the stress-strain diagrams are required for the motioned specimen and the original one. Figures

4.6 and 4.7 show stress-strain diagrams for the original sample and the 12 mm notch sample with CFRP specimen respectively.

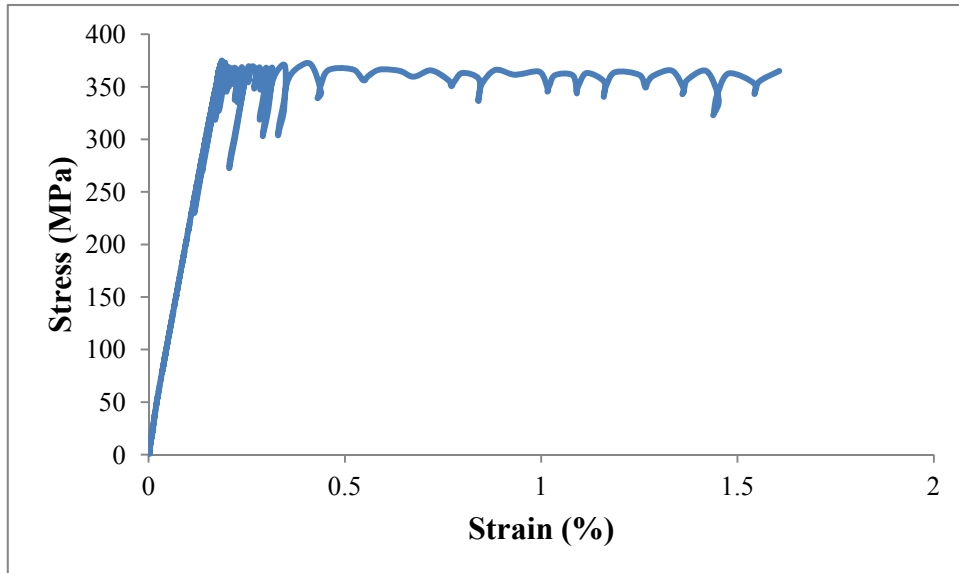


Figure 4.6: Stress-strain diagram for the original sample

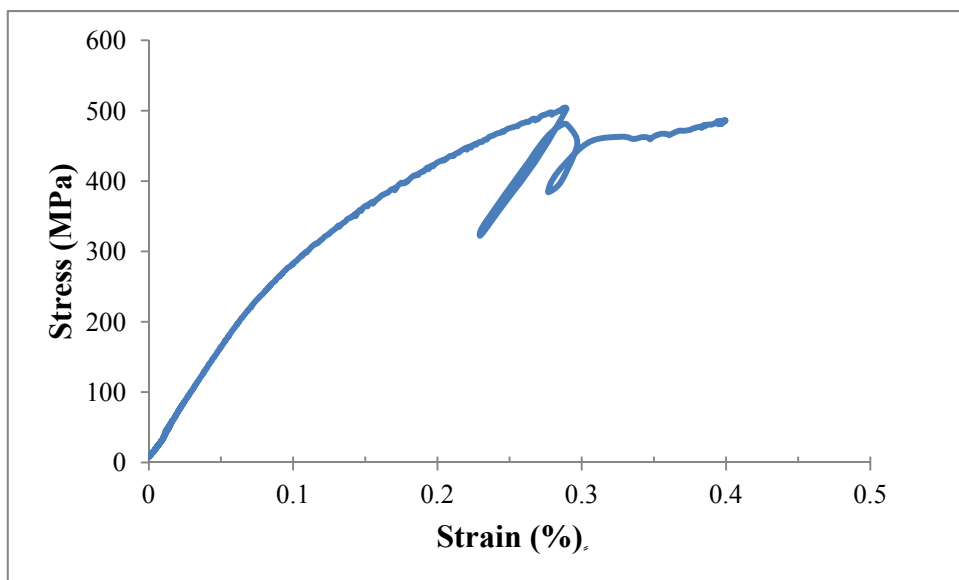


Figure 4.7: Stress-strain diagram for 12 mm notch with CFRP specimen

Figure 4.6 shows that the yield point of the initial steel sample takes place at strain about (0.18 %) or (0.0018), while Figure 4.7 shows that the delaminating of the CFRP of the 12 mm notch with CFRP specimen occurred approximately at strain about (0.29 %) or (0.0029). That means the yield of steel for 12 mm notched rehabilitated specimen happened before delaminating of CFRP and the maximum load noticed in the load-extension plot was the ultimate load of the sample. The strain gauge was attached to CFRP strip as shown in Figure 4.8. In Figure 4.7 the yield stress for 12 mm notched rehabilitated sample can be found at the strain value of 0.18% (about 400 MPa) and as the equivalent area was known, then the yield load was found to be 35456 N. Table 4.2 shows the yield stress values, delaminating occurrence and ultimate loads for all notched specimens with CFRP.



Figure 4.8: Attaching of strain gauge to CFRP strip

Table 4.2: Yield load, delaminating occurrence and ultimate loads for reinforced samples

Sample	Yield load (N)	Delaminating occurrence	Ultimate load (N)
Average of Steel alone	52125		73521
Average of 3 mm with CFRP	52268	Before the ultimate load.	63377
Average of 6 mm with CFRP	51856		53646
Average of 9 mm with CFRP	47133		53077
Average of 12 mm with CFRP	35456	At the ultimate load.	42898

Table 4.3 shows the increases in yield and ultimate loads for rehabilitated notched specimens compared with those without CFRP at the same notch. Based on the values presented in Table 4.3, the Figures 4.9 and 4.10 have been drawn. The results regarding the improvement of load carrying capacities agreed with previous research (Gillespie et al., 1996; Liu et al., 2001; Tavakkolizadeh and Saadatmanesh, 2001).

Table 4.3: Load increments for rehabilitated notched specimens

Sample	Yield load (N)			Ultimate load (N)		
	without CFRP	With CFRP	Increasing ratio %	without CFRP	With CFRP	Increasing ratio %
Average of Steel alone	52125			73520		
Average of 3mm notch	45803	52268	14.11	60608	63377	4.56
Average of 6mm notch	39133	51856	32.51	51222	53646	4.73
Average of 9mm notch	32311	47133	45.86	45321	53077	17.11
Average of 12mm notch	25836	35456	37.23	39128	42898	9.63

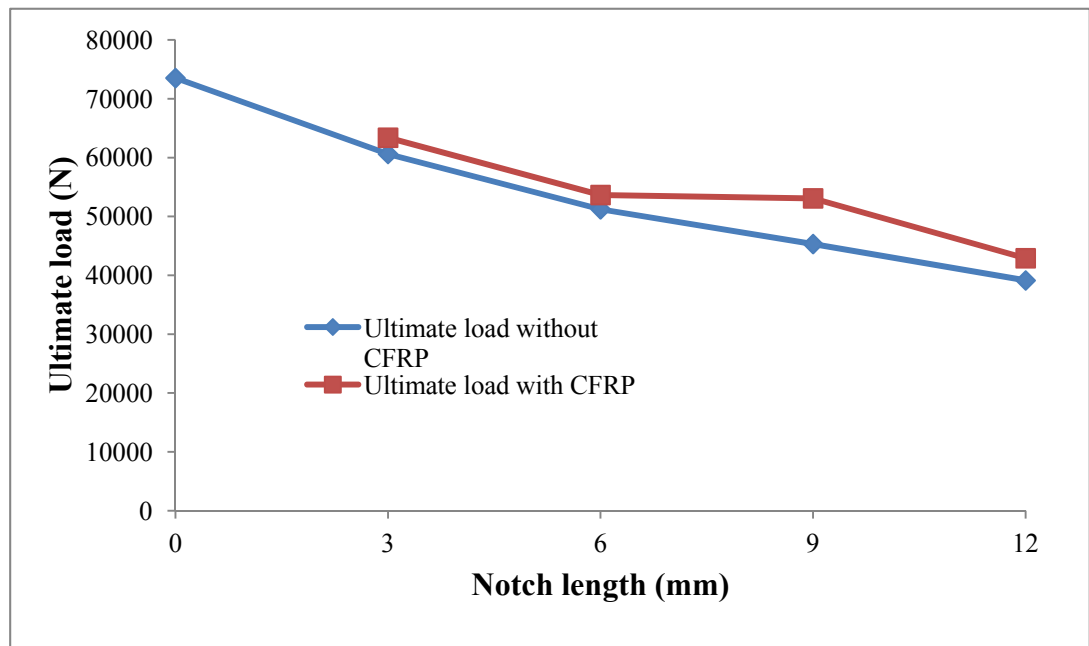


Figure 4.9: Increase in ultimate loads for rehabilitated notched samples

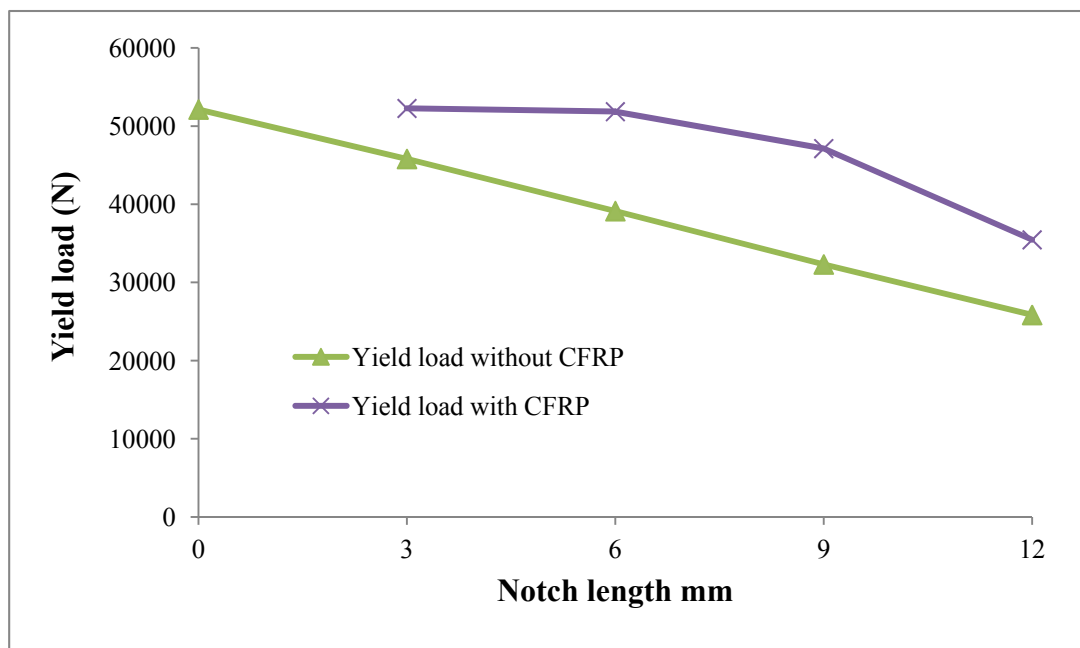


Figure 4.10: Increase in yield loads for rehabilitated notched samples

The Figures 4.9 and 4.10 demonstrate that attaching CFRP was still working up to the 9 mm notch or a corrosion percentage of about 38% where the maximum

increments in yield and ultimate loads were recorded compared with those without reinforcement. At 50% of corrosion or at the 12 mm notch, the steel overtook the elastic stage and stress-strain diagram was required to determine the yield stress which keeps the structure within the elastic strain.

It is necessary to find the equivalent area for specimens with CFRP so stress can be calculated. The required equivalent area can be found as follows:

$A_{s\ eq.} = A_s + A_c * (E_c/E_s) = A_s + 40.64\ mm^2\ (2\ layers\ of\ 0.8 * 25.4) * (125000\ MPa / 272433\ MPa)$ (Tables 3.1, 3.2 and 3.3 in Ch. 3).

$$A_{s\ eq.} = A_s + 40.64\ mm^2 * 0.4588 = A_s + 18.64\ mm^2 \dots\dots\dots (4.1)$$

Where:

$A_{s\ eq.}$ = equivalent area of steel,

A_s = Area of steel,

A_c = Area of CFRP,

E_s = Elastic modulus of steel, and

E_c = Elastic modulus of CFRP.

The above equation has been used to calculate the yield stresses for notched rehabilitated specimens based on their yielding loads and equivalent areas. The calculation here focused on yield stress because it is considered the most significant design factor in designing of steel trusses. Table 4.4 explains these calculations for notched samples rehabilitated by CFRP, while Figure 4.11 shows the relationship between the percent of carbon to steel area for notched reinforced specimens and yield stress.

Table 4.4: Equivalent area and yield stress for rehabilitated samples

Sample	As eq. mm ²	Yield load (N)	Yield stress (MPa)	Area Steel mm ²	Area CFRP mm ²	R ⁽¹⁾ %	R ⁽²⁾ %	Corrosion % ⁽³⁾
Average of Steel alone	142	52125	367	142	0	0	100	0
Average of 3 mm with CFRP	142.64	52268	366	124	40.64	33	87.32	12.68
Average of 6 mm with CFRP	124.64	51856	416	106	40.64	38	74.64	25.36
Average of 9 mm with CFRP	106.64	47133	442	88	40.64	46	61.97	38.03
Average of 12 mm with CFRP	88.64	35456	400	70	40.64	58	49.29	50.71

R⁽¹⁾ = 100* Ratio of areas: CFRP/steel

R⁽²⁾ = 100* Ratio of remaining areas of steel after notch/initial area of steel

⁽³⁾. Corrosion % = 100 - R⁽²⁾

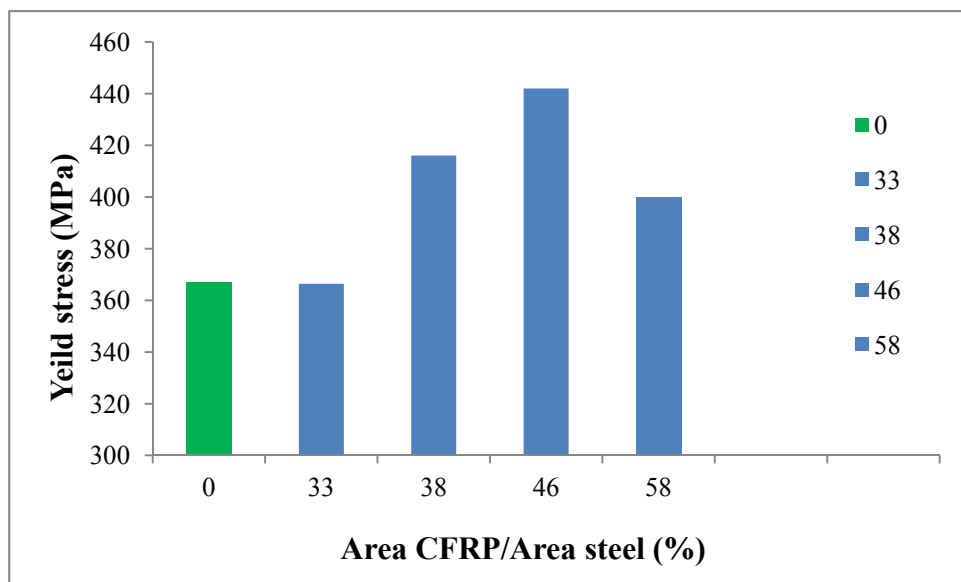


Figure 4.11: Relationship between percentage of CFRP to steel area for notched reinforced specimens and yield stress (from 3 to 12 mm notch, blue colour)

Figure 4.12 shows the increments obtained in stress by increasing the ratio of CFRP to corroded steel based on their cross sectional areas at the notch section. It was noticed that the sample of 3mm notch or 33% ($R^{(1)}$) recorded approximately the same yield stress as the original sample (green colour in Figure 4.11), when it was expected to record more than that value. At 6 mm and 9 mm notches or at 38% and 46% ($R^{(1)}$), the increase in yield stress was about 13.4% and 20.4% of the original yield respectively. When the area of CFRP to the remaining area of steel was about 58% ($R^{(1)}$), the steel member passed the elastic strain to plastic strain at ultimate stress while the yield stress was found through a stress-strain diagram in order to keep the corroded steel member within the allowable elastic zone.

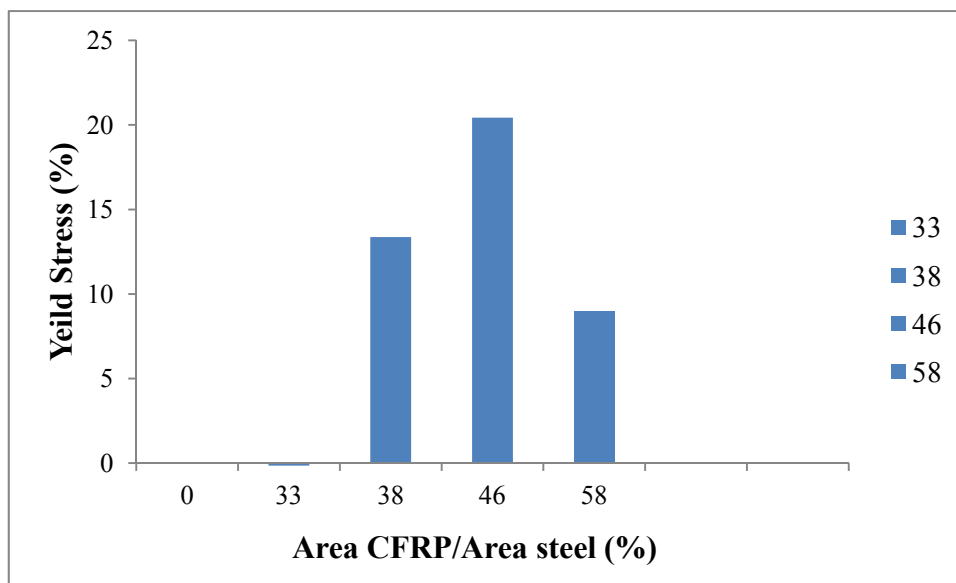


Figure 4.12: Stress increments by increasing the ratio of carbon to corroded steel

Therefore, the best use of this type of CFRP was when the percentage of CFRP area to remaining steel area after corrosion ($R^{(1)}$) is about 46% ,or in another words, when the amount of carbon area (40.64 mm^2) was attached to the corroded steel within 38% of corrosion (9 mm notched steel sample).

4.2.2 *Effect of environmental temperature*

Section 4.1.1 focused on yield and ultimate stresses because the comparison was between notched reinforced and notched non-reinforced specimens and the control sample. The control sample was the intact one which had a total cross-sectional area of steel, while the affected samples had different cross-sectional areas of steel. In Sections 4.1.2 and 4.1.3, all samples were chosen from the type of notched reinforced specimens and the notch of (9 mm) was chosen. The stress of the control sample (9 mm notched reinforced sample) has already been discussed in section 4.1.1, where the control was compared with samples when subjected to different temperature and moisture conditions (Table 3.8). The study focused on ultimate stress as it sought to determine the effect of environmental conditions on rehabilitation processes.

The general behaviour of loads carrying was approximately the same for all specimens under the different temperatures. Figures 4.13 and 4.14 show two examples of load-extension graphs for two specimens under -20 °C and 60 °C temperatures, respectively. These two Figures (4.13 and 4.14) confirm that in the first stage the load was carried by the steel and the two layers of the CFRP up to the yield point, then there was the delamination of the first layer of CFRP, which caused the sudden drop of load in the curves. Even after this point the specimens, area of steel and the second layer of the CFRP, were still carrying load. A second delamination of the remaining CFRP caused the second drop in the load curve. Then, the load was carried only by the remaining area of steel which gradually dropped down to the point of specimen failure.

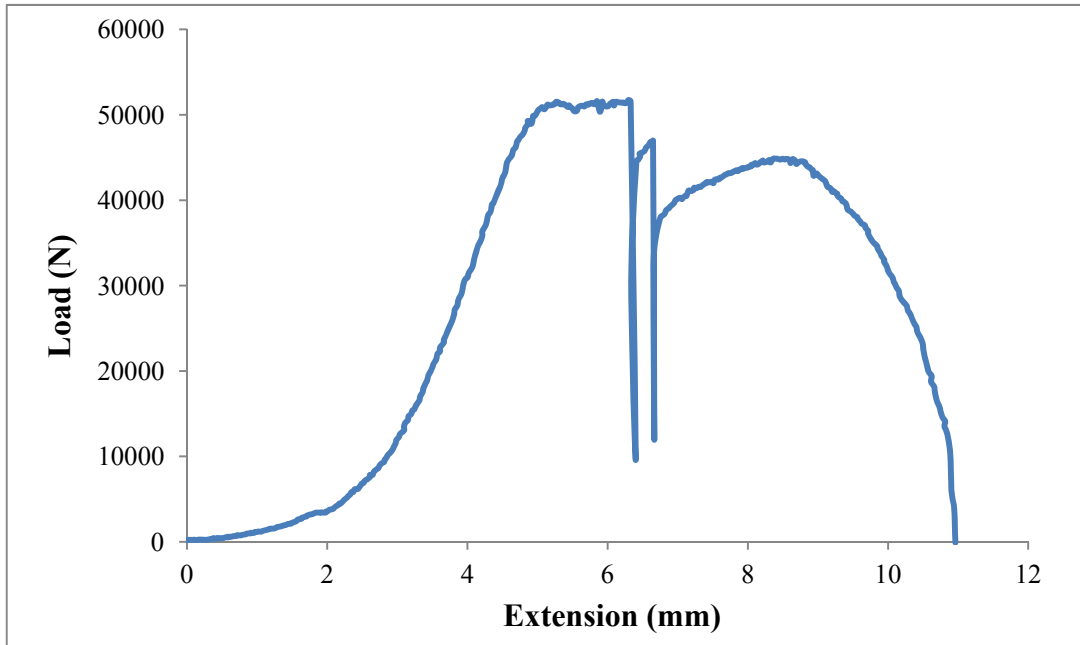


Figure 4.13: Load-extension graph for the specimen at -20° C

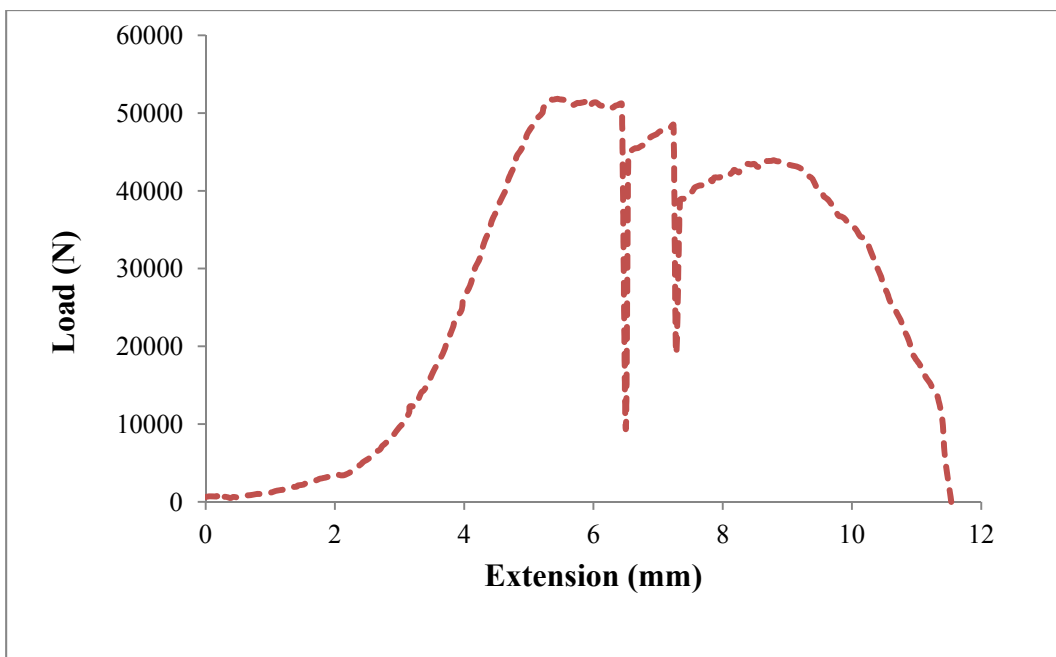


Figure 4.14: Load-extension graph for the specimen at 60° C

According to the program plan mentioned in Table 3.8, the tensile tests included the testing three of 9 mm notched reinforced specimens under each one of

these temperatures (-20°C , 20°C , 60°C , recycle of -20°C and 60°C) for 24 hours. The average for each of the three specimens under the target temperature was compared with the control sample. Figure 4.15 shows the comparison of average ultimate stresses with different temperatures. The ultimate stresses were calculated based on the ultimate loads and equivalent areas (As-eq.).

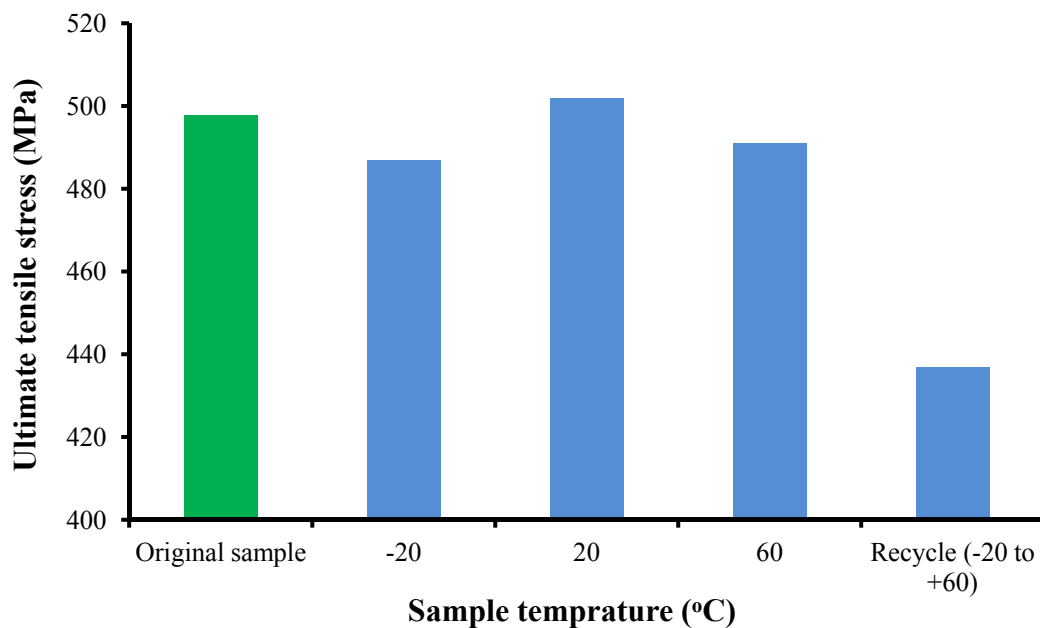


Figure 4.15: Average ultimate stresses with different temperatures

It can be seen from Figure 4.15, that the maximum tensile stress for both the original and the $+20^{\circ}\text{C}$ samples were the highest and very close to each other because 20°C temperature is very close to room temperature which makes the effect of temperature on the ultimate stress value minimal. The ultimate stress for samples at 60°C was a little more than that of sample at -20°C and both were less than the original sample by about 1.4% and 2.2% respectively. The lowest ultimate stress was for samples under recycle between -20°C and 60°C which was 13.9% less than the original sample. This happens because freeze-thaw cycles can lead to accelerated

degradation and that under zero temperature hardening and micro cracking of the composite can happen, then bond degradation occurs (Karbhari et al., 2003). Also, as the cycle of temperature aims to find the effect of temperature fluctuations, it must extend across suitable period of time which was 30 days in this study. The other samples were subjected to target temperatures for just 24 hours so they experienced the required temperature effects.

4.2.3 *Effect of moisture*

According to the program plan mentioned in Table 3.8, three of the 9 mm notched reinforced specimens were immersed for different lengths of time (from 500 hours to 2000 hours). The average for each three specimens at the target time was compared with the control sample which was tested at laboratory conditions and was seen to not be affected by moisture. Table 4.5 shows the results of the ultimate tensile stress for 9 mm notched rehabilitated samples compared with the original sample, and the ultimate stresses were calculated based on the ultimate loads and equivalent areas (A_s -eq.).

Table 4.5: Effect of moisture on ultimate tensile stress

Time under water (hrs.)	Ultimate tensile stress (MPa)	Reduction in ultimate tensile stress %
(Original specimen)	497.7	
500	489.1	1.76
1000	484.5	2.73
1500	478.8	3.95
2000	465.5	6.92

As the number of immersion hours increased, there was a gradual reduction in ultimate tensile stress. The reduction recorded small values particularly between 500

and 1500 hours, and after that the reduction rate increased with the lasting time recording a maximum value about 6.92% at 2000 hours compared with original sample. Smith et al.(2005) found a similar general effect of moisture exposure leading to a reduction of strength. Also, Karbhari et al. (2003) reported that the effect of long-term moisture exposure under certain conditions may cause degradation and decrease in the load carrying capacity. Figure 4.16 shows the effect of moisture on the ultimate tensile stress value of the samples.

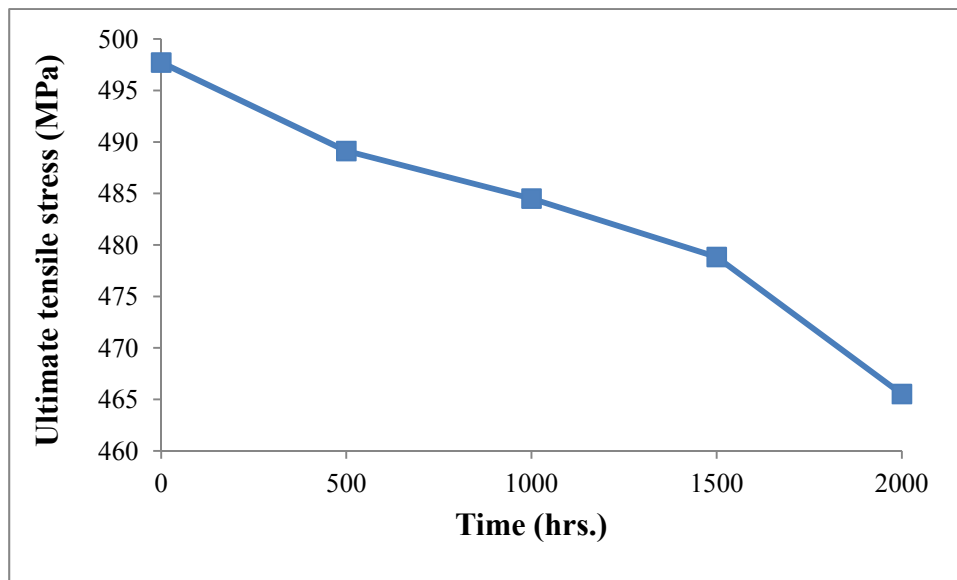


Figure 4.16: Moisture effect on ultimate tensile stress

4.2.4 Finite Element Model for notched reinforced tensile member

The Strand 7 program was used to develop a finite element model for the 9 mm notched rehabilitated specimen used in tensile test. The dimensions of this FE model were (25 mm equal legs angle x 3 mm thickness x 350 mm length) with a 9 mm edge notch in the middle length of the specimen. The tensile load was applied in the X direction which represented the length of the specimen, while Y was the width direction and Z was the thickness direction. The dimensions of modelling CFRP

laminates were (0.8 mm thickness x 25.4 mm width x 150 mm length) and it was assumed that a perfect bond was formed in between the CFRP layer and the steel. To represent the experimental tensile sample, a fixed boundary condition was selected and the load was applied to other end as per the following Figure 4.17.

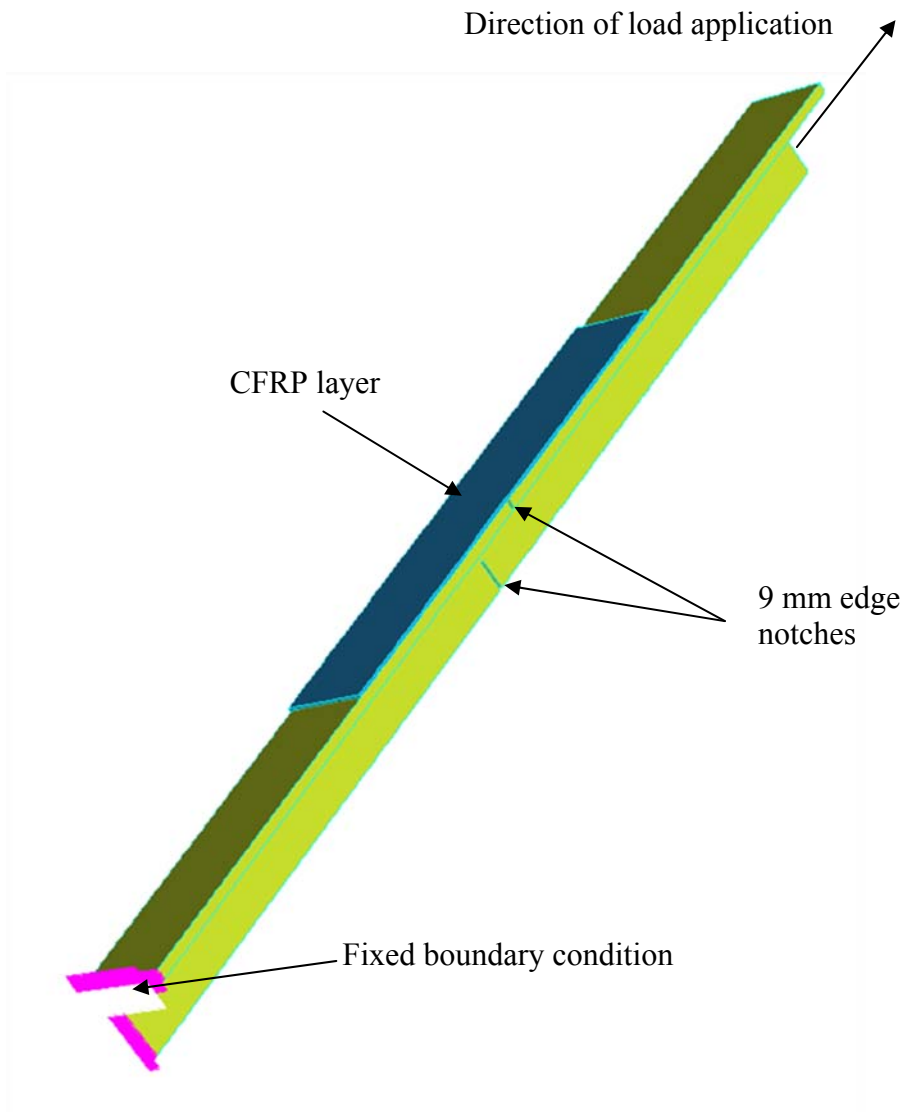


Figure 4.17: The mesh used for the FEA

The model was subjected to a 40 kN tensile load, and the values of strain on the CFRP surface were taken to compare with the values of strain of the CFRP strip recorded by the strain gauge attached to the specimen. Figure 4.18 shows a picture

that has been taken from the middle of the model. The picture presents the distribution of strain on the CFRP strip at the notch area.

As the strain gauge was attached to the surface of the CFRP strip (see Figure 4.8), it was necessary to choose points from the FE model which represent the strain on the same position of the strain gauge. These points were GP3, GP4, GP7 and GP8. The average reading of the points (GP3, GP4, GP7 and GP8), which are on the surface of the element, can be compared with the experimental strain reading provided by the strain gauge at approximately 40 kN load. This comparison is shown in Table 4.6. The strain dialogue box was enlarged, as shown in Figure 4.19, and the strain values of the mentioned points were conformed to the reading of the strain gauge.

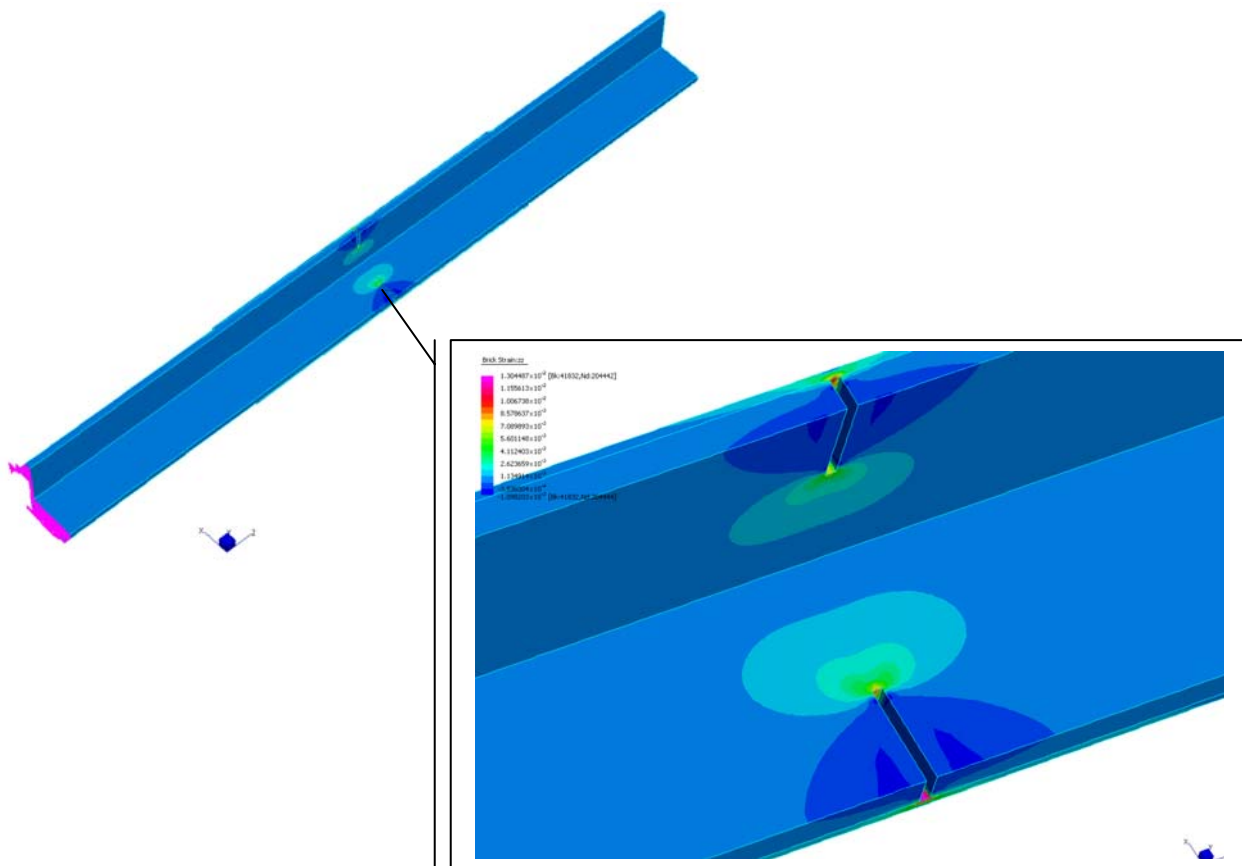


Figure 4.18: Strain distribution (FE model)

Table 4.6: Readings provided by strain gauge at 40 kN

Load (N)	Strain *10 ⁻³
39937	1.439 (Experimental)
Surface point GP3	1.450
Surface point GP4	1.418
Surface point GP7	1.450
Surface point GP8	1.418
Average of GP3, GP4, GP7 and GP8	1.434 (FE)

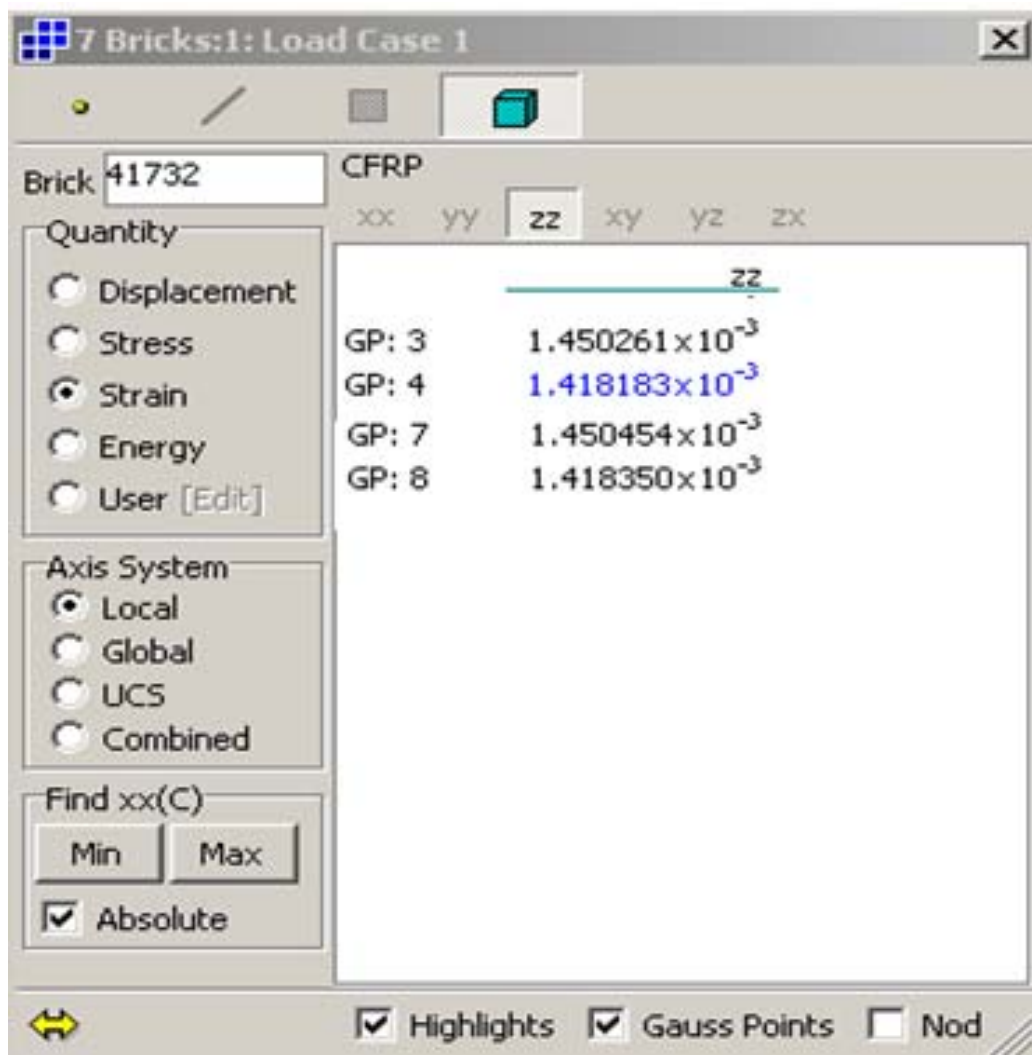


Figure 4.19: Enlarged view of the strain dialog box

4.3 Compressive characteristics of the rehabilitated steel

This section includes the results of all specimens subjected to compression test in order to find the effect of corrosion, temperature and moisture on rehabilitated steel members.

4.3.1 Influence of notch sizes

According to the plan mentioned in Table 3.9, a comparison of compression tests was made between the 9 mm notched sample and 9 mm notched reinforced sample. The 9 mm notched sample reinforced by CFRP was considered as an original (control) sample to compare later with those samples subjected to temperature and moisture effects. Figure 4.20 shows load-extension diagrams in the compression test for 9 mm notch samples with and without CFRP.

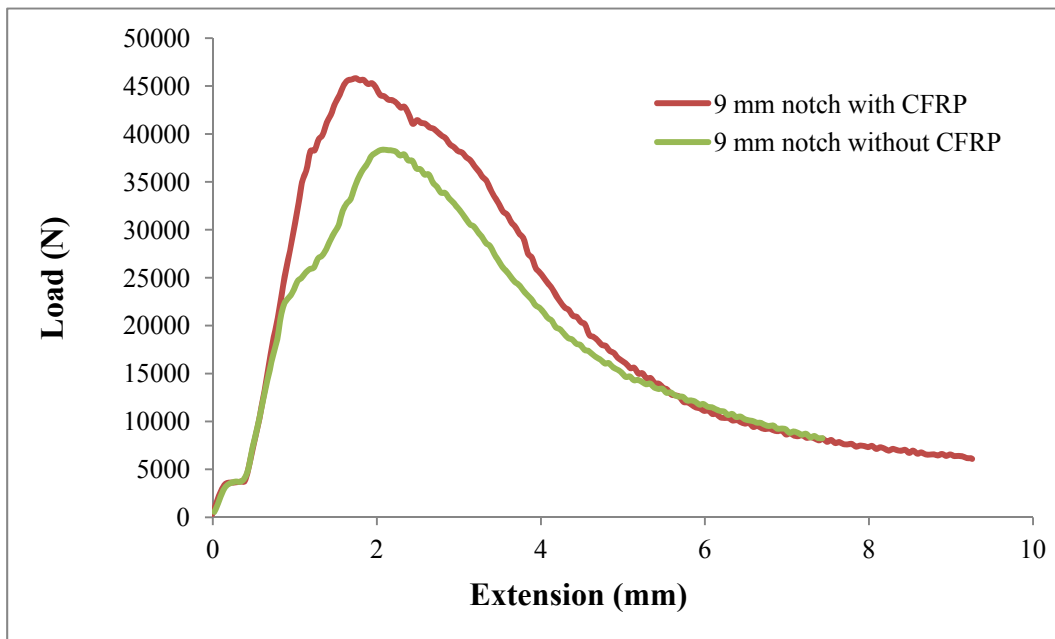


Figure 4.20: Compression load-extension diagrams for 9 mm notched samples with and without CFRP

The average ultimate compression load for the three notched specimens without CFRP was 36010 (N), while the average for those specimens with CFRP was 48280 (N). The ultimate compression stress was calculated depending on the steel area at notched section (88 mm^2) for specimens without CFRP and on an equivalent area at notched section (106.64 mm^2) for specimens with CFRP. Figure 4.21 shows the ultimate compression stresses for 9 mm notched samples with and without CFRP. It can be seen that the carbon increased the ultimate compression stress by about 10.63% compared with sample without CFRP. The positive effect of CFRP in the compression test showed agreement with the results of Shaat and Fam (2009), Ekiz and El-Tawil (2006) and Silvestre et al. (2008) regarding the increase in load carrying capacities.

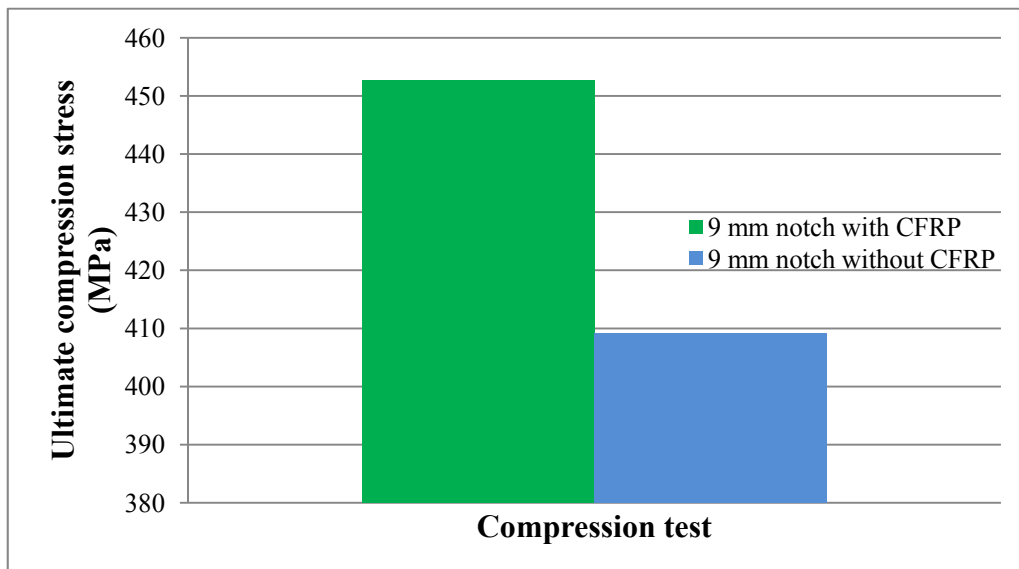


Figure 4.21: Ultimate compression stresses for 9 mm notched samples with and without CFRP

4.3.2 Effect of environmental temperature

According to the program plan mentioned in Table 3.9, the compression tests included testing three of the 9 mm notched reinforced specimens under each one of

these temperatures (-20° C, 20° C, 60° C, recycle of -20° C and 60° C) for 24 hours. The average for each of the three specimens under the target temperature was compared with the original sample (at laboratory temperature). The results of these samples and the original sample are shown in Table 4.7.

Table 4.7: Ultimate stresses in compression test

Sample type	Ultimate compression stress (MPa)
Original sample	452.7
Sample at -20° C	456.5
Sample at 20° C	457.2
Sample at 60° C	456
Recycle (-20° C to 60° C)	421.9

It was noticed that the ultimate compression stress for specimens subjected to (-20° C, 20° C and 60° C) were approximately the same, and so the difference between them can be disregarded. Hence, the results of temperature in the compression test did not present a remarkable effect between them or compared with the original sample under the laboratory temperature. However, the sample subjected to recycle between -20° C and 60° C was the lowest, at about 7.3% less than the original sample. The explanation used for the effect of recycle temperature on the tensile test also applies in compression (Karbhari et al., 2003) and exposure time (30 days) under recycle temperature. Figure 4.22 shows ultimate compression stresses under different temperatures and the original sample under laboratory temperature.

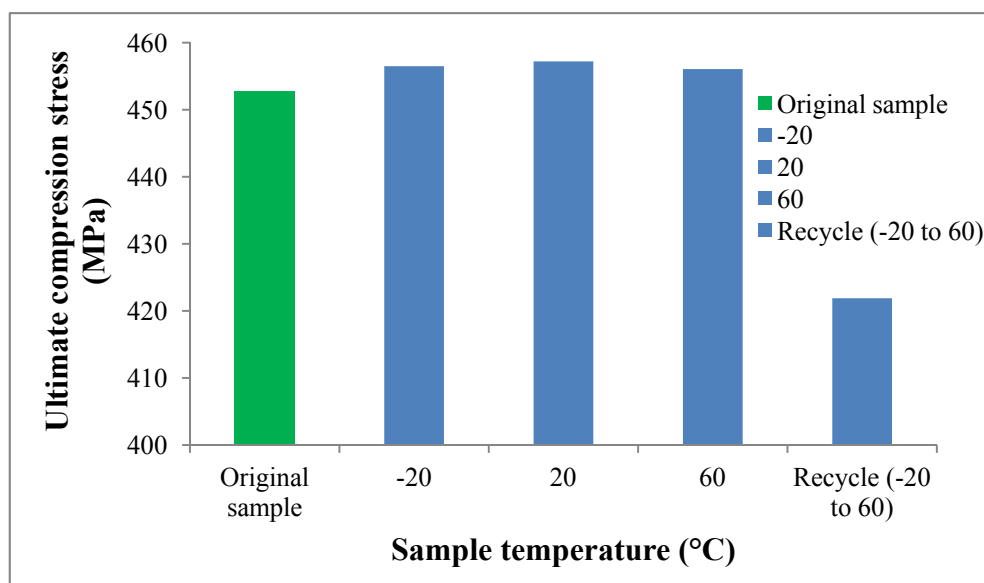


Figure 4.22: Ultimate compression stresses under different temperature

4.3.3 Effect of moisture

According to the program plan mentioned in Table 3.9, three of the 9 mm notched reinforced specimens at different times under water (from 500 hours to 2000 hours) were tested. The average for each three specimens at the target time was compared with the control sample which was tested at laboratory conditions and was seen to not be affected by moisture. Table 4.8 shows the results of these samples and the original sample. Figure 4.23 was drawn based on the values of Table 4.8 to show the effect of moisture on ultimate compression stress.

Table 4.8: Effect of moisture on ultimate compression stress

Time under water (hrs)	Ultimate compression stress (MPa)	Reduction in ultimate compression stress %
(Original specimen)	452.7	
500	437.2	3.55
1000	413.7	9.42
1500	408.5	10.81
2000	408.4	10.87

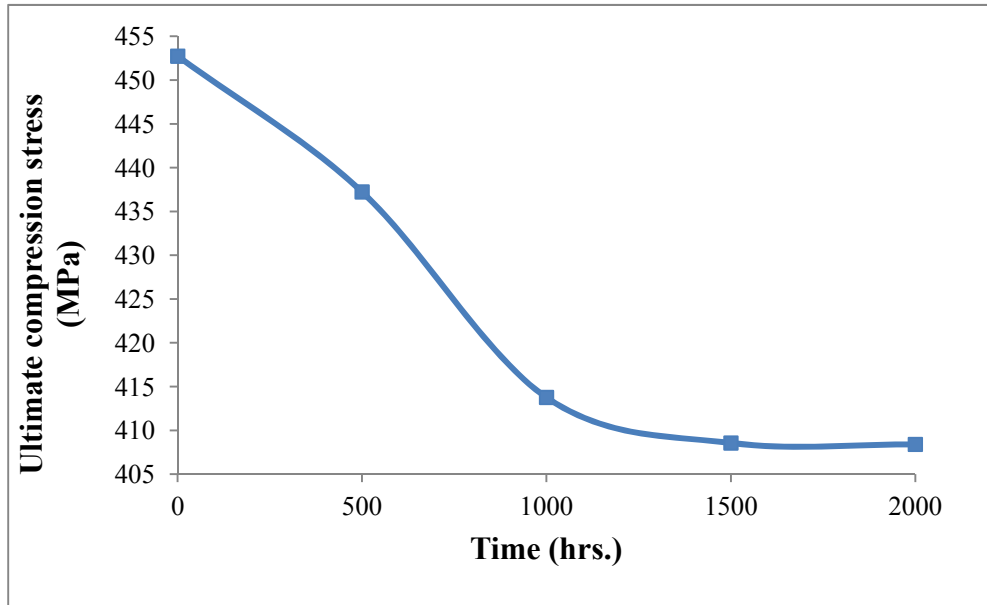


Figure 4.23: Moisture effect on ultimate compression stress

The results of moisture effects presented a significant decrease in ultimate compression stress with the lasting time under water up to 1000 hours, then, there was a slow decrease from 1000 to 1500 hours followed by an approximately straight line between 1500 and 2000 hours. These results correlate with those mentioned by Smith et al.(2005) and Karbhari et al., (2003). Yang et al. (2005) also reported in their experimental work, for man-made seawater environments, that water penetration through the interfaces causes strength reduction to a certain degree, after which a new balance system is formed that can reduce the movement of water molecules or even stop it. Thus, the decrease rate in strength will slow down since water penetration did not continue.

4.4 Failure modes

In general, delamination was found to be the dominating failure mechanism on most of the CFRP/steel angle tested specimens in both tensile and compression tests with few cases of debonding failure. This type of failure proved the good ability of

the adhesive material to transfer the load from the steel to the CFRP and keep transferring up to the last stage of testing. This also reflects that the preparing of the specimens in the laboratory was very good. Figures 4.24 to 4.25 show delaminating failures in both tensile and compression tests, and it can be seen that the inside part of CFRP was still attaching to steel specimen after failure.

However, debonding failure was the main failure mechanism for the specimens subjected to recycle temperature between (60°C and -20°C) and also for the specimens immersed under water for 2000 hrs. This type of failure means that the adhesive material has been affected by these environmental conditions and its ability to transfer the load was limited to the first stage of testing and then it failed to continue transferring the load. Figures 4.26 to 4.27 show debonding failures in both tensile and compression tests.

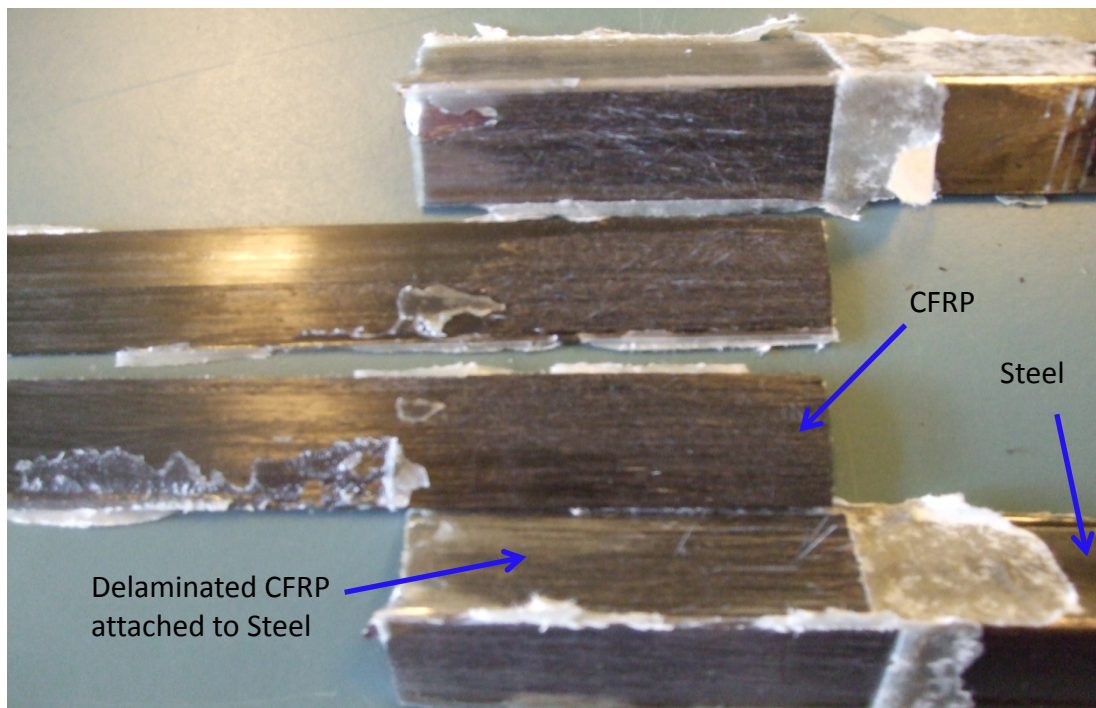


Figure 4.24: Delaminating failure in tensile test

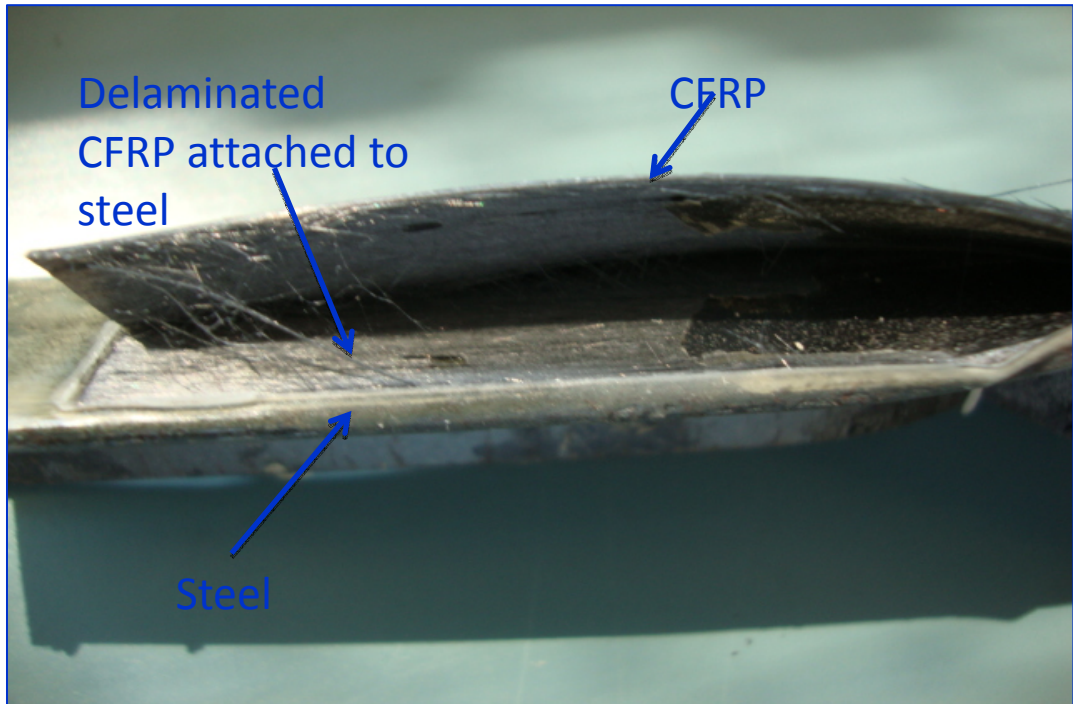


Figure 4.25: Delaminating failure in compression test

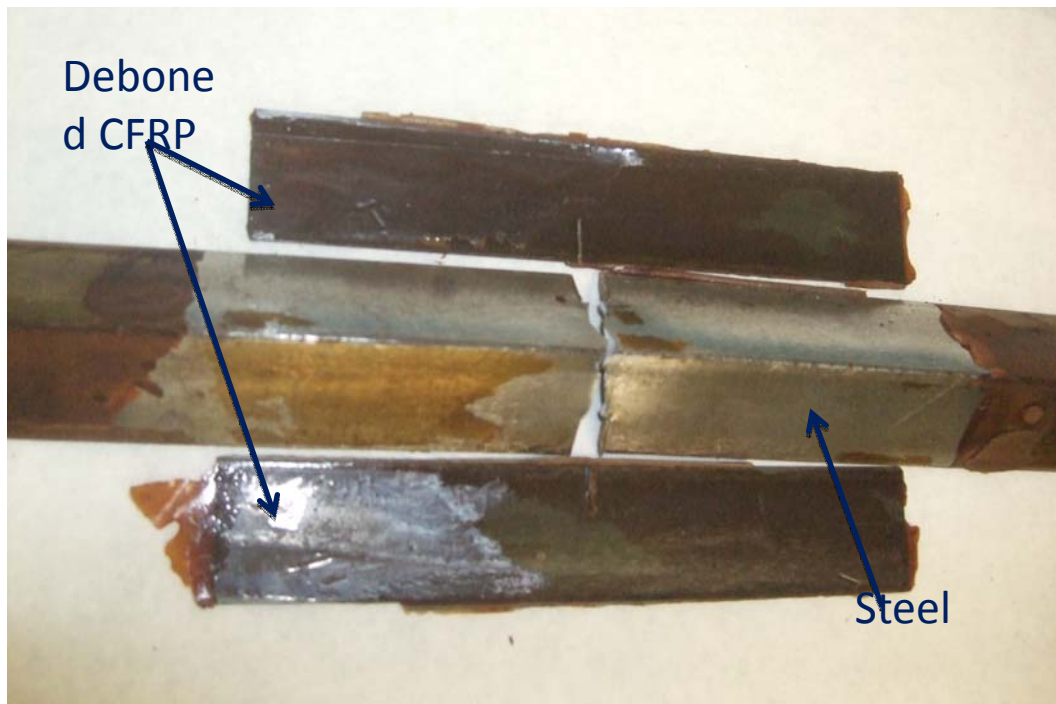


Figure 4.26: Debonding failure in tensile test

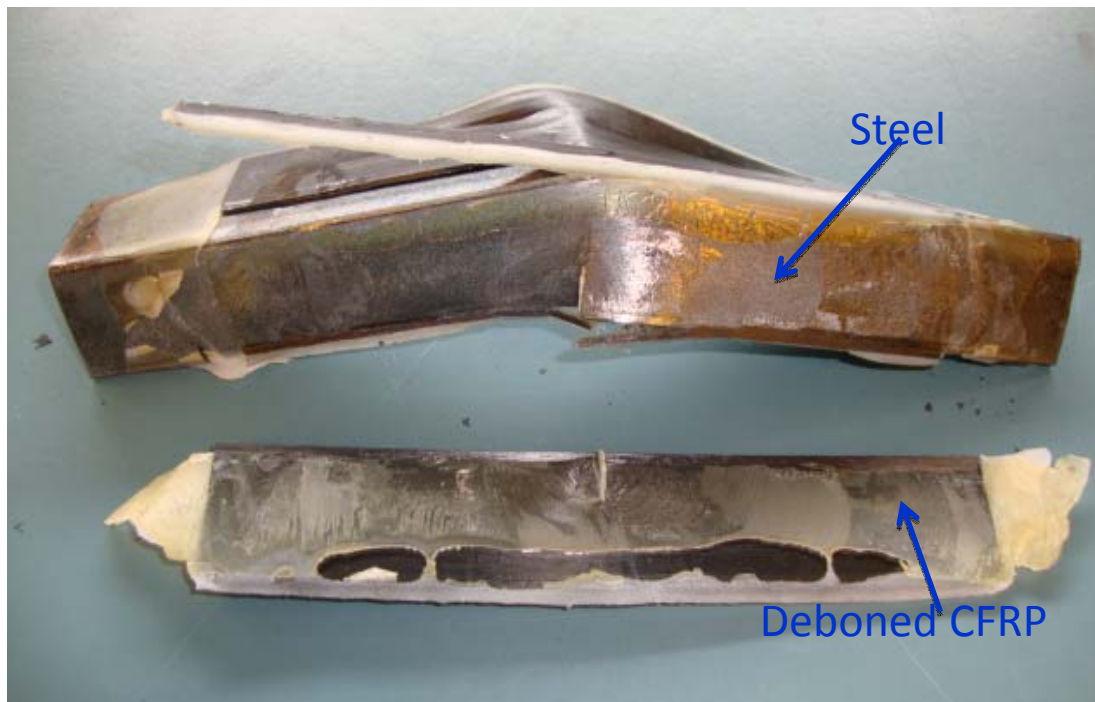


Figure 4.27: Debonding failure in compression test

4.5 Summary

The data provided by this chapter leads to the conclusion that CFRP strips were able to increase the load carrying capacity for notched samples whether they were subjected to tensile or compression tests. The recycling temperatures between (60° C and -20° C) affected the rehabilitation system in both tensile and compression tests, while the effect of the temperatures (-20° C, 20° C and 60° C) for 24 hours was not noticeable. In addition, the data showed that the moisture had a negative effect on both tensile and compression stresses, but this effect was seen gradually in tensile test and faster in compression test. Moreover, the failure modes have been illustrated in this chapter.

Chapter Five

Conclusions and recommendations

5.1 Introduction

This chapter contains conclusions based on the findings of this study. In addition, a several recommendations are provided. The value of each sample used in this study, whether in tensile or in compression test, represented the average value of three specimens which made these results reasonable and dependable.

5.2 Conclusions on tensile behaviour

Regarding the corrosion effect on tensile behaviour, the experimental work included testing two groups of samples. The first group represented samples of different artificial notches (3, 6, 9 and 12) mm without CFRP, the second group represented samples of the same notches but reinforced by CFRP. The results of both groups were compared with the intact sample. For temperature and moisture effect on tensile behaviour, the 9 mm notch was chosen to represent the effect of corrosion. Then, the reinforced sample of the 9 mm notch (second group) was compared with reinforced samples subjected to different temperatures (-20° C, 20° C, 60° C and recycle between -20° C and 60° C) and different periods of moisture (500, 1000, 1500 and 2000) hours under water. Temperature and moisture effects were tested separately. The analysis of these results led to the following conclusions:

- The influence of the artificial notch, even small sized, can sharply affect the ductility of the steel angle compared to the original one

- Load-deformation behaviour and stress distribution are largely affected by the shape, size and position of the notch
- The CFRP strips used in this study improved the ductile behaviour of deteriorated samples, especially at the 3 mm notch or at 12.6% of corrosion compared with deteriorated samples without CFRP
- The CFRP strips used in this study increased the load carrying capacities of deteriorated samples to reach maximum increments of about 45.8% in yield load and about 17.1% in ultimate load, both at 9 mm notch or at 38% of corrosion compared with deteriorated samples without CFRP
- The economical and proper use of this type of CFRP occurs when the percentage of carbon area to steel area at the corroded section ($R^{(1)}$) is about 46% and yield stress increases to about 20.4% compared with yield of the intact sample. At the same time, and within this value ($R^{(1)} = 46\%$), the corroded steel member was remained within the allowable elastic zone. Less than that value of ($R^{(1)} = 46\%$), when ($R^{(1)} = 38\%$) the increment in yield stress was about 13.4% which is also considered acceptable, but with more than ($R^{(1)} = 46\%$) there is a possibility that the corroded steel member will move into the plastic zone. In this case, stress-strain diagrams will be used to identify the allowable yield stress for the deteriorated member
- Samples exposed to temperatures (-20°C , 20°C and 60°C) for 24 hours did not show a noticeable effect on ultimate tensile stress compared with the original sample. The sample under 20°C recorded an ultimate tensile stress approximately similar to the original one, the sample under 60°C recorded 1.4% less than the original while the sample under -20°C was 2.2% less than the original. However, the periodic exposure to extreme temperatures like

recycle between -20°C and 60°C for 30 days seriously affected the ultimate tensile stress and it was reduced to about 13.9% less than the original sample

- Moisture effect caused a gradual reduction in ultimate tensile stress when the time under water increased. The reduction recorded a minimum value of about 1.76% less than the original sample at 500 hours, and a maximum value of about 6.92% less than the original sample at 2000 hours
- The strain values of the CFRP strip provided by both of the finite element program Strand7 and the strain gauge were similar. This gives a good agreement between the finite element model and the experimental work regarding the strain values of CFRP strip.

5.3 Conclusions on compression behaviour

Compression tests included a comparison of 9 mm notched specimens rehabilitated with CFRP and those having the same notch but without CFRP to find the effect of CFRP on the compression stress of corroded specimens. The 9 mm notched reinforced sample was chosen as a control sample to compare with other samples affected by different degrees of temperature or different periods of moisture in order to find the environmental effect on the compression stress of rehabilitated specimens. From the results of these tests, the following conclusions have been drawn:

- The CFRP strips used in this study increased the ultimate compression stress by about 10.7% compared to the non-rehabilitated sample
- Samples exposed to temperatures (-20°C , 20°C and 60°C) for 24 hours did not record a remarkable effect on ultimate compression stress compared with the original sample. Similar to tensile behaviour, the sample subjected to recycle temperature between -20°C and 60°C

for 30 days recorded the lowest point in ultimate compression stress of about 7.3% less than the original sample

- Moisture had a faster effect on ultimate compression stress than ultimate tensile, especially the first 100 hours which recorded a reduction of about 9.42% compared with the original sample. It seems, from moisture results, that water has nearly lost its negative effect on ultimate compression stress between 1500 and 2000 hours, with a maximum reduction about 10.87% less than the original sample recorded at 2000 hours
- The compression and tensile specimens have the same type of adhesive material and were affected by the same type of water (tap water) however, the effect of water penetration through the interfaces was different. In the compression test, balance system was reached between 1500 and 2000 hours. But at this lasting time, the tensile test did not reach balance system, and it can be concluded that water penetration could have the same effect on tensile stress but with a greater lasting time under water. It is expected that balance system may be achieved at a point between 2500 to 3000 hours or perhaps even later.

5.4 Recommendations and proposals for future works

In this section, some recommendations and proposals are made regarding the application of CFRP in the rehabilitation of corroded steel members. These recommendations and proposals are based the results of the current investigation:

- The shape of notch used to represent corrosion can change load-deformation behaviour and stress distribution. That means the

different shapes of notches, even if they have the same size of area, can provide different results of stress distribution and result in different yield loads and ultimate loads. Further experimental and numerical studies on the relationship between notch size and shape and its effect on stress are needed. To study the effect of environmental factors on the stresses of artificially corroded steel members, it is recommended that the same notch size and shape be chosen and located within the same position on all specimens, so that the unknown effects of the notch can be similar and equal for all specimens

- Due to the limited availability of resources, this study was limited to one type of CFRP with low elastic modulus. Study of the application of different types of CFRP with a wide range of elastic modulus, say 100 GPa to 400 GPa is recommended
- Due to the positive effects in this study, the use of the CFRP strips, utilised in this study, is recommended for the rehabilitation of deteriorated steel truss members. The recorded positive effects can be practically achieved by using the same type of steel, adhesive material and CFRP or when the modulus of elasticity for CFRP is about half the modulus of elasticity for steel ($E_c/E_s \approx 0.5$) using the same adhesive material
- The changing of adhesive material can substantially affect the results as the adhesive bond is considered to be the weakest point in this rehabilitation system. More research is required to identify an

adhesive material which is both suitable for bonding CFRP to steel, and highly resistant to environmental effects

- For field application, it is recommended that the percentage of CFRP area to steel area at the corroded section should be about 35% to 45%, to achieve the most economic use of the mentioned CFRP and keep the corroded steel member within the allowable elastic strain
- Although the effect of global buckling in the design of compression truss members can usually be avoided, research in the effect of CFRP in prevention of local buckling (plate buckling) is recommended
- The use of CFRP strips and the adhesive material, used in this study, in locations continually experiencing a very wide range of temperature differences (such as between -20°C and 60°C during the day and the night) is not recommended
- The results of the most extreme exposure to water lead to a recommendation that a suitable and cheap moisture barrier be applied to the rehabilitated area in order to reduce the moisture effect and increase the durability of rehabilitation system.

References

- ACI-Committee-440 (2007) Report on Fibre Reinforced Polymer (FRP) Reinforcement for Concrete Structures. American Concrete Institute (ACI), Committee 440.
- Akaro, C. (2006) Long-term performance of epoxy filled steel grate decking. *Department of Civil and Environmental Engineering*. Florida State University
- AL-Ibweini, M. & Ziara, M. (2011) Structural performance of repaired corroded reinforced concrete beams *The Islamic University Journal (Series of Natural Studies and Engineering)*, 19, 139-156.
- Al-Shawaf, A. (2011) Modelling wet lay-up CFRP-steel bond failures at extreme temperatures using stress-based approach. *International Journal of Adhesion and Adhesives*, 31, 416-428.
- Al-Shawaf, A., Al-Mahaidi, R. & Zhao, X.-L. (2008) Effect of elevated temperature on bond behaviour of high modulus CFRP/steel double-strap joints. *Australian Structural Engineering Conference (ASEC)*,. Melbourne, Australia.
- Albermani, F., Mahendran, M. & Kitipornchai, S. (2004) Upgrading of transmission towers using a diaphragm bracing system. *Engineering Structures*, 26, 735-744.
- Armstrong, K. B. (2003) Carbon fibre fabric repairs to metal aircraft structure. *The Third Technology Conference on Engineering with composites*. London, England.
- AS-1391 (2007) Metallic materials - Tensile testing at ambient temperature, Australian Standard.
- Bai, Y., Keller, T. & Vall e, T. (2008) Modeling of stiffness of FRP composites under elevated and high temperatures. *Composites Science and Technology*, 68, 3099-3106.
- Bambach, M. R., Elchalakani, M. & Zhao, X. L. (2009b) Composite steel-CFRP SHS tubes under axial impact. *Composite Structures*, 87, 282-292.
- Bambach, M. R., Jama, H. H. & Elchalakani, M. (2009a) Axial capacity and design of thin-walled steel SHS strengthened with CFRP. *Thin-Walled Structures*, 47, 1112-1121.
- Barkatt, A. (2001) Issues in predicting long-term environmental degradation of fibre-reinforced plastics. IN RH, J. (Ed.) *Environmental effects on engineered materials: Corrosion technology; 15*. . New York: Marcel Dekker.

References

- Bassetti, A., Liechti, P., Nussbaumer, A., Marquis, G. & Solin, J. (1999) Fatigue resistance and repairs of riveted bridge members. *European Structural Integrity Society*. Elsevier.
- Behncke, R. (2002) A strategy for major overhead line failures. *Power engineers line conference*. Sun Valley, Idaho.
- Bocciarelli, M., Colombi, P., Fava, G. & Poggi, C. (2009) Fatigue performance of tensile steel members strengthened with CFRP plates. *Composite Structures*, 87, 334-343.
- BS-4848-part4 (1972) Dimensions Properties (Superseded by BS EN 10056 - 1: 1999), British Standards.
- Colombi, P. & Poggi, C. (2006) Strengthening of tensile steel members and bolted joints using adhesively bonded CFRP plates. *Construction and Building Materials*, 20, 22-33.
- Ekiz, E. & El-Tawil, S. (2006) Inhibiting steel brace buckling using CFRP wraps. *Proceeding of the 8 th U.S. National Conference on Earthquake Engineering*. San Francisco, California, USA.
- El-Tawil, S., Ekiz, E., Goel, S. & Chao, S.-H. (2011) Retraining local and global buckling behavior of steel plastic hinges using CFRP. *Journal of Constructional Steel Research*, 67, 261-269.
- El Damatty, A. A., Abushagur, M. & Youssef, M. A. (2005) Rehabilitation of Composite Steel Bridges Using GFRP Plates. *Applied Composite Materials*, 12, 309-325.
- EN-ISO-527-5 (1997) Determination of tensile properties, Test conditions for unidirectional fibre-reinforced plastic composites, International Standard. Switzerland, ISO.
- Fam, A., MacDougall, C. & Shaat, A. (2009) Upgrading steel-concrete composite girders and repair of damaged steel beams using bonded CFRP laminates. *Thin-Walled Structures*, 47, 1122-1135.
- Fattaleh, A. (1984) *Professional Engineering (Civil) Licence Review Manual: Steel Design*, California, Professional Engineering Development Publications, Inc.
- Fawzia, S., Al-Mahaidi, R. & Zhao, X.-L. (2006) Experimental and finite element analysis of a double strap joint between steel plates and normal modulus CFRP. *Composite Structures*, 75, 156-162.
- Francis, R. (2000) *Bimetallic Corrosion: Guides to Good Practice in Corrosion Control* Teddington, Middlesex National Physical Laboratory

References

- Gillespie, J. W., Mertz, D. R., Kasai, K., Edberg, W. M., Demitz, J. R. & Hodgson, I. (1996) Rehabilitation of Steel Bridge Girders: Large Scale Testing. *Proceeding of the American Society for Composites 11th Technical Conference on Composite Materials*.
- Haghani, R. (2010) Analysis of adhesive joints used to bond FRP laminates to steel members - A numerical and experimental study. *Construction and Building Materials*, 24, 2243-2251.
- Harries, K. A., Peck, A. J. & Abraham, E. J. (2009) Enhancing stability of structural steel sections using FRP. *Thin-Walled Structures*, 47, 1092-1101.
- Hashim, S. A. (1999) Adhesive bonding of thick steel adherents for marine structures. *Marine Structures*, 12, 405-423.
- Hollaway, L. C. (2003) The evolution of and the way forward for advanced polymer composites in the civil infrastructure. *Construction and Building Materials*, 17, 365-378.
- Hollaway, L. C. (2010) A review of the present and future utilisation of FRP composites in the civil infrastructure with reference to their important in-service properties. *Construction and Building Materials*, 24, 2419-2445.
- Huawen, Y., König, C., Ummehofer, T., Shizhong, Q. & Plum, R. (2010) Fatigue performance of tension steel plates strengthened with prestressed CFRP laminates. *Journal of Composites for Construction*, 14, 609-615.
- Intelligent sensing for innovative structures (ISIS) (2000/01) Solution-oriented research. Canada research network.
- Jiang, S. & Zhao, X. (2007) Temperature distribution in Grouted sleeve connections subjected to fire and outdoor environment. *ISEC-4/ 4th International Structural Engineering and Construction Conference*. Melbourne, Australia.
- Karbhari, V., Chin, J., Hunston, D., Benmokrane, B., Juska, T., Morgan, R., Lesko, J., Sorathia, U. & Reynaud, D. (2003) Durability gap analysis for fibre-reinforced polymer composites in civil engineering. *Composites for Construction 2003*, 7, 238-47.
- Karbhari, V. M. & Shulley, S. B. (1995) Use of composite for rehabilitation of steel structures-determination of bond durability. *Materials in Civil Engineering*. ASCE, Vol. 7, pp. 239-245.
- Kerboua, B., Adda bedia, E. & Benmoussat, A. (2011) Strengthening of damaged structures with bonded prestressed FRP composite plates: an improved theoretical solution. *Journal of Composites Materials*, 45, 499-512.
- Kim, Y. J. & Harries, K. A. (2011a) Fatigue behavior of damaged steel beams repaired with CFRP strips. *Engineering Structures*, 33, 1491-1502.

References

- Kim, Y. J. & Harries, K. A. (2011b) Behavior of tee-section bracing members retrofitted with CFRP strips subjected to axial compression. *Composites Part B: Engineering*, 42, 789-800.
- Lee, L. S. & Jain, R. (2009) The role of FRP composite in a sustainable world. *Clean Techn Environ Policy*, 11, 247-249.
- Lees, J. M. & Winistörfer, A. U. (2011) Nonlaminated FRP strap elements for reinforced concrete, timber, and masonry applications. *Journal of Composites for Construction*, 15, 146-154.
- Lima, K., Robson, N., Oosterhof, S., Kanji, S., J.DiBattista & Montgomery, C. J. (2008) Rehabilitation of a 100-year old steel truss bridge. *CSCE 2008 Annual Conference*. Edmonton, Canada.
- Liu, H., Al-Mahaidi, R. & Zhao, X.-L. (2009) Experimental study of fatigue crack growth behaviour in adhesively reinforced steel structures. *Composite Structures*, 90, 12-20.
- Liu, X., Silva, P. F. & Nanni, A. (2001) Rehabilitation of Steel Bridge Members with FRP Composite Materials. *CCC2001, Composite in Construction*. Porto, Portugal.
- Mays, G. C. & Hutchinson, A. R. (1992) Adhesives in civil engineering. New York, NY, Cambridge University Press.
- McGeorge, D., Echtermeyer, A. T., Leong, K. H., Melve, B., Robinson, M. & Fischer, K. P. (2009) Repair of floating offshore units using bonded fibre composite materials. *Composites Part A: Applied Science and Manufacturing*, 40, 1364-1380.
- Mertz, D. R. & Gillespie, J. W. (1996) *Rehabilitation of steel bridge girders through the application of advanced composite materials*, University of Delaware, Final Report to the Transportation Research Board for NCHRP-IDEA Project 11.
- Moaveni, S. (1999) *Finite Element Analysis: Theory and Application with ANSYS*, Minnesota State University, Mankato, Prentice Hall, Upper Saddle River, New Jersey 07458.
- Naruse, T., Hattori, T., Miura, H. & Takahashi, K. (2001) Evaluation of thermal degradation of unidirectional CFRP rings. *Composite Structures*, 52, 533-538.
- Nguyen, T.-C., Bai, Y., Zhao, X.-L. & Al-Mahaidi, R. (2011) Mechanical characterization of steel/CFRP double strap joints at elevated temperatures. *Composite Structures*, 93, 1604-1612.
- Patnaik, A. K. & Bauer, C. L. (2004) Strengthening of steel beams with carbon FRP laminates. *Proceeding of the 4th Advanced Composites for Bridges and structures conference*. Calgary, Canada.

References

- Pendhari, S. S., Kant, T. & Desai, Y. M. (2008) Application of polymer composites in civil construction: A general review. *Composite Structures*, 84, 114-124.
- Radomski, W. (2002) *Bridge rehabilitation*, London; Singapore; River Edge, NJ, Imperial College Press ; Distributed by World Scientific Pub. Co.
- Selzer, R. & Friedrich, K. (1997) Mechanical properties and failure behaviour of carbon fibre-reinforced polymer composites under the influence of moisture. *Composites Part A: Applied Science and Manufacturing*, 28, 595-604.
- Shaat, A. & Fam, A. (2009) Slender steel columns strengthened using high-modulus CFRP plates for buckling control. *Journal of Composites for Construction*, 13, 2-12.
- Shaat, A., Schnerch, D., Fam, A. & Rizkalla, S. (2003) Retrofit of Steel Structures Using Fiber Reinforced Polymers (FRP): State-of-the-Art. Centre for Integration of Composites into Infrastructure.
- Silvestre, N., Young, B. & Camotim, D. (2008) Non-linear behaviour and load-carrying capacity of CFRP-strengthened lipped channel steel columns. *Engineering Structures*, 30, 2613-2630.
- Smith, S. T., Kaul, R., Sri Ravindrarajah, R. & Otoom, O. M. A. (2005) Durability considerations for FRP- strengthened RC structures in the Australian environment.
- Täljsten, B., Hansen, C. S. & Schmidt, J. W. (2009) Strengthening of old metallic structures in fatigue with prestressed and non-prestressed CFRP laminates. *Construction and Building Materials*, 23, 1665-1677.
- Tao, Y., Stratford, T. J. & Chen, J. F. (2011) Behaviour of a masonry arch bridge repaired using fibre-reinforced polymer composites. *Engineering Structures*, 33, 1594-1606.
- Tavakkolizadeh, M. & Saadatmanesh, H. (2001a) Galvanic Corrosion of Carbon and Steel in Aggressive Environments. *Journal of Composite for Construction ASCE*, 5, 200-210.
- Tavakkolizadeh, M. & Saadatmanesh, H. (2001b) Repair of Cracked Steel Girders Using CFRP Sheets. *SEC-01. Hawaii*.
- Tavakkolizadeh, M. & Saadatmanesh, H. (2003) Fatigue strength of steel girders strengthened with carbon fiber reinforced polymer patch. *Journal of Structural Engineering, ASCE*, 129, 186-196.
- Tawfik, Q. & Karunasena, W. (2010) Use of CFRP for rehabilitation of steel structures: a review. *2010 Southern Region Engineering Conference (SREC 2010)*. Toowoomba, Australia, Engineers Australia.

References

- Toutanji, H. & Dempsey, S. (2001) Stress modeling of pipelines strengthened with advanced composites materials. *Thin-Walled Structures*, 39, 153-165.
- Tsouvalis, N. G., Mirisiotis, L. S. & Dimou, D. N. (2009) Experimental and numerical study of the fatigue behaviour of composite patch reinforced cracked steel plates. *International Journal of Fatigue*, 31, 1613-1627.
- Ueda, T. (2005) FRP for construction in Japan. *Seminar on Concrete Engineering in Mongolia*. Ulan Bator, Mongolia.
- Vatovec, M., Kelley, P. L., Brainerd, M. L. & Kivela, J. B. (2002) Post strengthening of steel members with CFRP *47th International SAMPE Symposium and Exhibition 2002* Long Beach, California; USA, 12-16 May 2002, Simpson Gumpert & Heger Inc.
- Veselovsky, R. & Kestelman, V. (2002) *Adhesion of polymers*, New York, McGraw-Hill.
- Yang, Y., Yue, Q. & Peng, F. (2005) Experimental research on the bond behaviour of CFRP to steel. In Chen, J. & Teng, J. (eds.) *International Symposium on Bond Behaviour of FRP in Structure - BBFS - 2005*. Hong Kong, China, International Institute for FRP in Construction
- Young, W. C. & Budynas, R. G. (2002) *Roark's formula for stress and strain*, New York, McGraw-Hill.
- Zhao, X.-L., Fernando, D. & Al-Mahaidi, R. (2006) CFRP strengthened RHS subjected to transverse end bearing force. *Engineering Structures*, 28, 1555-1565.
- Zhao, X.-L. & Zhang, L. (2007) State-of-the-art review on FRP strengthened steel structures. *Engineering Structures*, 29, 1808-1823.

Bibliography

Bunsell, A. R. (2005) *Fundamentals of fibre reinforced composite materials*, Bristol, Institute of Physics Publishing.

Bank, L. C. (2006) *Composites for construction: structural design with FRP materials*, Hoboken NJ, John Wiley & Sons.

Callister, W. D. (2011) *Materials science and engineering*, Hoboken NJ, Wiley.

Appendix A

Tables of maximum loads

A.1 Maximum loads in tensile test

Section A.1 shows the maximum tensile load for each specimen subjected to the tensile test. These maximum values are provided by the testing machine, and the average value of three specimens was used for analysis, discussion and comparison.

Table A.1.1: Maximum tensile load of original samples (steel alone)

Original Sample	Maximum tensile load (N)
Sample 1	74029
Sample 2	73190
Sample 3	73343
Average value	73521

Table A.1.2: Maximum tensile load of 3 mm samples with and without CFRP

Samples of 3 mm notch	Maximum tensile load (N)	
	With CFRP	Without CFRP
Sample 1	64675	60695
Sample 2	62629	59554
Sample 3	62828	61575
Average value	63377	60608

Table A.1.3: Maximum tensile load of 6 mm samples with and without CFRP

Samples of 6 mm notch	Maximum tensile load (N)	
	With CFRP	Without CFRP
Sample 1	55472	50322
Sample 2	53016	51275
Sample 3	52451	52068
Average value	53646	51222

Table A.1.4: Maximum tensile load of 9 mm samples with and without CFRP

Samples of 9 mm notch	Maximum tensile load (N)	
	With CFRP	Without CFRP
Sample 1	53075	44943
Sample 2	52436	45709
Sample 3	53718	45310
Average value	53077	45321

Table A.1.5: Maximum tensile load of 12 mm samples with and without CFRP

Samples of 12 mm notch	Maximum tensile load (N)	
	With CFRP	Without CFRP
Sample 1	44714	39083
Sample 2	41478	36839
Sample 3	42501	41463
Average value	42898	39128

Table A.1.6: Maximum tensile load of samples affected by temperature

Samples affected by temperature	Maximum tensile load (N)			
	-20° C	20° C	60° C	Recycle between -20° C and 60° C
Sample 1	51734	53611	51840	49246
Sample 2	52054	52527	52741	45172
Sample 3	51947	54404	52497	45294
Average value	51912	53514	52359	46571

Table A.1.7: Maximum tensile load of samples affected by moisture

Samples affected by moisture	Maximum tensile load (N)			
	500 hrs.	1000 hrs.	1500 hrs.	2000 hrs.
Sample 1	51564	51047	51428	45996
Sample 2	52054	51703	50360	51032
Sample 3	52863	52252	51398	51901
Average value	52160	51667	51062	49643

A.2 Maximum loads in compression test

Section A.2 shows the maximum compression load for each specimen subjected to the compression test. These maximum values are provided by the testing machine, and the average value of three specimens was used for analysis, discussion and comparison.

Table A.2.1: Maximum compression load of 9 mm samples with and without CFRP

Samples of 9 mm notch	Maximum compression load (N)	
	With CFRP	Without CFRP
Sample 1	45820	36070
Sample 2	48090	33590
Sample 3	50930	38370
Average value	48280	36010

Table A.2.2: Maximum compression load of samples affected by temperature

Samples affected by temperature	Maximum compression load (N)			
	-20° C	20° C	60° C	Recycle between -20° C and 60° C
Sample 1	46240	49032	48666	47735
Sample 2	50436	49490	47857	43560
Sample 3	49368	47751	49383	43676
Average value	48681	48758	48635	44990

Table A.2.3: Maximum compression load of samples affected by moisture

Samples affected by moisture	Maximum compression load (N)			
	500 hrs.	1000 hrs.	1500 hrs.	2000 hrs.
Sample 1	49990	43981	43401	41330
Sample 2	44750	43829	43188	46255
Sample 3	45141	44561	44119	43070
Average value	46627	44124	43569	43552